Determination of Laterality in the Rabbit Embryo:

Studies on Ciliation and Asymmetric Signal Transfer

Dissertation zur Erlangung des Doktorgrades
der Naturwissenschaften (Dr. rer. nat.)

Fakultät Naturwissenschaften
Universität Hohenheim

Institut für Zoologie

vorgelegt von

Kerstin Feistel
aus Simmern

2006

Dekan:	Prof. Dr. Heinz Breer
1. berichtende Person:	Prof. Dr. Martin Blum
2. berichtende Person:	Prof. Dr. Heinz Breer
Eingereicht am:	27.11.2006
Mündliche Prüfung am:	30.01.2007

Die vorliegende Arbeit wurde am 29.11.2006 von der Fakultät Naturwissenschaften der Universität Hohenheim als „Dissertation zur Erlangung des Doktorgrades der Naturwissenschaften“ angenommen.

Mein herzlicher Dank gilt Prof. Dr. Martin Blum für die Chance, als Neuling in der Molekularbiologie diese Doktorarbeit in seiner Arbeitsgruppe durchführen zu können. Ich weiß sein Engagement und seinen Optimismus sehr zu schätzen und bedanke mich für seine Motivation, die mir besonders in der letzten Phase der Arbeit sehr weitergeholfen hat.

Ich danke Prof. Dr. Heinz Breer für sein Interesse an dieser Arbeit, die von ihm investierte Zeit sowie die Möglichkeit zum regen Austausch zwischen den Instituten.

Ich möchte mich bei Prof. Dr. Christoph Viebahn für sein Interesse an dieser Arbeit und die gute Zusammenarbeit bedanken, über die ich mich sehr gefreut habe.

Ich bedanke mich ganz herzlich bei Dr. Anja Rietema, die mir nicht nur mit Tricks und Kniffen aus der Molekularbiologie zur Seite stand, sondern mich auch mit den „haarigen“ Angelegenheiten dieser Arbeit vertraut gemacht hat.

Mein Dank gilt dem Boehringer Ingelheim Fonds und allen seinen Mitarbeitern, die mir mit ihrer Unterstützung ungeahnte Möglichkeiten eröffnet haben.

Danke an alle Kollegen! Es war eine klasse Zeit mit euch und ich werde die wilden Diskussionen, die Musik und den Kuchen vermissen!

Ganz lieben Dank meiner Familie für ihre Unterstützung und ihre Begeisterung und natürlich meinem Mann Torben, mit dem mir die gemeinsame Doktorarbeitszeit trotz (oder gerade wegen) des alltäglichen Wahnsinns so unheimlich viel Spaß gemacht hat!

Abstract

The midline of the vertebrate embryo plays a pivotal role in the regulation of left-right (LR) asymmetry. In mammals recent interest has focused on a structure situated at the caudal part of the notochord, the posterior notochord (PNC), which is homologous to Kupffer's vesicle (KV) in fish and the gastrocoel roof plate (GRP) in frog. Despite highly diverging embryonic architecture, the PNC/KV/GRP is the site where motile monocilia set up a directional fluid flow, an event indispensable for the generation of LR asymmetry. Signals created at the PNC/KV/GRP need to be transferred to the periphery of the embryo, where they initiate the left-specifying program in the left lateral plate mesoderm (LPM).

In this study morphogenesis and ciliogenesis of the notochordal plate as well as the signaling processes between midline and LPM were studied in the rabbit embryo. Rabbit development progresses through a flat blastodisc phase and represents the typical mode of mammalian embryogenesis. Transcription of ciliary marker genes, the first sign of beginning ciliogenesis, initiated in Hensen's node and persisted in the nascent notochord. Cilia emerged on cells leaving Hensen's node anteriorly to form the notochordal plate. Cilia lengthened to about 5µm and polarized from an initially central position to the posterior pole of cells. Electron microscopic analysis revealed 9+0 and 9+2 cilia and a novel 9+4 axoneme intermingled in a salt-and-pepper-like fashion. These data showed that the ciliogenic gene program essential for laterality determination is conserved at the midline of the rabbit embryo.

The present study also provided evidence that initiation as well as repression of the Nodal cascade crucially depended on communication between midline and lateral plate (LP). Separation of LP tissue from the midline before, during and after the 2 somite stage demonstrated that signals from the PNC induced and maintained the competence of LPM to express *Nodal*. Signals from the midline were necessary after the 2 somite stage to maintain a right-sided identity, i.e. absence of *Nodal* expression. Gap-junction-dependent intercellular communication (GJC) was shown to play a central role in this process. Previously, GJC had been involved in LR axis determination in cleavage stage frog embryos and early blastodisc stages in chick. This study for the first time demonstrates the role of GJC in mammalian embryos. GJs regulate the signaling between midline and periphery: permeable gap junctions

were required specifically at the 2 somite stage to repress *Nodal* induction in the right LPM, whereas closed GJs were a prerequisite for Nodal signaling on the left side. Establishment of the right-sided fate depended on FGF8, the signaling of which was regulated by the opening status of GJs. A 3-step model is proposed for symmetry breakage and induction of the LR signaling cascade in vertebrates: (1) Nodal protein synthesized at the lateral edges of the PNC diffuses bilaterally and confers competence for the induction of the Nodal cascade to the LPM, (2) at the same time the left-specific cascade is actively repressed by action of the GJC/FGF8 module, and (3) following the onset of leftward flow at the PNC repression gets released specifically on the left side at the 2 somite stage, presumably by transient inhibition of GJC. This model not only is consistent with the presented data, but also with published work in other model organisms.

Zusammenfassung

Im Wirbeltierembryo spielt die Mittellinie eine wichtige Rolle bei der Ausbildung der links-rechts (LR) Asymmetrie der inneren Organe. Das jüngste Interesse fokussiert sich insbesondere auf den caudalen Teil des Notochords im Säuger, das posteriore Notochord (PNC), eine Region die dem Kupfferschen Vesikel (KV) des Fisches und der Dachplatte des Gastrocoels (GRP, gastrocoel roof plate) der Amphibien homolog ist. Trotz der höchst unterschiedlichen Morphologie der Wirbeltierembryonen zeichnet sich die PNC/KV/GRP-Region immer dadurch aus, dass hier ein durch Monocilien getriebener gerichteter Flüssigkeitsstrom entsteht, welcher für die Entstehung von Asymmetrie unverzichtbar ist. Signale, die in diesem Bereich der Mittellinie entstehen, müssen in die Peripherie des Embryos gelangen, um die links-spezifische Signalkaskade im linken Seitenplattenmesoderm (SPM) in Gang zu setzen.

In der vorliegenden Arbeit wurden sowohl die Morphogenese und Ciliogenese der Notochordalplatte als auch die Signalprozesse zwischen Mittellinie und Seitenplatte im Kaninchenembryo untersucht. Die Entwicklung des Kaninchens durchläuft ein flaches Keimscheibenstadium und repräsentiert somit die grundlegende Morphologie der Säugerentwicklung. Die Transkription ciliärer Markergene, das erste Zeichen der Ciliogenese, begann im Hensenschen Knoten und setzte sich im auswachsenden

Notochord fort. Die ersten Cilien entstanden auf Zellen, die den Knoten als Teil der Notochordalplatte rostralwärts verließen. Diese Cilien wuchsen zu etwa 5µm Länge heran und nahmen sukzessive eine posteriore Position auf der Zelle ein. Die Analyse der Cilien im Elektronen-mikroskop zeigte, dass 9+0 und 9+2 Cilien sowie ein neu entdecktes 9+4 Axonem auf der Notochordalplatte vermischt vorkamen. Diese Daten bestätigten, dass das genetische Programm, welches die Ciliogenese steuert und für die Ausbildung der Organasymmetrie verantwortlich ist, in den Strukturen der Mittellinie des Kaninchens konserviert ist. Die vorliegende Arbeit zeigte zudem, dass sowohl Induktion als auch Repression der Nodal-Signalkaskade auf einem Austausch zwischen Mittellinie und Seitenplatte (SP) beruhen. Die Isolierung von SP-Gewebe vor, während und nach dem 2-Somiten-Stadium bewies, dass Signale aus dem PNC die Kompetenz zur Expression von Nodal im SPM induzierten und aufrecht erhielten. Nach dem 2-Somiten-Stadium waren Signale aus der Mittellinie notwendig, um die Identität der rechten Seite, d.h. fehlende *Nodal*-Expression, aufrecht zu erhalten. Es stellte sich heraus, dass gap-junction-vermittelte interzelluläre Kommunikation (GJK) eine zentrale Rolle in diesem Prozess spielt. Es ist bereits bekannt, dass GJK in Furchungsstadien von Froschembryonen sowie in der frühen Keimscheibe des Hühnchens an der Ausbildung der LR Asymmetrie beteiligt sind. Nun zeigt diese Arbeit zum ersten Mal, dass GJK auch im Säuger eine Rolle spielt. Gap junctions (GJs) regulieren den Signalaustausch zwischen Mittellinie und Peripherie: permeable GJs waren speziell im 2-Somiten-Stadium zur rechtsseitigen Repression von *Nodal* im SPM benötigt, während geschlossene GJs eine Voraussetzung für die Induktion von Nodal auf der linken Seite bildeten. Die Identität der rechten Seite war zudem von FGF8 abhängig, dessen Funktion durch den Öffnungsstatus der GJs reguliert wurde. Ein dreistufiges Modell für den Symmetriebruch und die Induktion der LR Signalkaskade in Wirbeltieren wird vorgeschlagen: (1) Nodal-Protein breitet sich beiderseits des PNC aus und überträgt die Kompetenz für die Nodal-Kaskade auf das SPM. (2) Die links-spezifische Kaskade wird durch das Zusammenspiel von GJK und FGF8 beidseitig aktiv unterdrückt bis (3) die linksgerichtete Flüssigkeitsbewegung diese Repression auf der linken Seite aufhebt, wahrscheinlich durch eine vorübergehende Inhibition von GJK. Das vorgeschlagene Modell stimmt nicht nur mit den hier präsentierten Daten, sondern auch mit bereits veröffentlichten Arbeiten an anderen Modellorganismen überein.

Table of contents

Introduction

Development of left-right asymmetry

Bilateral symmetry is the common feature of all animals belonging to the taxon of bilateria. It is produced by the alignment of the anterior-posterior and dorso-ventral axes creating a midsagittal plane at which both left and right side of the body are mirrored. In vertebrates, this ancestral symmetry is apparent in the bilaterally symmetrical appearance of the body as viewed from the outside. Yet, an asymmetric arrangement of the viscera exists: the internal organs can be displaced to the left and right sides of the body with respect to the midline or they may be medially located but constructed asymmetrically. Vertebrate left-right (LR) asymmetry is a trait which manifests itself during embryogenesis with the asymmetric development of organ primordia. The first morphological evidence of directionality is a rightward bend in the heart tube, which eventually results in the complex patterning of the embryonic heart and its leftward alignment. In the adult vertebrate, several other visceral organs are placed asymmetrically, such that the liver is on the right side, stomach and spleen are located on the left side and even the seemingly bilaterally symmetric lung has a diverging number of lobes between left and right side. The correct placement of the thoracic and abdominal organs is referred to as situs solitus, whereas the phenotype of a complete mirror-image reversal is called situs inversus. Disturbed laterality determination can also lead to heterotaxia, a state which is specified by the misplacement of single organs, whereas in a left or right isomerism, the identity of one side is reflected onto the other side resulting in the loss or duplication of single organs.

The detailed description and genetic analysis of laterality defects in human patients has contributed a great deal to the understanding of how the LR axis is determined.

Yet most of the information about how LR asymmetry is created during embryogenesis comes from studies using mouse models for laterality. Apart from mouse, LR asymmetry has been investigated in well established vertebrate model organisms such as zebrafish, *Xenopus* and chick. Although many of the general mechanisms of asymmetric organ placement seem to be conserved among those species, diverging and sometimes contradictory results have been obtained concerning the events that initiate asymmetric morphogenesis. It has been speculated that this might be due to the striking differences in embryonic architecture accompanying the various modes of development.

The rabbit as a mammalian model organism

Although in many aspects murine embryogenesis can serve as a general model for the development of mammals, rodent embryos are especially untypical for gastrulating/neurulating mammalian embryos, as up to the time of embryonic turning, they adopt an unusual cup-shaped 'egg cylinder' appearance. Typical mammalian development however is represented by a flat disc-shaped embryo, which closely resembles and is in many aspects comparable to the chicken blastodisc. Therefore, the rabbit, which develops via a flat blastodisc, can be used to study archetypical mammalian development as it is conserved in humans as well. A staging system for rabbit embryos based on the Hamburger-Hamilton (HH) staging system for chicken embryos has been developed (Fig. 1, reproduced with permission from Blum et al. 2006). Rabbit gastrulation starts with the appearance of the primitive streak in stage 3, when the first cells leave the epiblast, migrate through the streak and contribute to mesoderm and endoderm formation. Stage 4 is represented by a fully formed Hensen's node, which is discernible as a thickening at the anterior end of the primitive streak. The midline mesoderm is laid down during stage 5. It begins with the exit of prechordal mesodermal cells from the node, which are followed by notochordal cells in a way that the embryo grows anteriorwards. In stage 6, the embryo has elongated and becomes more slender. The node is located in the

posterior half of the blastodisc because the notochordal plate is now longer than the primitive streak. The subsequent somite stages are defined by the number of somites formed and are characterized by a waisted appearance of the embryo.

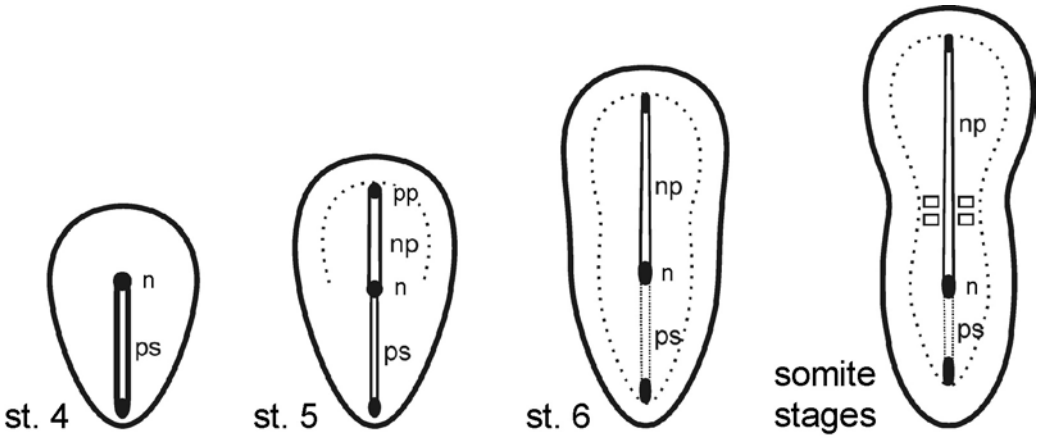

Fig. 1 Staging system of rabbit embryos. Between 7.0 and 8.0 dpc the rabbit embryo develops from stage (st.) 4 (characterized by the presence of Hensen's node, n), via stage 5 (notochordal plate, np, and prechordal plate, pp) and stage 6 (elongated notochordal plate and head fold) to somitogenesis. ps, primitive streak.

Despite the extremely diverging modes of early development, the morphogenetic events of organ placement in vertebrates are preceded and initiated by the action of a conserved set of factors which is expressed in the left lateral plate mesoderm (LPM) of the neurula stage embryo. This succession of gene expression is called the “Nodal cascade” and has been identified in all vertebrates examined up to date.

Nodal signal transduction and its regulation

Nodal is the first of three genes which are asymmetrically transcribed in the left lateral plate. It encodes a secreted molecule belonging to the transforming growth factor beta (TGFβ) superfamily of growth factors. TGFβ factors typically signal as dimers by binding to receptors of the serine/threonine kinase type. For signal transduction Nodal needs a heterodimeric complex of a receptor type I and type II (in

the case of Nodal these are ALK4,7 and ActR-IIB) as well as an accessory receptor of the EGF-CFC type, which facilitates binding of Nodal to the receptor. Bound Nodal activates the pathway so that both type I and type II receptors are phosphorylated and activate the transducer Smad2 also by phosphorylation. Activated Smad2 translocates into the nucleus and in a complex with Smad4 and the transcription factor Foxh1 activates target gene transcription (Whitman and Mercola, 2001; Massague, 2003). One of these targets is *Nodal* itself, so that it acts in a positive feedback loop on its own transcription.

Two different enhancers have been identified to drive LPM *Nodal* expression. The asymmetric expression of *Nodal* is mainly directed by the asymmetric enhancer ASE, which is located in the first intron of the *Nodal* gene and is Nodal-responsive, as revealed by its strict Foxh1-dependent activation (Norris et al., 2002). The second enhancer was termed LSE for left side-specific enhancer and is located about 4kb upstream of the transcription start site. Similar to the ASE, the LSE is Nodal-responsive but it seems to be dispensable for asymmetry, as neither *Nodal*$^{\Delta LSE/+}$ nor *Nodal*$^{\Delta LSE/\Delta LSE}$ mice show alteration of markers or situs defects (Saijoh et al., 2005).

Expression of *Nodal* during gastrulation

In mammals and chick, *Nodal* transcripts are detected at the site of gastrulation, the primitive streak, as well as in the organizer, the node or Hensen's node (Zhou et al., 1993; Levin et al., 1995; Blum et al., 2006). In *Xenopus* and zebrafish embryos, expression of early *Nodal* homologs resides in the equivalent structures: in the frog, it is found in the circumblastoporal collar and dorsal blastoporal lip (Jones et al., 1995) and in zebrafish embryos, it is circumferentially expressed in the germ ring and embryonic shield (Rebagliati et al., 1998). In these structures Nodal induces the epithelial-mesenchymal transition of cells and thus participates in mesoderm and endoderm formation during gastrulation (reviewed by Schier and Chen, 2000). Slightly later, concomitant with the first cells of the newly forming midline mesoderm

leaving the organizer, *Nodal* ceases to be expressed in the streak and organizer equivalents.

Paranotochordal expression of *Nodal*

Nodal expression reappears as a distinct domain which borders the posterior aspect of the notochordal plate (PNC) in mouse and rabbit, and the homologous structures in teleosts and amphibians, namely Kupffer's vesicle (KV) and the gastrocoel roof plate (GRP, Blum et al. 2006). As the PNC in mouse has been referred to as "Node" this is where the name "*Nodal*" originated from (Zhou et al., 1993). In mammals, *Xenopus* and zebrafish the paranotochordal domain of *Nodal* expression is bilateral and precedes initiation of the Nodal Cascade in the left LPM (Lowe et al., 1996; Long et al., 2003). However, in chick, where morphological asymmetries in Hensen's node precede asymmetric gene activity, the paranotochordal expression first establishes unilaterally and becomes bilateral only after the onset of lLPM expression (Levin et al., 1995).

In the mouse it has been genetically proven that the paranotochordal domain of *Nodal* expression is essential for the initiation of *Nodal* transcription in the left LPM (Brennan et al., 2002, Saijoh et al., 2003). When *Nodal* expression at the PNC is greatly reduced or completely absent in transgenic mice (Saijoh et al., 2003), asymmetric *Nodal* in the LPM does not appear. In these mice a reconstitution of the paranotochordal domain was sufficient to re-initiate *Nodal* in the LPM. The NDE, an enhancer which is located 9.5kb upstream of the transcription start site, is PNC specific (Adachi et al., 1999; Norris and Robertson, 1999). Different from the enhancers driving LPM expression, the NDE is not responsive to Nodal signaling (Saijoh et al., 2003), indicating that *Nodal* expression at the PNC is maintained by a factor other than *Nodal* itself. Additionally, the paranotochordal expression of *Nodal* persists in *cryptic* knock-out mice (Gaio et al., 1999) as well as in *Xenopus* embryos in which *Xcr1* has been knocked down with morpholino antisense oligonucleotides (Onuma et al., 2006). These findings demonstrate that the EGF-CFC co-receptor,

which is essential for Nodal signal transduction in the lateral plate, is not necessary for the midline domain.

The Nodal cascade in the lateral plate mesoderm

In rabbit, mouse and chick, *Nodal* is transcribed in the left LPM from the 2-3 somite stage onwards (Levin et al., 1995; Lowe et al., 1996; Fischer et al., 2002). Correspondingly, it is first detected in the left LPM at stage 19/20 in *Xenopus* as well as in 10-12 somite embryos of zebrafish (Rebagliati et al., 1998; Ohi and Wright, 2006). Transcription in the LPM starts in the LPM cells lying at the level of the paranotochordal domain. From here, *Nodal* signals propagate in a rostro-caudal fashion, eventually spanning a region from the posteriormost aspect of the embryo into the developing heartanlage.

Apart from positively feeding back upon itself to allow the fast rostro-caudal expansion in the LPM, Nodal signaling targets the expression of two genes important for regulation and perseverance of the gene cascade, namely *Lefty2* and *Pitx2*. Lefty, an untypical TGFβ family member, serves as a feedback inhibitor of Nodal signaling by competing for receptor as well as co-receptor binding (Schier and Shen, 2000). *Lefty2* expression in the lateral plate starts shortly after *Nodal* and co-expands rostrally and caudally, finally terminating *Nodal* expression (Ohi and Wright, 2006). The other target, the homeobox transcription factor Pitx2, remains expressed in the lateral plate and mediates the translation of the first asymmetric cues into asymmetric organ morphogenesis (Logan et al., 1998).

A role for embryonic cilia in laterality determination

Embryos tend to bear ciliated structures that enable them to move, feed or keep their surfaces clean. The focus of interest in the LR field recently cumulates in a ciliated

structure whose function is quite diverging as it seems to be specialized for the determination of laterality in vertebrates: the mammalian PNC and its homologs in fish and frog, KV and GRP.

Cilia at the PNC/KV/GRP

In all species described up to date, the PNC/KV/GRP can be located by the paranotochordal expression of *Nodal* in the neurula stage embryo (Blum et al., 2006). It consists of epithelialized mesodermal cells which will later on contribute to the notochord of the posterior body and tail. During the time that these cells are part of the PNC/KV/GRP they are all characterized by the presence of a single monocilium on their apical surface (Sulik et al., 1994; Shook et al., 2004; Essner et al., 2005). The PNC/KV/GRP is derived from the organizer, comes to lie rostrad of it and stands in direct continuity with the developing notochord anteriorly. Mutations specifically affecting PNC or KV morphogenesis in mouse or in zebrafish lead to tail malformation and specifically to left-right defects, indicating the requirement of this structure for posterior body elongation and highlighting its implication in setting up laterality (Herrmann and Kispert, 1994; Abdelkhalek et al., 2004). Yet the understanding of the importance of this very structure arose out of a study published in 1998 (Nonaka et al., 1998) that reported LR-defects in a mouse knockout of the *Kif3b* gene. In the absence of the Kif3b subunit of the heterotrimeric Kinesin-II-complex, the cells of the murine PNC lacked monocilia and the embryos showed either bilateral or a lack of LR-marker genes and randomized situs. It had been demonstrated before that cilia on the notochord of the mouse were motile (Sulik et al., 1994), but it became clear only then, that this motility resulted in a leftward-directed flow of extracellular fluid in the PNC region. The structure in the mouse at that time was erroneously referred to as “Node”, reflecting the assumption that it represented the embryonic organizer, called Hensen’s node in rabbit and chick. Hence, the fluid motion set up by the motile monocilia was termed “Nodal Flow” and

made its way into the primary literature and even textbooks as the symmetry breaking event in the mouse.

The “Nodal Flow” hypothesis

The subsequent characterization and manipulation of leftward fluid flow in the mouse further approved its role in the determination of the LR axis (Okada et al., 1999; Nonaka et al., 2002). It was shown that the classical mouse models for LR defects, *iv* and *inv*, both had irregularities in the setup of flow (Okada et al., 1999). *Iv* harbors a mutation in the left-right dynein gene (*lrd*), encoding an axonemal dynein heavy chain indispensable for motility of the cilium (Supp et al., 1997). In this mutant, PNC cells still produced cilia, but those were paralyzed due to the deficiency in motor protein function and thus no “Nodal Flow” was detected in these mice. The function of Inversin, the gene product of *inv*, is still enigmatic. In the mutant mouse, PNC cilia arise and show motility, however this results only in aberrant fluid flow, which is slow and turbulent (Okada et al., 1999; Okada et al., 2005).
Experimental manipulations of the flow yielded two main results: (1) the randomized markers of *iv* mice could be directed and rescued by the application of external flow and (2) in wild type mice, LR marker genes could be inverted by reverting the intrinsic flow (Nonaka et al., 2002). Based on the finding of this extracellular fluid flow a model was put forward which proposed that the leftward directed flow served to redistribute a symmetrically released morphogen across the PNC resulting in its accumulation on the left side (Nonaka et al., 1998; Nonaka et al., 2002). This morphogen flow model was supported by the demonstration that exogenously applied molecules of appropriate size are indeed subject to asymmetric distribution by intrinsic fluid flow (Okada et al., 2005). It also made sense in the light that several genes coding for morphogens such as Shh, FGF8 or Nodal are expressed in or in the vicinity of the PNC. Although different from the initial suggestion, morphogenic molecules might also be packed in membranous vesicles, as so called NVPs (“Nodal Vesicular

Parcels") loaded with RA and Shh were found in the PNC region and as a cargo those NVPs might be transported leftward by the fluid flow (Tanaka et al., 2005).
A modification of the "Nodal Flow" hypothesis was presented by Tabin and Vogan (2003) who reasoned against the morphogen model and proposed that the flow might instead be set up and sensed by two different populations of cilia, namely by such of motile vs. sensory character. This idea was confirmed experimentally by Brueckner and colleagues (McGrath et al., 2003) who showed that all PNC cilia were positive for the ion channel polycystin-2, but that a subset of those cilia was immotile as indicated by the lack of Lrd protein. Those immotile and thus most probably sensory cilia were located at the lateral borders of the PNC whereas Lrd-positive cilia were found on cells located centrally in the PNC (McGrath et al., 2003).

Ciliary architecture

Cilia are ancient and conserved organelles all sharing the same principal biogenesis, structure and function. At the cell's apical surface, a cilium originates from its template structure, the basal body, and protrudes into the extracellular space. A motor-protein driven process called intraflagellar transport (IFT; Rosenbaum and Witman, 2002) delivers all necessary components and thus assembles the ciliary axoneme, which is entirely covered by the cell membrane. The axoneme as the inner scaffold of the cilium consists of nine microtubule doublets arranged in a circular fashion. A vast variety of proteins is attached to the microtubules, such as the inner and outer arm dynein complexes which are essential for motility of the cilium. These motor proteins produce a sliding movement between adjacent doublets and as the tubules are all proximally attached to the basal body, the sliding force results in bending of the cilium (Wemmer and Marshall, 2004). This ciliary motility is controlled in part by the central pair apparatus (CP), two single central microtubules tethered together to make them act as a doublet. In some species the CP rotates during bending of the cilium, thereby modulating outer doublet dynein activity via the radial spokes, which may account for the variety of waveforms and beating frequencies

observed in different cilia and flagella (Omoto et al., 1999; Wargo and Smith, 2003). In cells with planar ciliary beat, the CP is fixed in its position and the plane of beating is perpendicular to the CP (Gibbons, 1981). As the CP plays such an important role in the modulation of motility, it is not surprising that most cilia lacking the central pair of microtubules are immotile and that cilia with this 9+0 structure were considered to fulfill sensory functions.

PNC monocilia are exceptional

There are, however, exceptions, the most prominent example being the monocilia on the PNC cells of the mouse . Those PNC cilia with 9+0 axonemes are indeed motile (Sulik et al., 1994), but probably due to the lack of a regulatory CP, they show a stereotype conical rotation rather than changing wave forms or planar beating (Nonaka et al., 2002; Nonaka et al., 2005; Okada et al., 2005). Interestingly, Kupffer's vesicle cilia, while performing rotational beat patterns in all cases, display 9+2 axonemes in zebrafish (Kramer-Zucker et al., 2005) and 9+0 axonemes in medaka (Okada et al., 2005).

Creating a leftward-directed fluid flow

The typical whip-like beat pattern of an epithelial 9+2 cilium is planar and biphasic: it consists of a fast power stroke "pushing" the surrounding fluid, and a slow recovery stroke which brings the cilium back into its initial position without moving the fluid. The orientation of the CP dictates the plane of beating and hence the direction of fluid movement. As indicated above, the CP is not essential for motility of the cilium per se, it rather modulates beat pattern. Therefore, 9+0 cilia lacking CP structures are only capable of rotational movements. Such rotational motion was supposed to produce local whirls and vortices only, but how clockwise rotation could be transformed into directional movement was modeled by (Cartwright et al., 2004). The

authors proposed that in order to make up a leftward directed fluid flow above the mouse PNC, cilia would need to be tilted in a posterior direction. Indeed it was shown that cilia on PNC cells of mouse and rabbit are localized posteriorly relative to the cell center (Nonaka et al., 2005; Okada et al., 2005). As epithelial cells typically show a mound-like appearance, displacement of the cilium towards the posterior results in a tilt and hence modulates motility: 180° of the rotation occur in the vicinity of the cell surface creating a slow and inefficient phase. The rest of the circulation is faster as it is unhindered by the surface and can be compared to the effective stroke of a 9+2 cilium. As a matter of fact, the effective stroke of a posteriorly tilted, clockwise rotating cilium is leftward and thus the rotation of PNC cilia is conveyed into unidirectional fluid flow to the left (Blake and Sleigh, 1974; Nonaka et al., 2005).

Evolutionary conservation of laterality determining fluid flow

Even before the first asymmetrically expressed genes were described, Brown and Wolpert (1990) proposed a theoretical model in which a chiral structure termed the F-molecule could confer LR asymmetry by its alignment along the existing anterior-posterior and dorso-ventral axes. They suggested that the microtubule cytoskeleton, which has intrinsic chirality, might be involved in this process. Thus a mechanism like the “Nodal Flow” nicely fulfilled the criteria of this long-sought module: microtubule-based, chirally constructed cilia which are oriented in an epithelium and evoke a leftward-directed fluid-flow. The first demonstration that in other vertebrate species cilia reside at structures homologous to the mouse PNC (Essner et al., 2002) made the scenario even more convincing and allowed the anticipation, that fluid flow might be found in other vertebrates, too. And indeed, fluid movement was described in Kupffer’s vesicle in zebrafish and medaka (Essner et al., 2002; Okada et al., 2005), in the rabbit (Okada et al., 2005) as well as in *Xenopus* (Schweickert et al., 2007), proving the evolutionary conservation of leftward-directed fluid-flow in vertebrates. In zebrafish gene knockdown by the injection of morpholino antisense oligonucleotides against Lrd targeted specifically to KV cells have also shown that the motility of

monocilia is necessary for L-R determination, as upon Lrd knock-down fluid flow was not observed and the embryos showed altered L-R development (Essner et al., 2005).

Gap junctions and the transfer of laterality cues

Leftward directed fluid flow across the PNC/KV/GRP is a conserved module of LR axis determination and seems to be the mechanism on which the early events of symmetry breaking in vertebrates converge. It may thus account for the first phase of the development of LR asymmetry which is (1) the breakage of bilateral symmetry at the PNC. This creation of LR asymmetric information at the midline must be followed by (2) the asymmetric transfer of cues to the LPM where those (3) initiate the Nodal cascade which eventually results in (4) the asymmetric morphogenesis of organ primordia. There is good evidence that it is leftward directed fluid flow which brakes symmetry at the PNC in phase (1). However, it still remains to be explained how in phase (2) this newly created asymmetric information is transferred from the midline to the lLPM to run the left-determining program.

Gap junctions are involved in the early creation of asymmetry

One way for epithelia to propagate signals is by means of cytoplasmic coupling via gap junctional complexes. Gap junctions (GJs) allow the intercellular passage of small molecules like ions, nucleotides and second messengers up to a molecular weight of 1.2kD. GJs are constructed by linking of the membrane-spanning connexons of two cells; connexons being hexameric assemblies made up from connexin (Cx) proteins. Gap junctional communication (GJC) is essential for many patterning processes in embryos, such as for the chick limb bud (Makarenkova et al., 1997; Makarenkova and Patel, 1999), for morphogenesis of the heart (Ewart et al.,

1997; Ya et al., 1998) as well as for left-right axis determination (Levin and Mercola, 1998; Levin and Mercola, 1999). In human patients, regulatory mutations in Cx43 have been reported to result in laterality disorders (Britz-Cunningham et al., 1995). In *Xenopus* and chick GJs are actually involved in left-right asymmetry creation, yet an early role for GJC has been proposed which precedes the formation of midline mesoderm and the function of cilia on the PNC/KV/GRP (Levin and Mercola, 1998; Levin and Mercola, 1999).

In the 8-16-cell-stage *Xenopus* embryo, all blastomeres were connected via GJs. However, cells were disconnected ventrally as the ventral gap junctions were regulated to be closed (Levin and Mercola, 1998). Application of drugs as well as misexpression of connexins, both inhibiting GJC, resulted in organ heterotaxia and loss of leftsided marker-gene expression. Treatments were most effective when applied to embryos between stage 5 and stage 12, which is prior to neural plate formation and hence prior to asymmetric gene expression in *Xenopus* (Levin and Mercola, 1998). The circumferential contiguity of cells together with the ventral isolation provide a system in which molecules can be transported between the left and right side of the embryo.

Although the embryonic anatomy of the chick embryo is very different from frog, GJs function upstream of asymmetric gene expression in the chick as well (Levin and Mercola, 1999). *Cx43* was circumferentially expressed in the epiblast of stage 2-3 chick embryos but was absent from the primitive streak and node (Levin and Mercola, 1999). Interfering with GJC in the chick by either pharmacologically blocking GJs, by downregulating GJ transcription or by disconnecting left and right sides microsurgically, led to a loss of asymmetric gene expression in Hensen's node and a mostly bilateral expression of *Nodal* in the LPM (Levin and Mercola, 1999). Levin and Mercola therefore proposed that GJC throughout the blastodisc of chick is needed during streak stages where it might be involved in asymmetric patterning of the node. The morphological asymmetry of the node is later on translated into a molecular asymmetry which is essential for the left-sided initiation of *Nodal* in the lateral plate (Levin et al., 1995). In mammals, however, there is no asymmetry of the node, yet GJs are involved in the establishment of organ asymmetry (Britz-Cunningham et al.,

1995). GJC may thus be required for events taking place after node formation. It has been proposed that the fibroblast growth factor FGF8 might act directly in a gap-junction based vectorial transfer of LR-relevant signals from the midline to the lateral plate (Fischer et al., 2002). FGF-signaling interacts with GJs in several processes during development. In chick lens cultures, it controls the opening status of GJs and enhances GJC (Le and Musil, 2001), whereas in chick limb bud cultures, application of FGF4/8 enhances the expression of the gap junction gene Cx43 (Makarenkova et al., 1997). Additionally, down-regulation of Cx43 protein level by introduction of antisense oligonucleotides reduces the expression of FGF4/8 in the limb bud (Makarenkova and Patel, 1999). These experiments suggested a feedback loop between FGF and signaling mediated by Cx43.

The role of FGF8 in left-right asymmetry

FGF8 is a secreted growth factor which plays important roles in many processes of embryonic development. The transduction of FGF8 signaling is initiated by binding of the growth factor to the FGF receptor 1 (FGFR1), a receptor-tyrosine-kinase. In many systems, the FGF8 signal is then transduced via the Ras-MAPK/ERK pathway, resulting in cell type- and context-specific responses like proliferation or differentiation . FGF8 is a central determinant for left-right asymmetry with diverging roles reported in different model systems. In mouse, FGF8 induces *Nodal* expression in the left lateral plate (Meyers and Martin, 1999), whereas in chick, FGF8 acts as a right determinant in the setup of LR-asymmetry by suppressing activation of the Nodal Cascade on the right side (Boettger et al., 1999). In a previous study using the rabbit embryo as a model system for typical mammalian development (Fischer et al., 2002), the function of FGF8 in laterality determination has been investigated. In the rabbit, FGF8 acts as a right determinant which blocks *Nodal* transcription in the right LPM *in vivo*. Inhibition of FGF signaling on the right side leads to ectopic activation of the Nodal cascade in the right LPM. Additionally, beads soaked in recombinant FGF8

protein placed on the left side next to the PNC could inhibit the expression of *Nodal* and its targets on the left side (Fischer et al., 2002).

In the midline, transcripts of *Fgf8* are not only found in the primitive streak during gastrulation, but expression extends into the node and PNC during the phase of cilia-driven fluid flow (Fischer et al., 2002; Sirbu and Duester, 2006). Inferred from these experimental and expression data, FGF8 might be involved in regulating the transfer of signals from the midline to the LPM. As indicated above, this could be accomplished by regulating GJC in the periphery of the node and PNC and would also present a potential link between cilia-driven leftward fluid flow at the midline and GJC.

Aim of this work

The initial aim of this Ph. D. thesis was to utilize the specific advantages of the rabbit embryo, i.e. the organization into the archetypical flat blastodisc and the availability of manipulative techniques and embryo culture, to assess the two conflicting hypothesis of symmetry breakage, the so-called ‚nodal flow' and ‚ion flux' models. As the prerequisite for the latter model, namely asymmetric voltage and/or pH-gradients were not found in rabbit embryos, the focus shifted early on to a) characterization of cilia at the site of ciliary flow (PNC), and b) analysis of the transfer mechanism from the PNC to the left side. Specific questions addressed in this thesis involved:

1. How is the genetic program of PNC ciliation configured?
2. What is the ultrastructure of PNC cilia?
3. Does PNC morphogenesis correlate with cilia-driven fluid flow?
4. Is the epithelial organization of the blastodisc (GJC) involved in signal transfer from the midline to the periphery?
5. How is the repressive activity of the growth factor FGF8 mediated asymmetrically?

Results

Cilia on the notochordal plate of the rabbit

Cilia on the rabbit PNC are functionally homologous to those found in mouse, as they set up a leftward-directed fluid flow during early somite stages (Okada et al., 2005). To investigate whether rabbit cilia are also moleculary and structurally similar to those of mouse, a study on the PNC and notochord was performed in which ciliary gene expression, the morphology of the notochordal plate and its ciliated cells as well as ciliary ultrastructure were analyzed.

Ciliary gene expression initiates in Hensen's node and persists in the nascent notochordal plate of the rabbit neurula embryo

In order to molecularly characterize PNC cilia in rabbit a marker gene analysis with fragments of five ciliary genes (see *Supplementary Data*) cloned by RT-PCR was performed. Expression patterns were analyzed by whole-mount in situ hybridization of defined embryonic stages (see *Introduction* section). Two transcription factors involved in the control of ciliary gene expression were analyzed. In mouse the Forkhead transcription factor *Foxj1* (formerly known as *HFH-4*) is expressed in cells bearing motile rather than sensory cilia (Blatt et al., 1999; Brody et al., 2000). Interestingly, loss-of-function mutations resulted in absent airway cilia without affecting PNC ciliogenesis, yet LR axis formation was compromised (Brody et al., 2000). In rabbit *Foxj1* was first expressed in Hensen's node at stage 4 (Fig. 2A). From stage 5 to the 2-3 somite stage strong signals persisted in Hensen's node (Fig. 2B-E). A gradient of signal intensities was found in the midline such that signals were

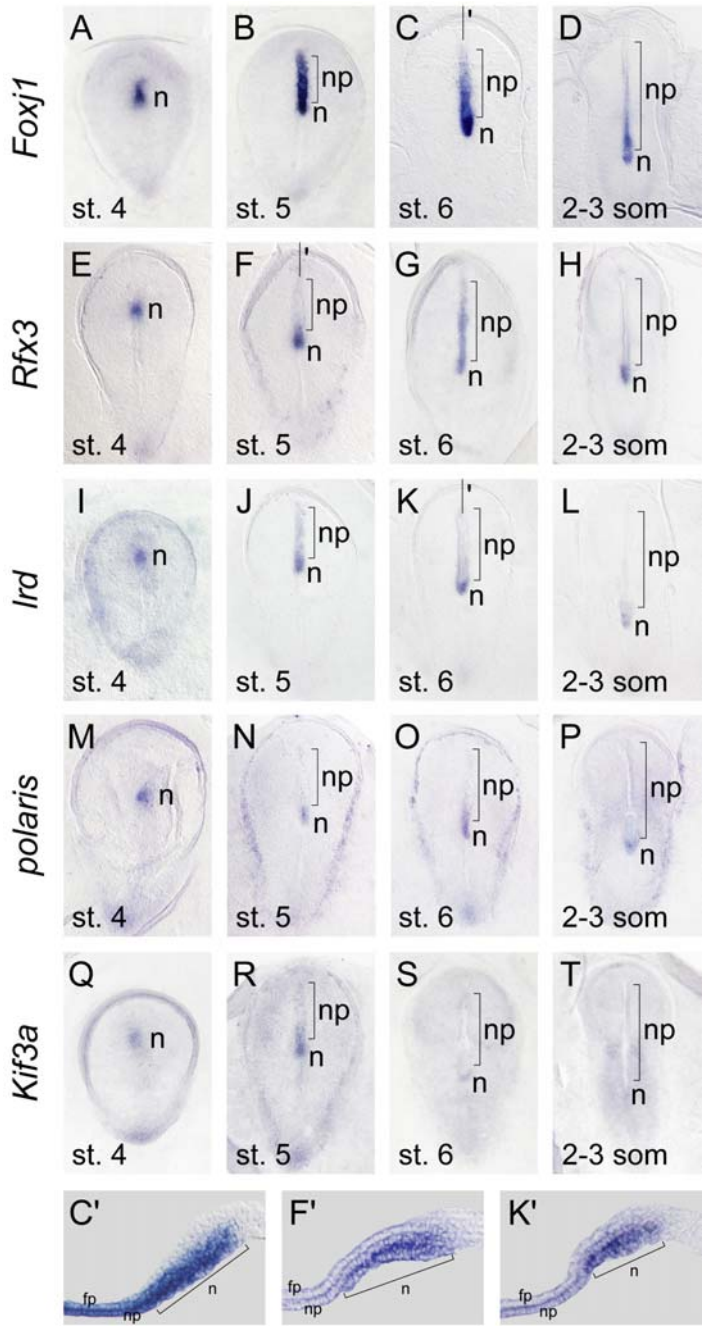

Fig. 2 Expression of ciliary marker genes in the node and notochordal plate of the rabbit embryo. Whole-mount in situ hybridization of rabbit embryos of defined stages using antisense probes specific for the transcription factors *Foxj1* (**A**-**D**) and *Rfx3* (**E**-**H**), the dynein motor protein *Ird* (**I**-**L**), the intraflagellar transport protein *polaris* (**M**-**P**), and the kinesin motor protein *Kif3a* (**Q**-**T**). Specimens are shown in ventral view with anterior to the top. Note that all genes were transcribed in the node (n) from stage (st.) 4 through early somite (som) stages, and more transiently in the notochordal plate (np) at stage 5 (**B**, **F**, **J**, **N**, **R**), and stage 6 (**C**, **G**, **K**, **O**, **S**) with consistently stronger signals in the posterior notochordal plate. Sagittal midline sections through specimens in (**C**), (**F**) and (**K**) demonstrate specificity of expression in the ventral part of the node and in the notochordal plate (**C**', **F**', **K**'), and lack of signals in the overlying floor plate (fp) in **F**' and **K**'.

strongest close to the node and getting weaker towards the anterior end (Fig. 2B-E). A sagittal section of the embryo in (C) identified strong signals in the ventral layers of Hensen's node and in the notochordal plate, whereas transcripts in the floor plate were significantly weaker (Fig. 2C'). Members of the Regulatory Factor X (RFX) family of winged-helix transcription factors regulate ciliogenesis in nematodes, insects and vertebrates (Swoboda et al., 2000; Dubruille et al., 2002; Bonnafe et al., 2004). A gene knockout of *Rfx3* in the mouse resulted - among others - in stunted PNC cilia and laterality defects (Bonnafe et al., 2004). Expression of rabbit *Rfx3* (Fig. 2E-H) was overall weaker but showed very similar characteristics to that of *Foxj1* (cf. Fig. 2A-D). Signals in Hensen's node were much stronger ventrally, i.e. in cells from which the notochordal plate emerges, although no notable difference of transcript levels between floor plate and notochordal plate were discernable (Fig. 2F'). Additionally, very transient expression was found for both genes in the first cells leaving the node, namely the prechordal mesodermal cells, which will form the prechordal plate anterior of the notochord from the 4 somite stage onwards (not shown).

Next the expression of the axonemal marker gene *lrd* was investigated. This gene encodes an axonemal dynein, which is required for PNC cilia motility in mouse (Supp et al., 1997; Okada et al., 2005). The *iv* mouse mutant defective in LRD function displays randomization of LR marker genes and organ placement (Supp et al., 1997). Rabbit *lrd* was expressed in Hensen's node, starting at stage 4 and becoming down-regulated at the 3 somite stage (Fig. 2I-L). Similar to *Foxj1* and *Rfx3*, *lrd* was expressed in the midline in a graded manner along the rostro-caudal axis (Fig. 2J, K). Signals were found in the ventral node and the notochordal plate with very low levels in the overlying floor plate (Fig. 2K'). The two IFT genes analyzed in this study, *polaris* (Fig. 2M-P) and *Kif3a* (Fig. 2Q-T) were only weakly expressed in node and notochordal plate. Particularly the notochordal plate expression was very transiently observed around stage 5 and 6 (Fig. 2N, O, R, S). The lack of signals for *lrd*, *polaris* and *Kif3a* in cells of the prechordal mesoderm, which were positive for *Rfx3* and *Foxj1*, may be a reflection of the overall much weaker expression levels of the axonemal and IFT genes compared to the transcription factors analyzed in this study.

Taken together the marker analysis showed that transcription of genes which are functionally required for PNC cilia in mouse was initiated in Hensen's node when the node first formed at stage 4, and that transcripts had short half-lives as their levels readily declined once cells moved out of the node into the forming notochordal plate and floor plate.

Development of the notochordal plate in the rabbit

The expression of marker genes indicated that ciliated cells could be expected from stage 4 onwards on Hensen's node, and slightly later on the prechordal mesoderm, the notochordal plate and the PNC. It was previously shown by TEM analysis and immunohistochemistry that Hensen's node and the notochordal process are covered by hypoblast initially, which during the following stages progressively becomes replaced by definitive endodermal cells originating from the node such that at stage 5 single endodermal cells appear interspersed among hypoblast cells, and by stage 6 a rim of definitive endodermal cells a few cells wide borders the notochordal plate on either side (Christoph Viebahn, personal communication). Cilia only appear after the presumptive notochordal cells emerge as notochordal plate during stage 5 of development (Blum et al., 2006). Therefore the early phase of notochord development was analyzed in osmium stained specimens by light microscopy, which allows for visualization of different tissue thickness and thus differentiation of node and prechordal mesoderm (Fig. 3A-C). Very dynamic morphogenetic processes were recorded in individual specimens from the beginning to the end of stage 5, which lasts about 4-6 hours. The first event was the exit of prechordal mesodermal cells from the node (Fig. 3A), followed by a cranial displacement and thus physical separation from the node through the extension of the notochordal process (Fig. 3B). The notochordal process lengthened to about three times the cranio-caudal dimension of the node (Fig. 3C) before the first cells, now epithelially organizing into the notochordal plate, emerged through the hypoblast/endoderm layer towards the end of stage 5 and became visible in scanning electron micrographs (Fig. 3D-H). The

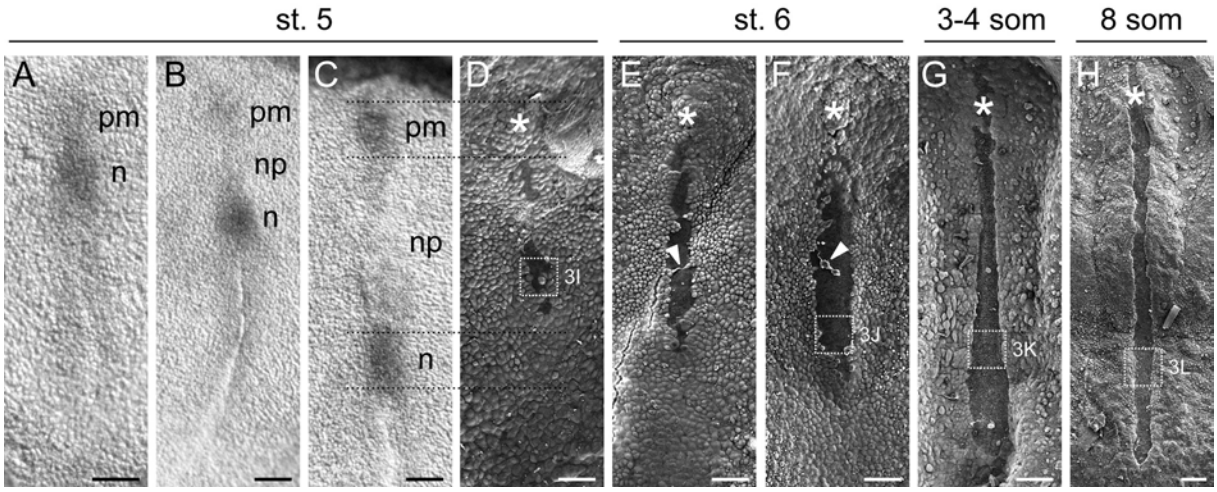

Fig. 3 Development of the notochordal and prechordal plate in the rabbit. Light (**A**-**C**) and scanning electron (**D**-**H**) micrographs of embryos from stage (st.) 5 to the 8 somite (som) stage. Specimens for light microscopy were osmium fixed such that darkness correlated with tissue thickness, and thus, node (n) and prechordal mesoderm (pm) were easily recognizable. During stage 5 successive exit of prechordal mesoderm and notochordal process (np) from the node (**A**, **B**) was followed by lengthening of the notochordal process and gradual emergence from the underlying hypoblast/endoderm (**C**, **D**). Embryos in (**C**) and (**D**) show matching stages, dashed lines indicate levels of node and prechordal mesoderm. (**E**-**H**) Progressive plate-like organization and further lengthening of the notochordal process before (st. 6, **E**, **F**) and during (**G**, **H**) early somitogenesis. Arrowheads indicate hypoblast/endoderm cells adhering to notochordal plate in (**E**, **F**). Asterisks in (**E**, **F**) mark prechordal mesoderm covered by endoderm, and exposed prechordal plate in (**G**, **H**). Note the characteristic widening of the posterior portion of the notochordal plate (PNC) from stage 6 (**E**, **F**) to the 4 somite stage (**G**), which was lost by the 8 somite stage (**H**). Stippled boxes in (**D**) and (**F**-**H**) indicate areas evaluated for polarization of cilia in Fig. 3. Embryos shown in ventral views, anterior to the top. Scale bars: 100µm.

prechordal region, which gradually appeared darker in light microscopy and thus consisted of a growing number of cells (Fig. 3A-C), could be discerned from late stage 5 onwards as a small mound under the hypoblast/endoderm at the anterior end of the notochordal plate (cf. Fig. 3C and Fig. 3D-F, mound indicated by asterisks). From the end of stage 5 to the end of stage 6, the notochordal plate fully emerged, allowing the direct monitoring of notochordal plate and PNC morphogenesis by SEM. First, the hypoblast/endoderm cells continuously receded from the notochordal plate surface in a caudal to cranial fashion (Fig. 3D-F). Occasionally, apparently dying cells - as judged by detachment and a degenerating microvillous coat - remained on the surface (arrowheads in Fig. 3E and F). At late stage 6 the notochordal plate was about 16-18 cells wide in the caudal region (Fig. 3F). At the 3-4 somite stage the

notochordal plate retained its broadened appearance in its caudal part, the PNC, with about 18 cell diameters width, but narrowed to about 10-12 cell diameters from about the level of the first somites to the anterior pole (Fig. 3G). The notochordal plate was completely free of adhering cells by the 3-4 somite stage. Concomitantly, the endodermal cells retracted from the rostral-most part of the ventral midline as well and revealed the surface of the underlying prechordal mesodermal cells, which were organized in an epithelial plate (Fig. 3G, H). The widening of the PNC was no longer seen at the 8 somite stage, when the notochordal plate had remarkably narrowed and comprised only about 5 cell diameters (Fig. 3H). In summary the analysis showed that the ventral midline epithelia undergo dynamic morphogenetic changes with the PNC as a clearly discernable but very transient structure.

Cilia lengthen and polarize during notochordal plate development

The first cilia appeared in late stage 5 embryos in which patches of notochordal cells could just be seen through gaps in the hypoblast/endoderm layer (Fig. 3D, Fig 4A, E). Cilia were stunted (Fig. 4E) with a mean length of 1.5µm. At that stage many cells still lacked cilia (indicated by asterisks in Fig. 4A and red dots in Fig. 4I). By the end of stage 6 cilia had not significantly lengthened, but most cells then carried a monocilium (Fig. 4B, F, J-L). Cilia extended to a length of about 3µm at the 3 somite stage (Fig. 4G) and reached their maximal length of about 5µm at the 5 somite stage (not shown). No significant differences in length were recorded at the 8 somite stage (Fig. 4H). At the 3-4 somite stage ciliary rudiments could also be seen on the prechordal mesodermal cells, which had surfaced from the endoderm (Fig. 4C). Prechordal cilia obviously continued to grow (Fig. 4D), however, patches with bald cells and shortened cilia were observed in the very same area as well (indicated by asterisks in Fig. 4D). Concomitant with lengthening the positioning of cilia on the apical cell surface changed from an initially central to a posterior localization (Fig. 4E, F, I-L). While at stage 5 about 70% of cilia were centrally oriented (Fig. 4I), 55% of cilia analyzed were posteriorly displaced at stage 6, further increasing to 81% at the

3-4 somite stage. In addition regional differences were observed such that cilia in immediate proximity to the node were generally shorter and more centrally organized, while cells displaced cranially showed longer and posteriorized cilia (not shown). Taken together, dynamic changes in ciliary length and polarization at the PNC and the notochordal plate were observed during neurula stages in the rabbit.

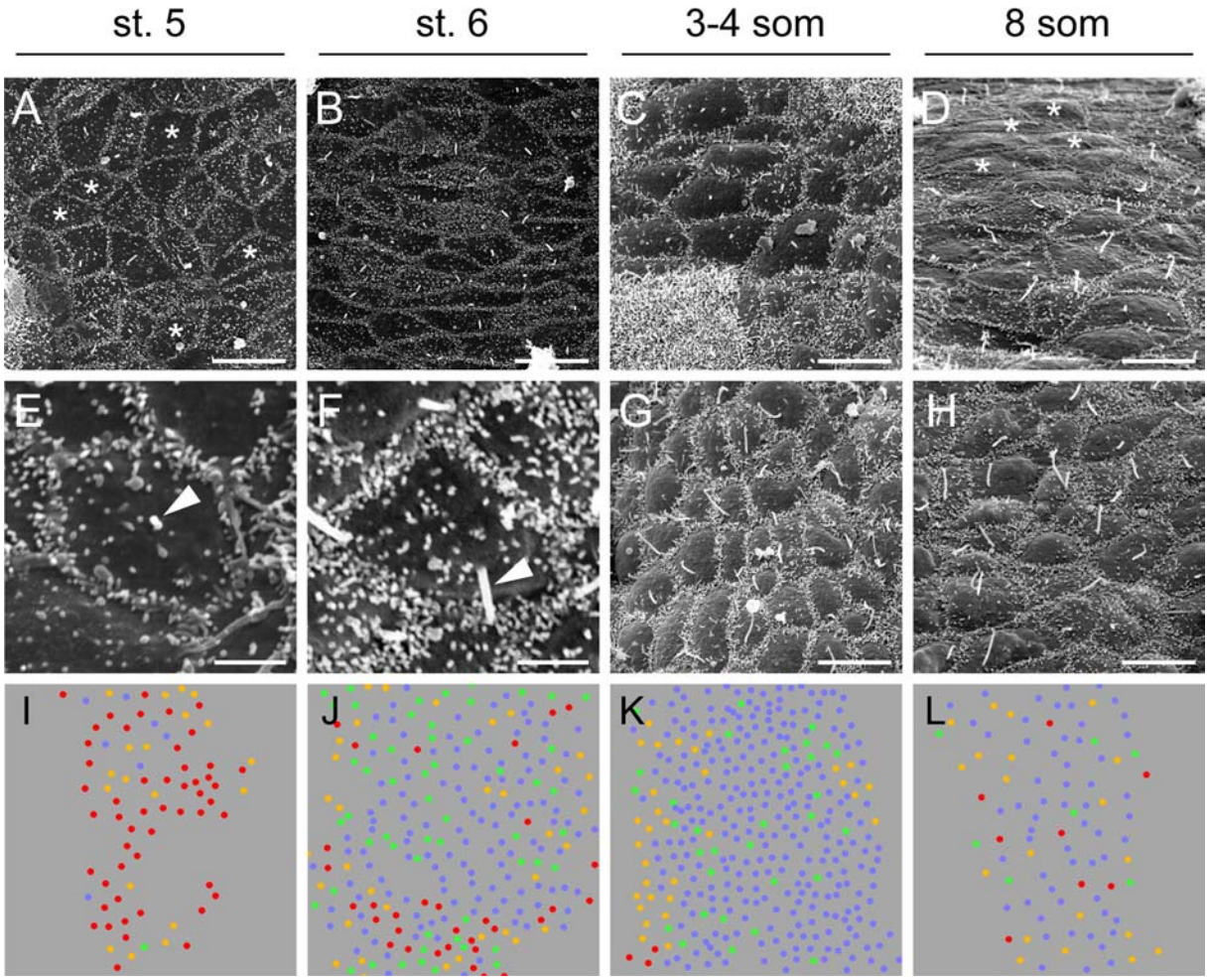

Fig. 4 Notochordal monocilia lengthen and polarize from stage 5 to early somitogenesis. (**A**-**H**) Scanning electron microscopy of ciliated cells at stage (st.) 5 (**A**, **E**), stage 6 (**B**, **F**), 3-4 somites (som; **C**, **G**) and 8 somites (**D**, **H**) in the notochordal (**A**, **B**, **E**-**H**) and prechordal (**C**, **D**) plate. (**I**-**L**) Position of ciliary base relative to the cell surface, which changed from a predominantly central (**I**) to a mostly posterior localization (**J**-**L**). Cells lacking cilia indicated by red dots, posterior cilia by blue, central cilia by yellow, and cilia with unclear insertion by green dots. Note that at stage 5 many cells lacked ciliary protrusions (asterisks in **A**), while from stage 6 onwards almost all cells were monociliated. Scale bars in (**A**-**D**, **G**, **H**) represent 10µm, in (**E**, **F**) 2µm.

A novel 9+4 axoneme revealed by ultrastructural analysis of notochordal cilia

PNC (“node”) cilia in the mouse lack the central pair microtubules (Sulik et al., 1994), while cilia of the homologous Kupffer’s vesicle in zebrafish display axonemes of the 9+2 type (Kramer-Zucker et al., 2005). In order to investigate the PNC axonemes in rabbit an ultrastructural TEM analysis was performed. Surprisingly, three types of monocilia were detected on notochordal plate cells, 9+0 axonemes as in mouse (Fig. 5A), cilia with a CP of the 9+2 type similar to zebrafish (Fig. 5B), and a novel cilium consisting of 9 outer doublet and 4 inner singlet microtubules (Fig. 5D-F). The central microtubules of the 9+4 cilium were in most cases arranged in a four-leaf clover fashion (Fig. 5D, E). Occasionally, an apparent 2 x 2 arrangement was observed, which indicated an underlying organization of two central microtubule pairs (dashed circles in Fig. 5F). Asymmetric projections emanating from the central microtubules could be distinguished in much the same way as in 9+2 cilia (black arrowheads in Fig. 5B, D, E). Dynein arms attached to the A-microtubule were found in each type of cilium (white arrowheads in Fig. 5A, B, D). In some cases the tri-branched structure of the outer arm was apparent (white arrowhead in Fig. 5B). The CP of the 9+2 and the 9+4 cilia as well as the absence of a CP in the 9+0 cilia seemed to persist throughout the length of the cilium, as transverse sections at the proximal end of the cilium, indicated by a tight arrangement of the outer microtubule doublets and extracellular matrix around the cilium shaft, showed the three different CP states (Fig. 5G-I). The basal bodies were normal as judged by the individual triplet microtubule structure and the perpendicular arrangement of the mother and daughter centriole to each other (Fig. 5C).

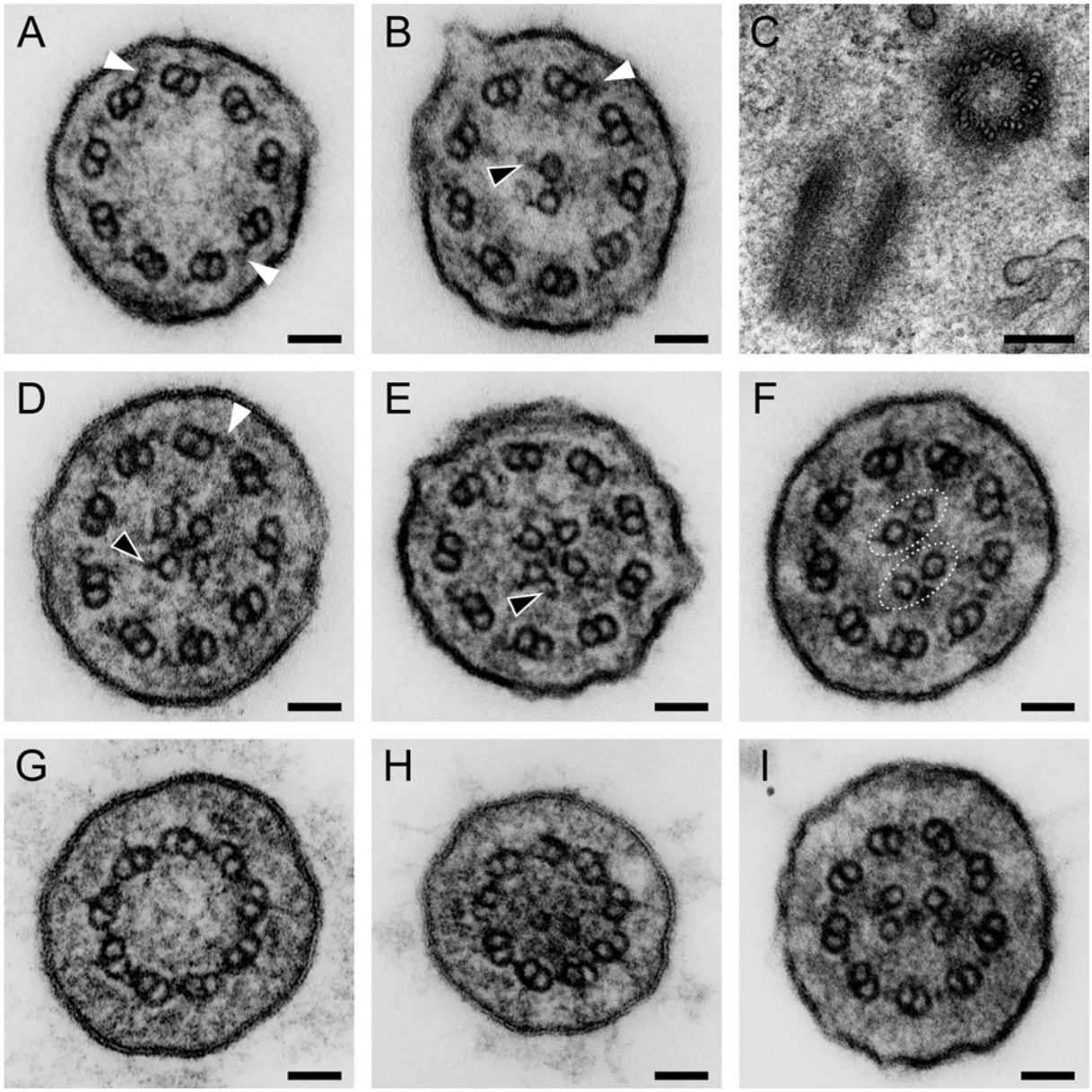

Fig. 5 Three types of axonemes on notochordal plate cells in the rabbit. Transmission electron microscopy of cross sections through notochordal cilia. (**A**) Monocilium of the 9+0 type. (**B**) Monocilium of the 9+2 type. (**C**) Basal body consisting of 9 microtubule triplets. (**D**-**F**) Characteristic examples of a new cilium type consisting of 9 outer doublets and 4 inner singlets. Note that all outer doublets possessed dynein arms (representative examples highlighted by white arrowheads), the tri-branched structure of which is apparent in (**B**), and that central microtubules showed typical protrusions (examples indicated by black arrowheads). Note also that the four inner singlets were arranged in two groups of two singlets each (indicted by dashed circles in **F**). (**G**-**I**) Proximal sections of 9+0 (**G**), 9+2 (**H**) and 9+4 (**I**) cilia demonstrating continuity of central apparatus to base of cilium. Scale bars represent 50µm in (**A**, **B**, **D**-**I**) and 200µm in (**C**).

Intermingled but uneven distribution of the three types of axonemes along the notochordal plate

To investigate whether the three different cilia types might be allocated to distinct domains of the notochordal plate, TEM samples were prepared from embryos dissected into three fragments containing the cranial notochordal domain (anterior fragment), a medial fragment covering the posterior aspect of the narrowed notochordal plate as well as the anterior part of the PNC, and a posterior fragment which contained the PNC region immediately cranial to Hensen's node (Fig. 6). In total 357 axonemal structures could be determined with certainty out of more than 800 cross sections examined. Evaluation of sections revealed that the three cilia

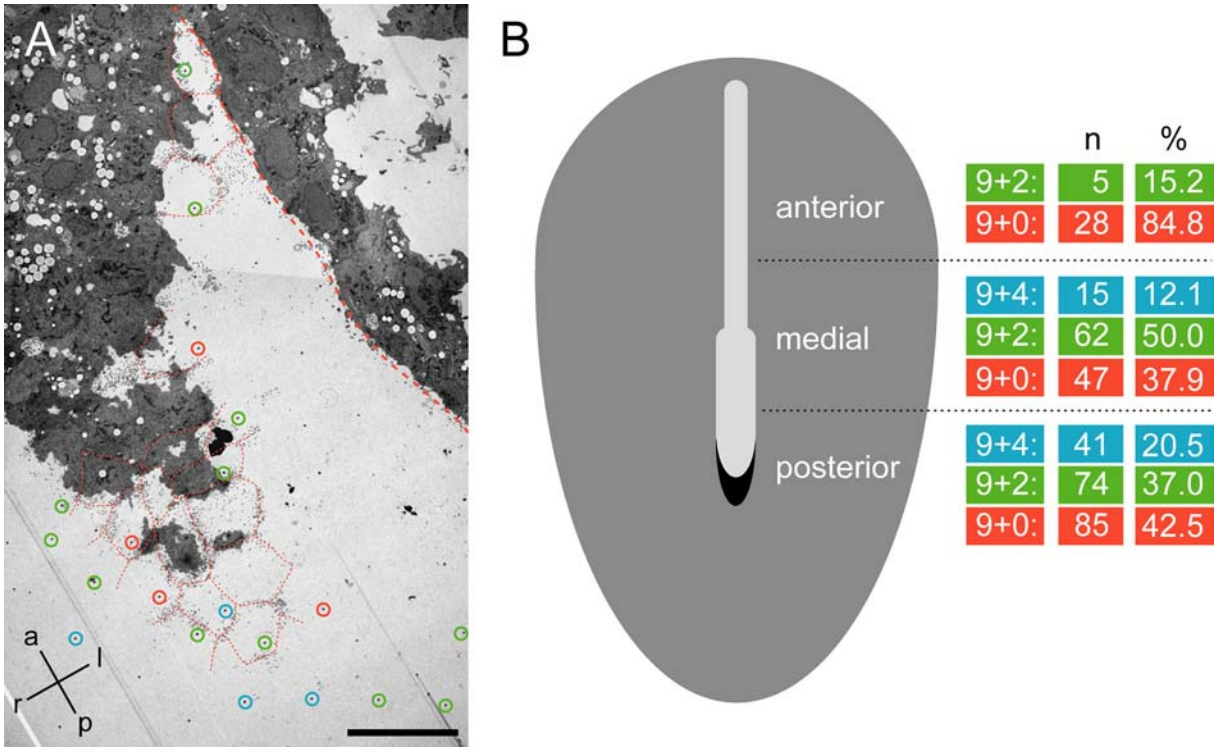

Fig. 6 Intermingled but uneven distribution of different cilia-types along the notochordal plate. (**A**) Overview of an ultrathin section in the plane of the notochordal plate at the transition between wide and narrow regions of a stage 6 embryo. Cell boundaries are outlined for clarity where possible (red stippled lines), and cilia types, identified at high magnification, are color-coded (red: 9+0; green: 9+2; blue: 9+4). Red dashed line marks lateral boundary of notochordal plate. Scale bar represents 10µm. (**B**) Schematic representation of an idealized stage 6 - early somite embryo. Hensen's node is indicated in black, the notochordal plate in light grey. The approximate levels of dissections into anterior, medial and posterior fragments are indicated, and the absolute and relative numbers of observed cilia types are shown.

types occurred intermingled in a salt-and-pepper like distribution (Fig. 6A). However, the relative abundance of axonemes along the notochordal plate apparently changed in a caudal to rostral fashion: 9+4 cilia were exclusively found in the posterior and middle fragment of the notochordal plate (Fig. 6B), roughly corresponding to its posterior widening, i.e. the PNC. Remarkably, axonemes of the 9+0 type were the predominant species found in anterior fragments, while the proportion of 9+2 cilia, though almost absent from the anterior fragment, was not significantly different in the posterior and middle fragment. Taken together these data suggest that the ciliogenic gene program which acts at the PNC is highly conserved and initiated in the organizer, but that axonemal structures vary between the vertebrates with - most notably - a novel cilium in the rabbit.

Analysis of ciliation in the pig embryo

The finding of three different types of cilia including a novel 9+4 axoneme on the notochordal plate of the rabbit was unexpected, as monocilia on the PNC of the mouse, the only other mammal examined up to now, all lack a central apparatus. As the mouse embryonic egg cylinder is uncommon for mammalian development it might well be that anatomic divergence is also reflected in certain morphological differences. It was thus examined whether another archetypic mammal, the pig, has different types of cilia as well. Pig embryos from timed matings were harvested from uteri and prepared for in-situ hybridization, immunohistochemistry (IHC) as well as for transmission electron microscopy. As described above, the PNC in mouse and rabbit harbors cilia and is the site of cilia-driven leftward fluid flow. This special ciliated entity is marked in its rostro-caudal extension by the paranotochordal expression domain of *Nodal*. The localization of this domain was thus used to track down the PNC in the pig. A gene fragment of pig *Nodal* (see *Supplementary Data*) was cloned by PCR from genomic DNA and gene expression was assessed using whole-mount

in situ hybridization. *Nodal* expression bordered the posterior notochord unilaterally on the left side in embryos equivalent to stage 6 rabbit embryos (Fig. 7A). As revealed in cross-sections, *Nodal* transcripts were found in the lateral-most cells of the notochord marking the transition towards the endodermal cell layer (Fig. 7A'). The histological analysis of different stages of notochord development (stages equivalent to stage 5, 6 and somite stages in the rabbit) showed that the notochord was always multilayered and covered ventrally by cells in continuity with the endoderm (not shown). An antisense probe against *Foxj1*, a ciliary marker gene which was found in the node and notochordal cells in st.5 rabbit embryos (cf. Fig. 2B), marked the node of pig embryos at the equivalent stages (Fig. 7B). The staining demonstrated that the transition from the primitive streak to the node and notochord of the pig embryo was slightly asymmetric. The indentation of the primitive pit could be discerned in sagittal sections (Fig. 7B'). In whole-mount views a displacement of the pit to the left side was apparent (Fig. 7B and inset in Fig. 7B). The boundary of the node reached more posterior on the right side of the primitive pit than on the left side (indicated by arrowhead in inset in Fig. 7B). This asymmetry was not seen in embryos older than stage 5 (Fig. 7A). IHC using a monoclonal antibody directed against acetylated tubulin revealed monocilia on endodermal cells all over the ventral surface of notochord stage pig embryos which were equivalent to stage 5-6 rabbit embryos (Fig. 7C). However, those cilia were extremely short and not detected on every single cell. In confocal optical sections through the embryos the notochord appeared as a solid rod of tightly packed cells covered ventrally by endoderm and clearly delimited from the mesoderm laterally. Within the notochord only few signs of mitosis were detected as judged by the presence of mitotic spindles (Fig. 7D). Probably due to their small size and low abundance as seen in the anti-tubulin stained specimens, no cross sections of cilia on endodermal cells were detected on ultrathin sections prepared for TEM. In summary these data show that despite a conserved archetypic mammalian embryonic architecture in the pig, asymmetry of the node, mode of notochord formation as well as unilateral appearance of *Nodal* at the PNC suggest that in the pig a mechanism of LR asymmetry formation acts which is comparable to that found in chick embryos.

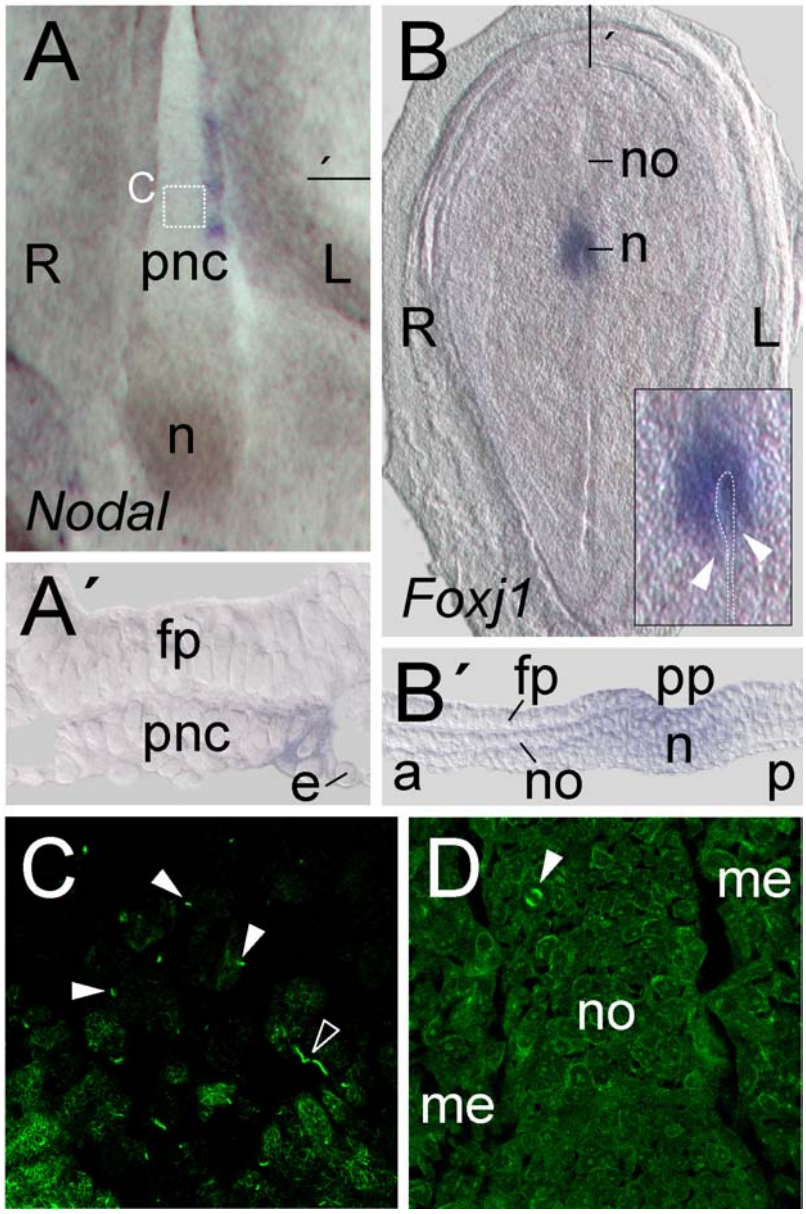

Fig. 7 Analysis of node, notochord and cilia in the pig embryo. Whole-mount in situ hybridization (**A**, **A**', **B**, **B**') and immunohistochemistry (**C**, **D**) were used to localize ciliated structures. (**A**) An antisense probe specific for the pig *Nodal* gene marked the left (L) margin of the posterior notochord (pnc) continuous with the node (n) in a stage 6 embryo. (**A**') Cross-section through specimen shown in (**A**) revealed *Nodal* transcripts in cells at the transition from posterior notochord to endoderm (e). (**B**) and inset in (**B**): An antisense probe specific for rabbit *Foxj1* marked the node of a stage 5 pig embryo. At that stage, an asymmetry of the node was apparent as seen by a leftward shift of the primitive pit (pp, indicated by stippled white line). Note that staining reached more posterior on the right (R) side of the node (indicated by arrowheads). (**B**') A sagittal section of specimen in (**B**) showed *Foxj1*-positive cells in the bulk of the node as well as in the presumptive floor plate (fp) and notochord (no). (**C**) Confocal images of anti-acteylated tubulin staining showed cilia (white arrowheads) and midbodies (outlined arrowhead) on endodermal cells above the posterior notochord (approximate region indicated by stippled box in **A**). (**D**) A confocal section in the plane of the embryo revealed the notochord as a solid rod distinct from the surrounding mesoderm (me). Arrowhead indicating a mitotic spindle. Embryos are shown in ventral view with anterior to the top, a: anterior, p: posterior.

Gap junctions and the transfer of laterality cues

In the following part of this thesis work it was tested whether gap junctional communication (GJC) is necessary for the transfer of LR asymmetry cues in the rabbit blastodisc and how fibroblast growth factor 8 (FGF8) cooperates with a potential gap-junction (GJ) -based mechanism.

Cx43 is expressed during LR relevant stages in the rabbit embryo

Cx43 encodes a protein belonging to the family of connexins which constitute the subunits of gap junctional complexes. *Cx43* has been described in the chick embryo, where it is circumferentially expressed in the blastodisc but transcripts are absent from the primitive streak (Levin and Mercola, 1999). The expression of *Cx43* was analyzed in rabbit gastrula and neurula stage embryo using in situ hybridization to determine whether a gap-junction-based mechanism might operate during stages which are relevant for LR asymmetry determination in the rabbit embryo.

At stage 4b, when Hensen's node was discernible as a marked thickening at the anterior end of the primitive streak, *Cx43* was expressed circumferentially in the rabbit blastodisc (Fig. 8A). Expression was very pronounced in the epiblast rostral and lateral of Hensen's node (Fig. 8A and 8A'), weaker but continuous caudally and nearly absent from Hensen's node itself. During the elongation of the notochordal process at stage 5 (Fig. 8B), *Cx43* expression was continuous anteriorly and became stronger in the vicinity of the primitive streak yet leaving the node almost free of transcripts. During stage 6 (Fig. 8C), when the notochordal process epithelialized and displaced the endoderm ventrally, a marked regionalization of *Cx43* in the ectoderm became apparent: the highest level of expression was detected in the future head neuroectoderm, whereas the ectodermal layer above the somitogenic mesoderm showed the lowest transcript level. In views of whole-mount embryos from stage 6 to the 3 somite stage (Fig. 8C-F) the midline mesoderm appeared almost free of

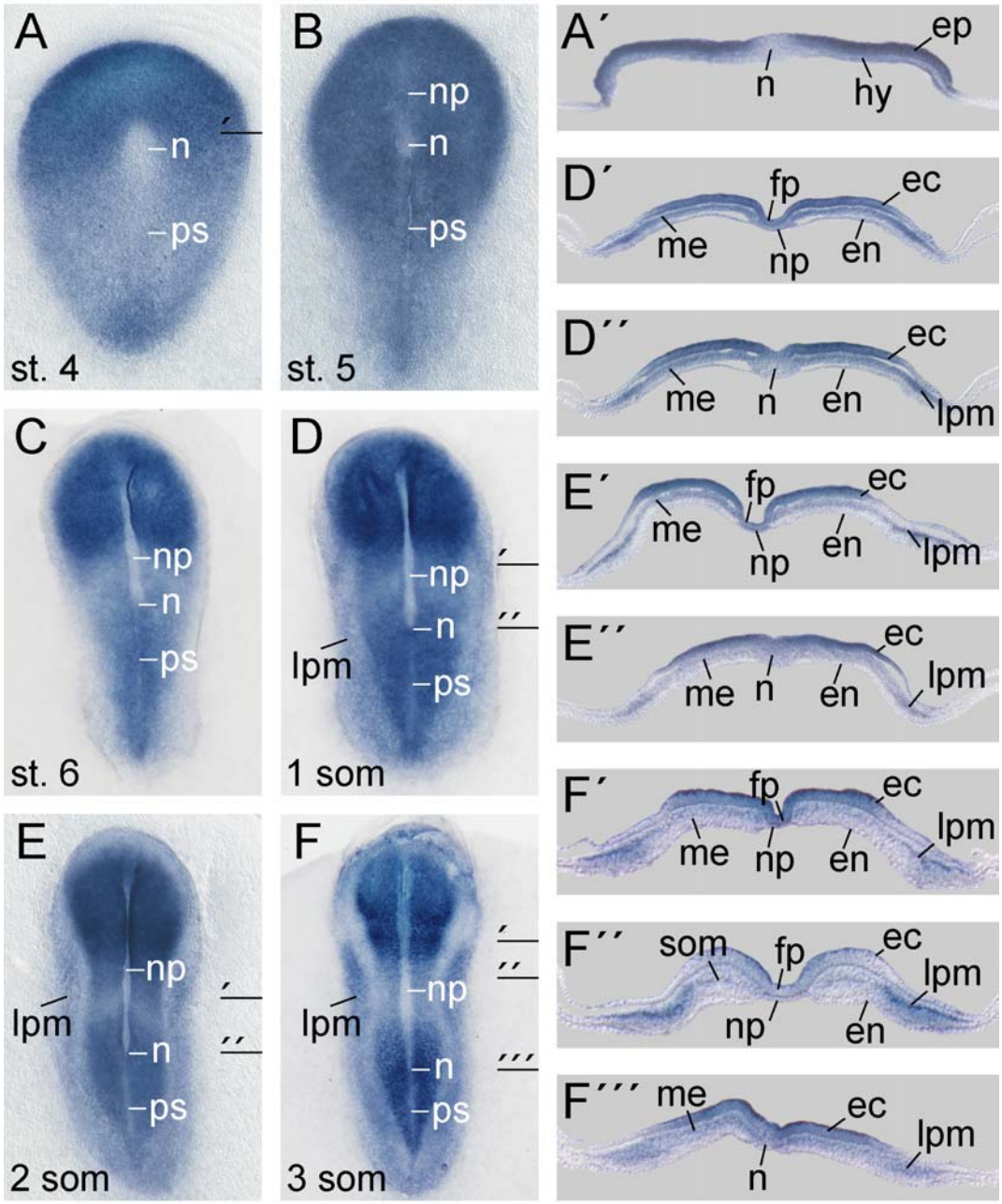

Fig. 8 Expression of *Cx43* in rabbit gastrula and neurula stage embryos. Whole-mount in situ hybridization of rabbit embryos of defined stages with an antisense probe specific for the gap junction gene *Cx43*. In stage (st.) 4 (**A**, **A**') the node was free of expression. *Cx43* transcripts were found in the epiblast (ep) at stage 4 (**A**, **A**') and in the ectoderm (ec) at later stages (**B**-**F**, **D**'-**F**'''). After the notochordal process (np in **B**) epithelialized into the notochordal plate (np in **C**, **D**, **D**', **F**', **F**'') the bilaminar midline mesoderm consisting of floorplate (fp) and notochordal plate appeared as a light strip in whole-mount embryos (**C**-**F**) and expressed *Cx43* (**D**', **E**', **F**', **F**''). From stage 6 onwards, the primitive streak (ps) was discernible as a light strip as well (**C**-**F**). Note that beginning with the 1 somite (som) stage, mesoderm (me) expression (**D**'-**F**''') became regionalized in the lateral plate mesoderm (lpm, **D**-**F** and **D**''-**F**'''). At the 3 somite stage, the condensed somites were almost free of expression (**F**''). *Cx43* transcripts were found in the hypoblast (hy, **A**') whereas the definitive endoderm (en, **D**'-**F**''') was almost free of expression. Embryos are shown in ventral views with anterior to the top.

expression. Sections (D', E', F', F'') revealed that this was mostly due to the thin bilaminar arrangement of notochordal plate and floor plate which made the midline mesoderm half-translucent. The midline cells showed *Cx43* transcription as well, although at a lower level as compared to the ectoderm. The paraxial and intermediate mesoderm which connect midline and lateral plate mesoderm (LPM) consist of loosely arranged cells which also expressed *Cx43* (Fig. 8D', D'', E', E''). This expression markedly declined at the 3 somite stage (Fig. 8F', F'') and was especially down-regulated in the condensed somitic mesoderm (Fig. 8F''). Between the 1 and 3 somite stage the endoderm did not express *Cx43* (Fig. 8E', E'') or showed expression at very low levels only (Fig. 8D', D''). A new domain of *Cx43* expression was evident from the 1 somite stage onwards, when cells of the LPM on both sides of the embryos became positive for *Cx43* transcripts. At the 1 somite stage this expression was broad throughout the LPM (Fig. 8D, D', D''), but it became more regionalized and pronounced during the 2 somite stage (Fig. 8E, E', E''). At the 3 somite stage, along with the condensation of somitic mesoderm and neurulation processes, the embryo adopted a curved and waisted appearance. At this stage, the LPM at the level of the presomitic and somitic mesoderm showed the most pronounced expression (Fig. 8F, F''). *Cx43* expression thus indicates that epithelial cells of the rabbit blastodisc, which might be involved in the transfer and spreading of LR cues, are coupled via GJs.

No asymmetries in pH or membrane potential in the early blastodisc

In the chick blastodisc, where *Cx43* is circumferentially expressed, cells in front of the primitive streak are coupled via GJs, and this coupling has been shown to be essential for the asymmetric patterning of Hensen's node (Levin and Mercola, 1999). Differences regarding pH/membrane potential between the left and right side of the primitive streak have been observed as well (Levin et al., 2002), creating a voltage gradient across the blastodisc. It has been speculated that GJs allow for the

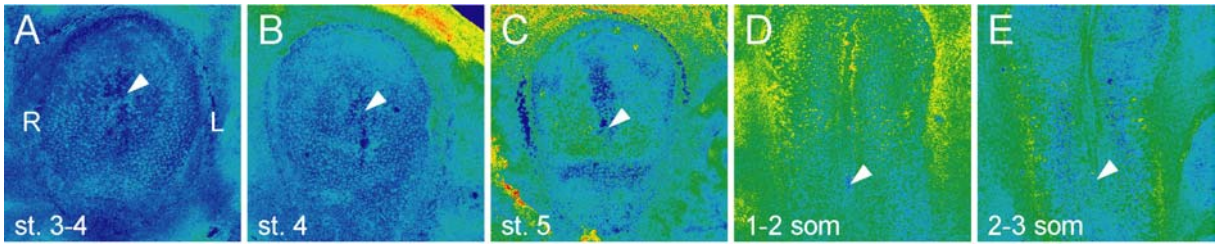

Fig. 9 No left-right asymmetric allocation of pH-values in the rabbit blastodisc. (**A**-**E**) Compiled confocal images of embryos treated with the pH-sensitive dye BCECF-AM. Fluorescence intensity is color-coded with blue representing low intensity and red representing high intensity. White arrowheads indicate the anterior limit of the primitive streak in (**A**) and the level of the node in (**B**-**E**).

dispersal of small molecular weight LR determinants, an intercellular exchange which may be driven by the voltage gradient (Levin et al., 2002).

To test whether a comparable gradient exists in the rabbit blastodisc, embryos were treated with the pH-sensitive fluorescent dye BCECF-AM and fluorescence was monitored using confocal laser scanning microscopy (Fig. 9). Higher fluorescence intensities are represented by yellow and red coloring and indicate more alkaline pH. To reveal a possible pH-based gradient across the rabbit blastodisc, fluorescence intensities between left and right sides of the embryo were compared. Out of a total of 26 embryos from primitive streak to somite stages (Fig. 9A-E) none showed a LR-asymmetric signal. Spots of higher intensity were occasionally detected in non-confocal overviews of embryos, but these were exclusively observed at sites with high cell density (e.g. at the primitive streak, in extraembryonic tissue artificially folded or at Hensen's node) and did not exhibit stronger fluorescence when examined confocally. However, overall fluorescence intensity increased from stage 3 to the 3 somite stage. These results suggest that pH in the rabbit blastodisc becomes more alkaline during gastrulation. However, asymmetric pH/voltage gradients as described in the chick embryo do most likely not exist in the rabbit blastodisc. GJC may thus be required in an alternative process during the process of laterality determination.

GJs mediate FGF8-dependent repression of *Nodal* in the right LPM

Control cultured rabbit embryos show altered expression of marker genes

As a reference for the following treatments of rabbit embryos in culture, untreated embryos were incubated as described in the *Methods* section and assessed for the expression of asymmetric marker genes by in situ hybridization. Control cultures yielded mostly normal morphology as judged by the appearance of axial mesodermal structures, the progression of somitogenesis, the development of the heart anlage and overall shape of the embryo. Apart from morphological landmarks, the paranotochordal expression domain of *Nodal* (see *Introduction* section) was used as an indicator for correct development before the onset of LR signal transfer. This domain is indispensable for the later asymmetric expression of *Nodal* in the LPM (Brennan et al., 2002; Saijoh et al., 2003). As in the following experiments the transfer of LR signals from the midline to the LPM was examined, only those embryos were evaluated which developed normally and showed paranotochordal expression of *Nodal*. Although most embryos developed normally, the control culture resulted in a disturbed expression of asymmetric marker genes as described (Fischer et al., 2002). When embryos were taken into culture at stage 5, 6 or the 1 somite stage (n= 39) and assessed for marker gene expression by in situ hybridization after they had reached the 4-6 somite stage, normal left-sided expression of *Nodal* was found in about 15.4% of cases (n= 6, Fig. 10A, B), however, most embryos expressed *Nodal* bilaterally (53.8%, n= 21, Fig. 10A, D). To a lesser extent, either right-sided expression of *Nodal* was observed (7.7%, n= 3, Fig. 10A, C) or both lateral plates (LPs) lacked *Nodal* transcripts completely (23.1%, n= 9, Fig. 10A, E). Cultured embryos developed normally from the 2 somite stage onwards (n= 11), as 90.9% (n=10) of embryos explanted at this stage developed left-sided marker gene expression and only 9.1% (n= 1) of embryos showed expression in the right LP additional to the normal left-sided domain (Fig. 10A). Embryos that were taken into culture at the 3 somite stage or later (n= 3), when *Nodal* was already established in the LPM, always developed normal left-asymmetric expression (Fig. 10A).

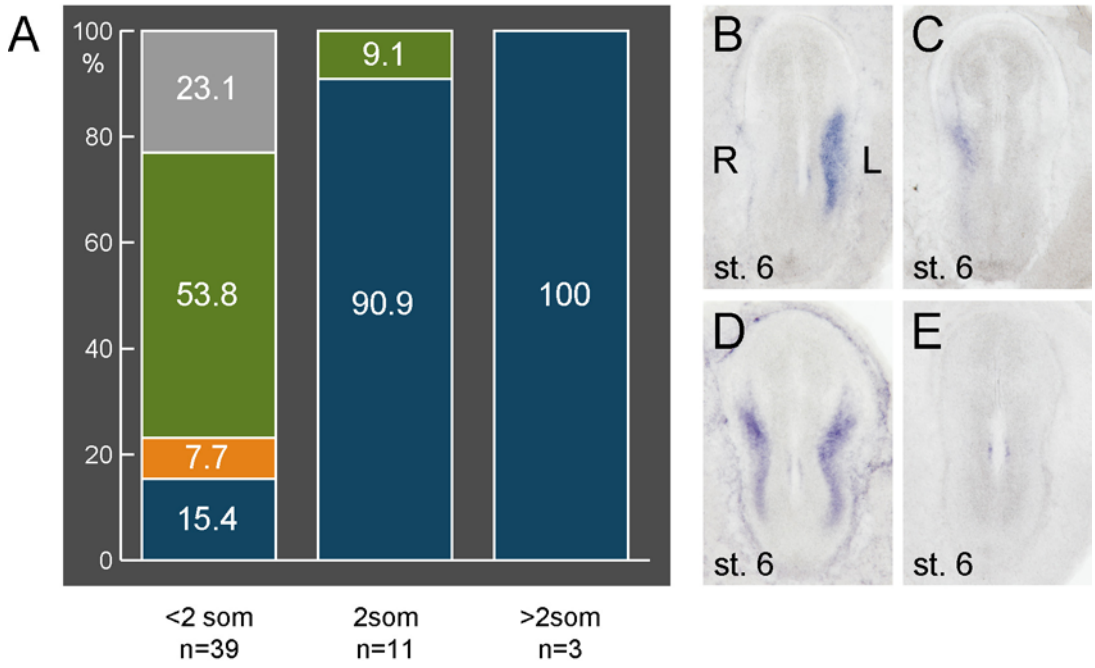

Fig. 10 Untreated control cultures show altered expression of *Nodal* when taken into culture before the 2 somite stage. (**A**) Diagram showing relative number of embryos explanted before, during or after the 2 somite stage with left-sided (blue), right-sided (yellow), bilateral (green) or lack of *Nodal* expression (grey) after *in vitro* culture. (**B**-**E**) Representative examples of embryos explanted at stage 6 with left-sided (**B**), right-sided (**C**), bilateral (**D**) or lack of *Nodal* expression (**E**). Embryos are shown in ventral view with anterior to the top.

The deregulated expression of *Nodal* in untreated control cultures shows that expression of the marker gene is highly variable on either side. Apart from being normally transcribed in the left LPM, *Nodal* was also found (1) bilaterally, cases in which the right LPM expressed the marker gene in addition to the left LPM, or (2) right-sided only, indicating a loss of *Nodal* on the left side and a gain of *Nodal* induction in the right LPM. In some cases, (3) both sides lacked *Nodal* expression, representing the regular fate of the right LPM, but a loss of *Nodal* induction on the left side. In order to unravel the induction processes that take place on either side, *Nodal* expression was evaluated by scoring the left or right side of the embryo separately, a method which reveals incidences of ectopic expression or loss of induction (Fig. 12A). Embryos were thus positive for left-sided expression when they had either left-sided or bilateral *Nodal* expression and positive for right-sided expression when right-sided or bilateral *Nodal* was found. Most specimens explanted between stage 5 and

the 1 somite stage (n= 39) developed *Nodal* expression in the normal domain spanning the left LPM (69.2%, n= 27, Fig. 12A). All embryos that had reached or were older than the 2 somite stage when explanted (n= 11) showed expression in the left LPM. Ectopic expression in the right LP was found in 61.5% (n= 24) of cases when embryos were explanted between stage 5 and the 1 somite stage (n= 39), whereas only 9.1% (n= 1) of embryos explanted at the 2 somite stage (n= 11) expressed *Nodal* in the right LPM. These data show that the deregulation of *Nodal* expression which arises during *in vitro* culture of rabbit embryos was primarily characterized by ectopic right-sided expression in embryos explanted between stage 5 and the 1 somite stage. It also indicates that the culture yielded stable left-sided marker gene expression when embryos were explanted from the 2 somite stage onwards.

GJC is required for right-sided repression of *Nodal*

To test the role of GJC in the establishment of LR-asymmetry, gastrula and neurula stage rabbit embryos were cultured in the presence of the gap junction blocker heptanol. This aliphatic alcohol interferes with gap junction based intercellular exchange without affecting conductance of the non-junctional membrane, cytosolic Ca^{2+} or pH (Chanson et al., 1989) and has already been used to inhibit GJC in frog embryos (Levin and Mercola, 1998). Embryos were cultured in normal medium into which heptanol had been diluted 10^5-fold, equating a 0.07mM solution. This treatment yielded overall normal morphological development as compared to the untreated control cultures. Embryos were assessed for marker gene expression by in situ hybridization after they had reached the 4-6 somite stage. Heptanol had no visible effect on *Nodal* transcription per se, as *Nodal* appeared in the paranotochordal domain, and the LPM domain of *Nodal* expression showed its characteristic dynamic rostro-caudal expansion throughout the LPM. However, embryos explanted and cultured in the presence of heptanol at stage 5, 6 or the 1 somite stage (n= 28) showed a disturbed expression of marker genes (Fig. 11A),

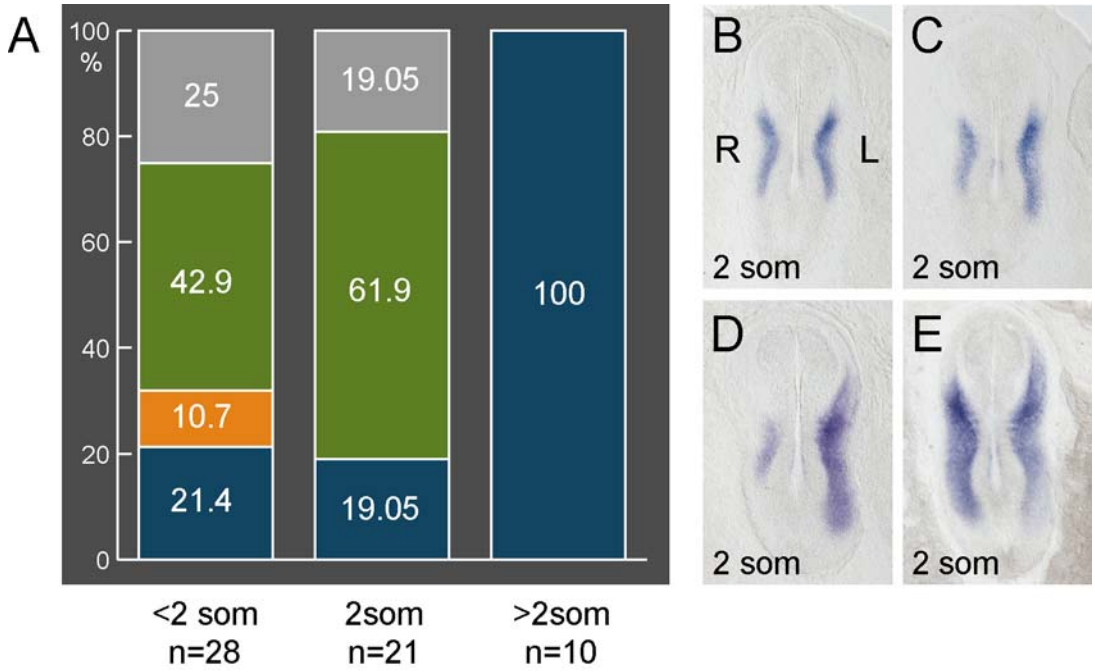

Fig. 11 Heptanol induces bilateral expression of *Nodal* specifically in the 2 somite stage. (**A**) Diagram showing relative numbers of embryos explanted before, during or after the 2 somite stage with left-sided (blue), right-sided (yellow), bilateral (green) or lack of *Nodal* expression (grey) after culture in the presence of heptanol. (**B**-**E**) Representative examples of embryos explanted at the 2 somite stage, showing bilateral expression of *Nodal* after treatment with heptanol in culture. Expression was either symmetric (**B**) or asymmetric (**C**-**E**). Embryos are shown in ventral view with anterior to the top.

comparable to that in untreated control cultures. *Nodal* expression at these stages was predominantly bilateral (42.9%, n= 12) and 21.4% (n= 6) of embryos showed normal left-sided expression. *Nodal* transcripts were restricted to the right LPM in 10.7% of cases (n= 3) and transcripts were found in neither left nor right LPM in another 25% of embryos (n= 7). Of the embryos that had reached the 2 somite stage before explantation, 90.9% developed left-asymmetric expression of marker genes in the control culture (cf. Fig. 10A). However, when 2 somite embryos were explanted and treated with heptanol during the culture period (n= 21), normal asymmetry as compared to the control culture was disturbed, as 61.9% of embryos (n= 13) showed bilateral expression of *Nodal* (Fig. 11A-E). When embryos were cultured from the 3 somite stage onwards (n= 10), treatment with heptanol showed no effect on asymmetric marker gene expression (Fig. 11A). The ectopic right-sided domain of *Nodal* which appeared in 2 somite stage embryos was variable, as in 3 out of 13

embryos expression was found to be bilaterally symmetrical (Fig. 11B), whereas in 10 out of 13 embryos expression was asymmetric (Fig. 11C-E). In embryos cultured up to the 4, 5 or 6 somite stage, the right-sided domain varied in size but was always smaller than the left-sided domain. However, in an embryo that had been cultured up to the 7 somite stage, the right-sided domain was apparently larger than the left-sided domain (Fig. 11D). It spanned the whole length of the left LPM including the heart anlage, whereas expression on the right side reached more anterior but was less expanded in cranio-caudal direction. In wild-type embryos at the 6 somite stage, the *Nodal* domain reaches its full length while during the 7 somite stage, *Nodal* starts to regress from the posterior-most LPM causing the expression domain to shrink in its rostro-caudal extension. The ectopic domain on the right side caused by treatment with heptanol was not smaller as compared to endogenous left-sided *Nodal* expression, but represented the normal extension of *Nodal* in a 6 somite stage embryo. The endogenous left-sided expression domain however expanded normally for a 7 somite stage embryo. This indicates that initiation of the ectopic right-sided expression in heptanol-treated embryos was delayed as compared to the left side.

Assessing *Nodal* expression by separately considering each side of the embryo revealed that treatment with heptanol specifically affected the right LPM of 2 somite stage embryos (Fig. 12B). In control untreated cultures, the right LPM expressed *Nodal* in 61.5% of cases when embryos were explanted before the 2 somite stage. Treatment with heptanol (n= 28) slightly lowered this ratio to 53.6% (n= 15), this moderate effect however was statistically not significant ($p>0,05$; all p-values calculated using the χ^2-test). When embryos were explanted and treated with heptanol at the 2 somite stage (n= 21), a statistically highly significant increase of expression in the right LPM was observed as compared to the untreated control cultures (9.1% in control untreated cultures vs. 61.9% in heptanol cultures, n= 13, $p<0,01$). The left-sided expression of *Nodal* was only slightly affected by the treatment with heptanol, as 64.3% (n= 18) of embryos younger than the 2 somite stage (n= 28, cf. 69.2% in control) and 80.95% (n= 17) of 2 somite stage embryos (n= 21) showed *Nodal* expression (cf. 100% in control). In both cases, reduction of *Nodal* was not statistically significant ($p>0.05$). Taken together these experiments

suggest that intercellular communication via GJs specifically during the 2 somite stage is required to inhibit activation of the Nodal cascade in the right LPM.

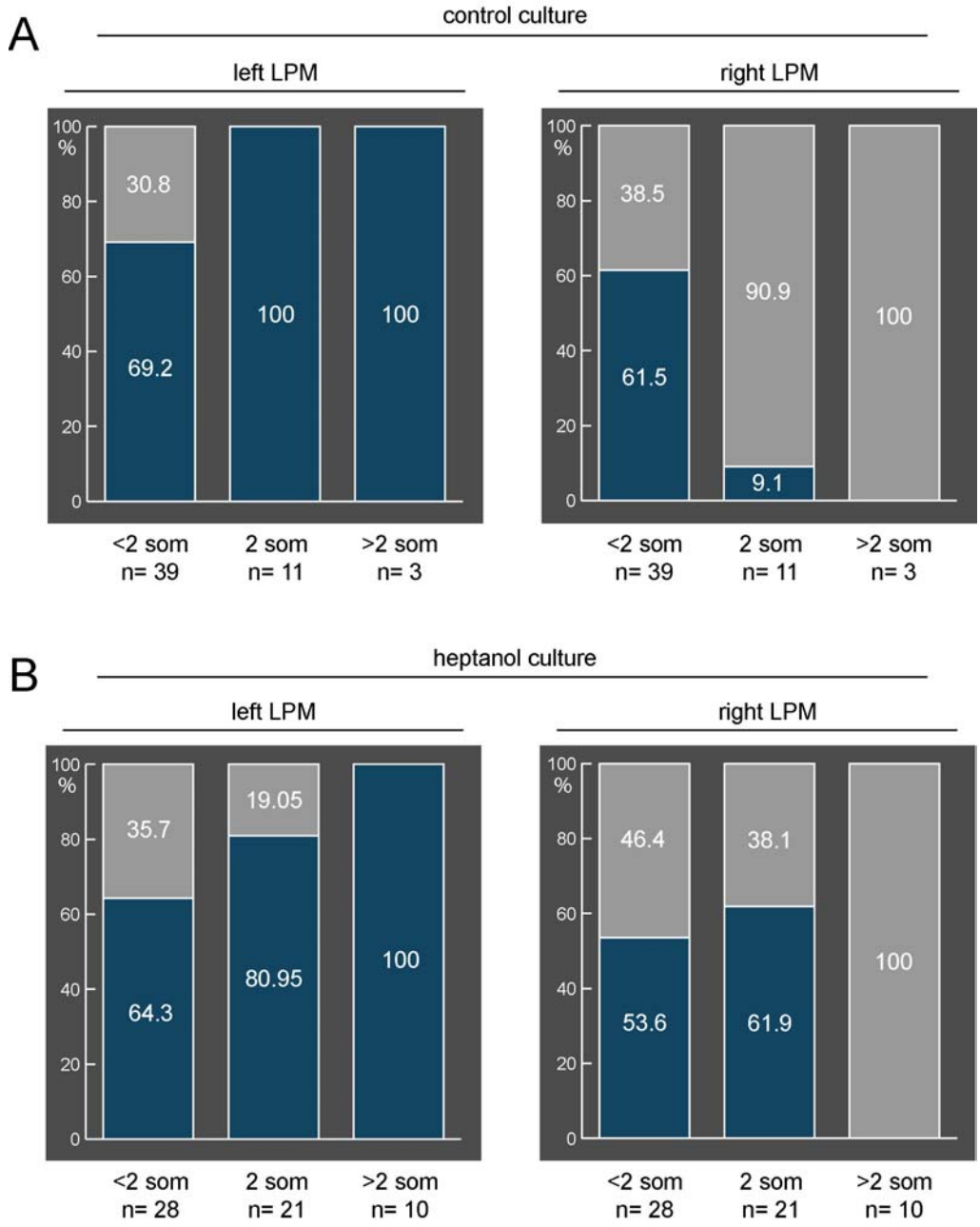

Fig. 12 The right lateral plate is specifically affected by treatment with heptanol during the 2 somite stage. (**A**, **B**) Diagrams showing percentage of *Nodal* expression in right or left lateral plate mesoderm (LPM) in untreated control cultures (**A**, cf. Fig. 9) compared to heptanol treated cultures (**B**, cf. Fig. 10). Relative numbers of embryos expressing *Nodal* are shown in blue, grey bars represent embryos lacking *Nodal* expression. Note that in heptanol treated embryos (**B**) expression in the right lateral plate was highly significantly elevated at the 2 somite stage as compared to control untreated cultures (**A**; $p<0.01$).

Inhibition of GJC reduces the repressive function of FGF8 on *Nodal*

In the rabbit embryo FGF8 acts as an inhibitor of *Nodal* expression on the right side *in vivo* (Fischer et al., 2002). This inhibitory effect can be demonstrated *in vitro* by the application of FGF8 protein onto the left side of the embryo, which results in the suppression of the left-sided Nodal cascade. As it has been shown that FGF8 interacts with GJC in chick lens and limb bud cultures (Makarenkova and Patel, 1999; Le and Musil, 2001) it was tested whether the inhibitory effect of FGF8 on *Nodal* was dependent on GJC. Beads soaked in FGF8 protein were placed onto the left side of the embryo next to the PNC and cultures were allowed to develop to the 4-6 somite stage in the presence of heptanol. The results were evaluated by assessing expression of *Nodal* on the left side of the embryo. When the left-sided

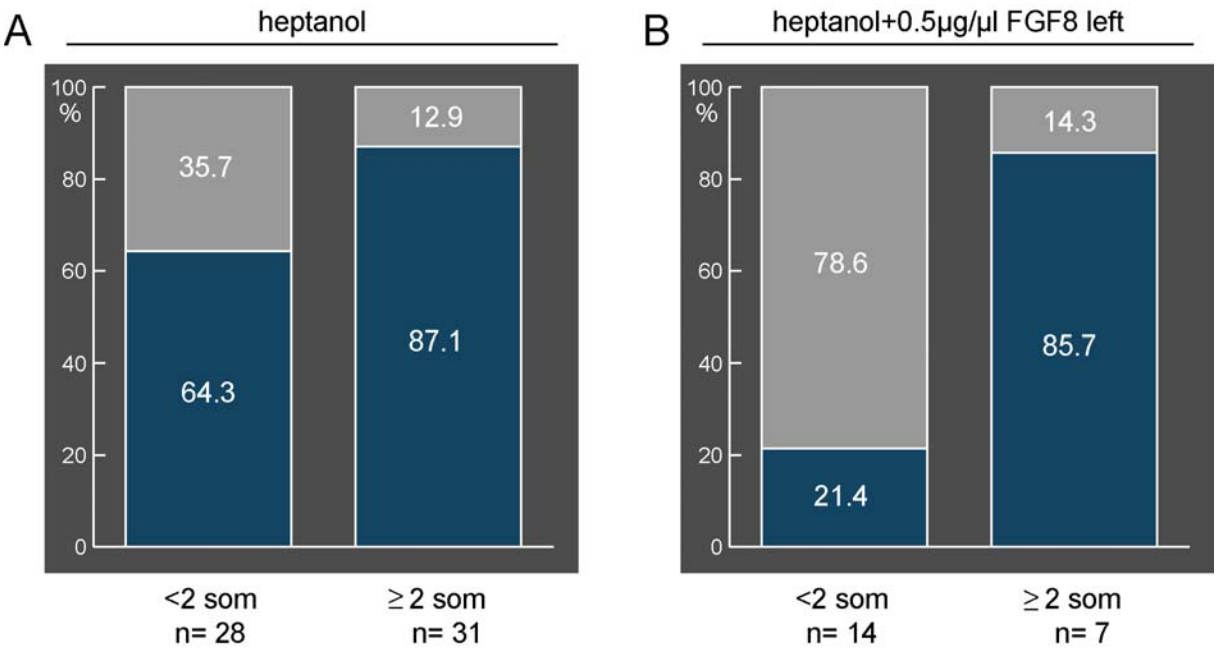

Fig. 13 Left lateral plate mesoderm expression of *Nodal* in heptanol-treated embryos is reduced by elevated doses of FGF8. Embryos were taken into culture before or during and after the 2 somite stage and assessed for *Nodal* expression by in-situ hybridization. (**A**) Expression of *Nodal* in the left lateral plate mesoderm of embryos treated with heptanol (cf. Fig. 12B). (**B**) Expression of *Nodal* in the left lateral plate mesoderm of embryos treated with heptanol and a left-sided FGF8 bead. Relative numbers of embryos expressing *Nodal* are shown in blue, grey bars represent embryos lacking *Nodal* expression. Note that in (**B**) initiation of the Nodal cascade was highly significantly reduced by application of 0.5µg/µl FGF8 ($p<0.01$), but expression was not completely blocked.

Nodal signal in heptanol+FGF8-treated embryos was unaltered as compared to stage-matched embryos treated with heptanol only, the expression was scored as unaffected by FGF8. If the *Nodal* expression domain was missing, considerably smaller or if *Nodal* was down-regulated around the bead upon treatment with FGF8, expression was scored as affected by FGF8-treatment.

In untreated embryos explanted before the 2 somite stage *Nodal* transcripts were found in the left LPM in 69.2% of cases (cf. Fig. 12A) and comparable embryos treated with heptanol showed left-sided *Nodal* expression in 64.3% of cases (Fig. 13A, and cf. Fig 12B). When at those stages a bead soaked in 0.3µg/µl FGF8 protein was applied onto the left side of the embryo (n= 8), left-sided expression of *Nodal* was unaffected in 62.5% (n= 5) of embryos examined (not shown), representing no significant reduction in left-sided expression ($p>0.05$). However, when the concentration of FGF8 was increased to 0.5µg/µl (n=14), only 21.4% (n= 3) of the embryos had unaffected expression on the left side (Fig. 13B). The treatment with 0,5µg/µl FGF8 thus caused a highly significant ($p<0.01$) down-regulation of *Nodal* expression as compared to heptanol treated control cultures. It should be noted that in otherwise untreated embryos, in which a left-sided FGF8 bead had been placed at concentrations of either 1µg/µl, 0.5µg/µl or 0.3µg/µl, left-sided *Nodal* expression was always absent (Fischer et al., 2002, and own observation). A repression of FGF8 on *Nodal* in otherwise untreated embryos was only observed when embryos were taken into culture and treated before they had reached the 2 somite stage (Fischer et al., 2002). Likewise in this study, *Nodal* expression was not affected by the application of 0.5µg/µl FGF8 onto the left side of heptanol-treated embryos that had reached the 2 somite stage or were older when taken into culture (n= 7, Fig. 13B). These results demonstrate that the repressive function of FGF8 on *Nodal* can be prevented by the inhibition of GJC and thus suggest that *in vivo* an inhibition of GJC on the left side may be necessary to initiate the Nodal cascade.

Rescue of GJ-dependent ectopic right-sided induction of *Nodal* by FGF8

FGF8 signaling can be inhibited by SU5402, a compound which specifically interferes with the catalytic center of the FGF-receptor 1 (FGFR1) and thus disrupts FGF8 signal transduction (Mohammadi et al., 1997). Application of SU5402 onto the right side of the rabbit blastodisc eliminated the repressive function of FGF8 up to the 2 somite stage and induced an ectopic right-sided domain of *Nodal* (Fischer et al., 2002, and own observation). As shown in the previous experiment, a global inhibition of GJC during the 2 somite stage by the use of heptanol had the same effect as an interruption of FGF8 signaling on the right side of the embryo, namely ectopic right-sided expression of *Nodal*. It was thus tested whether additional FGF8 protein could counteract ectopic *Nodal* expression caused by the inhibition of GJC with heptanol during the 2 somite stage. When embryos were taken into culture and treated with heptanol at the 2 somite stage they developed ectopic expression of *Nodal* in the right LPM in 61.9% of cases (Fig. 14, cf. Fig. 12B). In heptanol-treated 2 somite stage embryos onto which a bead with 0.5µg/µl FGF8 was placed on the right side next to the PNC, the ectopic *Nodal* domain was conspicuously smaller in 4 out of 5 cases (not shown). When the dose of FGF8 was elevated to 1µg/µl protein (n= 9), an ectopic right-sided domain was seen in 11.1% (n= 1) of the 2 somite stage embryos whereas the remaining embryos (n= 8) showed no *Nodal* expression on the right side (Fig. 14). Ectopic expression of *Nodal* induced by the treatment with heptanol was thus significantly reduced from 61.9% in heptanol-treated embryos to 11.1% in heptanol-treated embryos with a FGF8-bead placed onto the right side ($p<0,05$). This implies that a sufficiently high dose of FGF8 could repress the heptanol-induced ectopic expression of *Nodal* in the right LPM. Taken together these results strongly suggest that ectopic right-sided expression of *Nodal* caused by the blockage of GJC during the 2 somite stage was due to an impairment of FGF8 function.

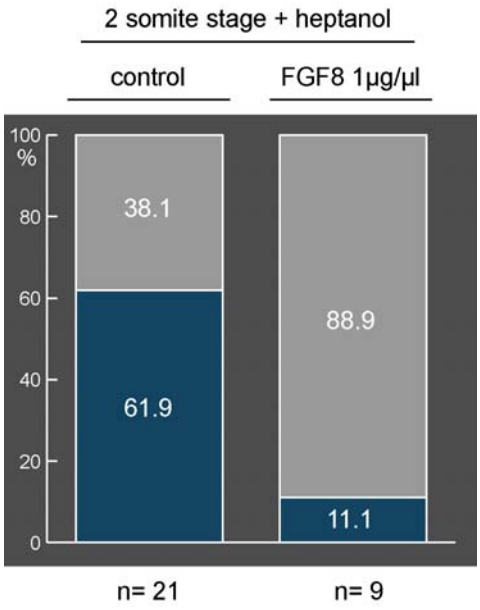

Fig. 14 Ectopic right-sided *Nodal* expression caused by inhibition of gap junctional communication during the 2 somite stage is rescued by FGF8. Embryos were taken into culture at the 2 somite stage, treated with heptanol and a right-sided FGF8 bead. Relative numbers of control heptanol and heptanol+FGF8-treated embryos expressing *Nodal* in the right lateral plate mesoderm are shown in blue, grey bars represent embryos lacking *Nodal* expression. Note that application of FGF8 significantly reduced *Nodal* expression in the right lateral plate mesoderm ($p<0.05$).

Retinoic acid induces right-sided expression of *Nodal*

Retinoic acid (RA) is a known inhibitor of FGF8 during mouse embryogenesis (Diez del Corral et al., 2003). RA signaling is found in a rostro-caudal gradient, overlapping with the expression of *Fgf8* in the floorplate at the level of the PNC, where RA probably controls the anterior limit of *Fgf8* transcription (Sirbu and Duester, 2006). As in mouse embryos, excess RA leads to bilateral expression of marker genes (Chazaud et al., 1999; Wasiak and Lohnes, 1999), the effect of RA on *Nodal* expression was tested in the rabbit.

When embryos were taken into culture before the 2 somite stage and treated with 1µM RA (n= 8), they mostly developed aberrant expression of *Nodal* (Fig. 15A). The expression ratio found upon treatment with RA was comparable to the disturbance recorded in untreated control cultures (cf. Fig. 10A) and heptanol treated cultures (cf. Fig. 11A). Most embryos showed bilateral expression of *Nodal* (50%, n= 4) while normal left-sided as well as lack of expression was found in 25% of cases each (n= 2, Fig. 15A). Unlike in control or heptanol treated embryos, expression exclusively on the right side was never observed. Similar to heptanol treated embryos, specimens cultured from the 2 somite stage onwards in the presence of RA

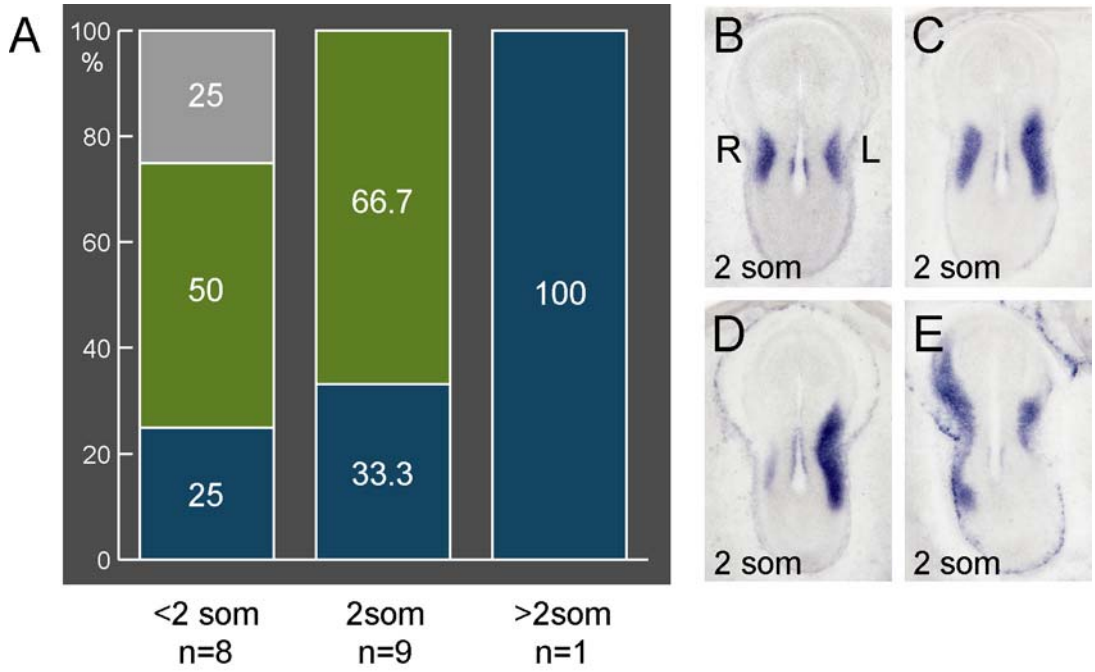

Fig. 15 Retinoic acid induces bilateral expression of *Nodal* specifically in the 2 somite stage. (**A**) Diagram showing relative numbers of embryos explanted before, during or after the 2 somite stage with left-sided (blue), bilateral (green) or lack of *Nodal* expression (grey) after culture in the presence of retinoic acid. (**B**-**E**) Representative examples of embryos explanted at the 2 somite stage, showing bilateral expression of *Nodal* after treatment with heptanol in culture. Expression was either symmetric (**B**) or asymmetric (**C-E**). Embryos are shown in ventral view with anterior to the top.

(n= 9) showed bilateral expression of *Nodal* in 66.7% of cases (n= 6, Fig. 15A-E). RA specifically induced ectopic right-sided expression in the 2 somite stage, as in embryos expressing *Nodal* bilaterally, the normal left-sided expression domain was always present and unaltered. One embryo taken into culture after the 2 somite stage showed normal left-sided expression (Fig. 15A). Comparable to the results obtained with heptanol, the bilateral *Nodal* domain in RA treated embryos was mostly asymmetric (5 out of 6 embryos expressing *Nodal* bilaterally; Fig. 15C-E), while only one embryo showed symmetric expression (Fig. 15B). Analysis of expression on both sides of the embryos showed that the right-sided domain was consistently initiated after the onset of left-sided expression. In embryos cultured from the 2 somite stage to the 4-6 somite stage this became evident by a small domain on the right side and a slightly (Fig. 15C) or significantly (Fig. 15D) increased rostro-caudal expansion of the left-sided domain. In an embryo cultured up to about the 7-8 somite stage, the

left-sided expression was reduced to a small patch inside and caudal to the heart anlage as is typical for *Nodal* expression at that stage. The *Nodal* domain on the right side however had reached a rostro-caudal extension similar to a 6-7 somite stage embryo. These results show that, similar to heptanol, RA induces a delayed ectopic expression of *Nodal* in the right LPM and suggest that RA may be required on the left side of the embryo to induce the Nodal cascade.

GJs and FGF8 act in the relay of initial asymmetric cues

Activation of the Nodal cascade in the LPM depends on signals from the midline

The culture of rabbit embryos in the presence of heptanol identified the 2 somite stage as a critical phase for GJC. This is shortly before *Nodal* transcripts are first detected in the left LPM in wild-type embryos. The question is raised whether LR-decisive cues, of either inhibitory or inducing nature, are transferred to the LP in a gap-junction-dependent manner during the 2 somite stage, a phase that lasts about 1.5hrs. To test whether the signals received by the LPM originate from the midline and if so, when these signals are needed, LP tissue was dissected at different time points and taken into culture. Both parts of the embryos, one consisting of LP tissue only and the other consisting of the contra-lateral LP as well as adhering axial mesoderm and paraxial tissue (Fig. 16A), were cultured in separate dishes and assessed for marker gene expression. Both parts were allowed to develop in culture until the 4-6 somite stage. The progression of somitogenesis indicating the developmental stage was observed in the part of the embryo with adhering midline and paraxial tissue.

Explanted LP tissue in culture developed mostly normal as judged by three criteria: (1) the paranotochordal expression of *Nodal* was initiated correctly in cells marking the transition between notochordal plate and endoderm in explants that carried midline and paraxial structures (Fig. 16B, B'); (2) whenever *Nodal* expression was

observed in the LP explants it was restricted to mesodermal cells irrespective of the side from which the explant was taken (Fig. 16C, C'); and (3) explants of either side which were allowed to develop beyond the stages during which *Nodal* was expressed developed a contracting heart anlage (not shown).

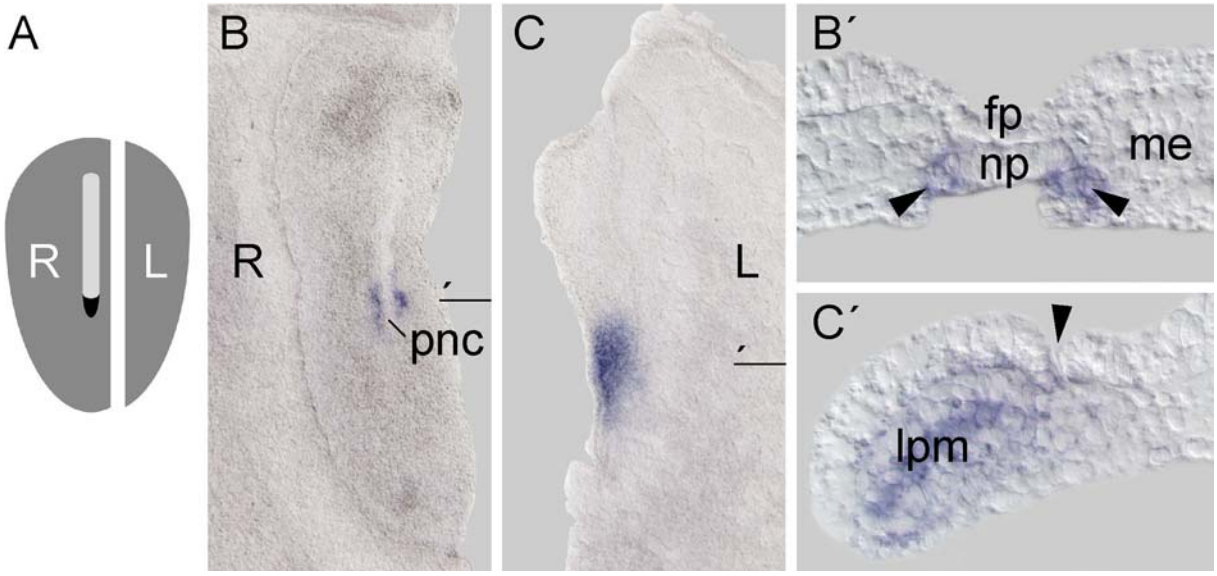

Fig. 16 Development of lateral plate tissue explanted in pre-somite stages. Lateral plate tissue was dissected and analyzed for *Nodal* expression by in-situ hybridization following culture to the 4-6 somite stage. (**A**) Schematic representation of lateral plate dissection. In the case depicted here, the left (L) lateral plate was removed and midline as well as paraxial tissues remained attached to the right (R) side. (**B**) Right-sided explant showing paranotochordal expression of *Nodal* at the site of the posterior notochord (pnc). (**B**') Section through right explant (level indicated in **B**) revealed expression in cells bordering the notochordal plate (np) on both sides (indicated by arrowheads). Note that cells expressing *Nodal* were not in contact with the overlying floorplate (fp). (**C**) Left lateral plate expressing *Nodal* in a posterior domain. (**C**') Section through left lateral plate (level indicated in **C**) showing that lateral plate mesoderm (lpm) specifically expressed *Nodal*. Arrowhead indicating border between embryonic and extraembryonic tissue. Embryos are shown in ventral view with anterior to the top, sections with dorsal side up.

In the mouse it has been shown that paranotochordal expression of *Nodal* is indispensable for activation of the Nodal cascade in the left LPM (Brennan et al., 2002; Saijoh et al., 2003). In the rabbit this domain of *Nodal* transcription appears towards the end of stage 5. Left LP explants that were dissected at stage 4 or at early stage 5 did not develop *Nodal* expression. This suggests that similar to mouse, in the rabbit LPM-*Nodal* depends on signals emanating from the cells expressing

Nodal on both sides of the PNC. Therefore, only embryos that had reached stage 5b were included in the subsequent experiment.

When left LP tissue was explanted before the 2 somite stage and cultured away from the midline (n= 36, Fig. 17A) the tissue expressed *Nodal* in 47.2% of cases (n= 17). If the left LP was explanted together with the adhering midline structures (n= 16), the rate of expression was elevated so that 56.25% (n= 9) of all specimens showed *Nodal* transcripts in the LPM (Fig. 17C). This slight increase in expression however was not statistically significant ($p>0.05$). A significant effect of the adhering midline tissue on *Nodal* expression in the left LPM was observed during the 2 somite stage. In left LPs without midline tissue (n= 19) *Nodal* transcripts were found in only 21.1% of cases (n= 4, Fig. 17A), whereas 80% (n= 4) of LPs cultured in the presence of the midline (n= 5) expressed *Nodal* ($p<0.05$, Fig. 17C). All LPs with adhering midline also expressed *Nodal* when explanted later than the 2 somite stage (n= 5, Fig. 17C), and only 20% (n= 2) of those without adhering midline (n= 10) lacked *Nodal* expression following culture ($p>0.05$, Fig. 17A).

LP tissue from embryos younger than the 2 somite stage that was dissected from the right side of the embryo and cultured without the midline (n= 15) showed only a low percentage of *Nodal* expression. Interestingly, even on the right side the presence of midline tissue (n= 37) considerably elevated the rate of expression in these early stages. While explants without midline revealed *Nodal* transcripts in only 20% of cases (n= 3, Fig. 17B), expression highly significantly increased to 62.2% (n= 23) in explants with adhering midline (n= 37, $p<0.01$, Fig. 17D). None of the right-sided explants without midline expressed *Nodal* when the tissue was removed during the 2 somite stage (n= 3, Fig. 17B) and only 20% (n= 3) of the embryos which were cultured in the presence of the midline (n= 15) showed expression when taken into culture at that stage ($p>0.05$, Fig. 17D). The presence of the midline stabilized the lack of expression in right explants after the 2 somite stage, as in such explants *Nodal* transcripts were never detected (n= 13, Fig. 17D) whereas 80% (n= 4) of explants without midline structures performed in older embryos (n= 5, Fig. 17B) did express *Nodal*, which was statistically very highly significant ($p<0.001$).

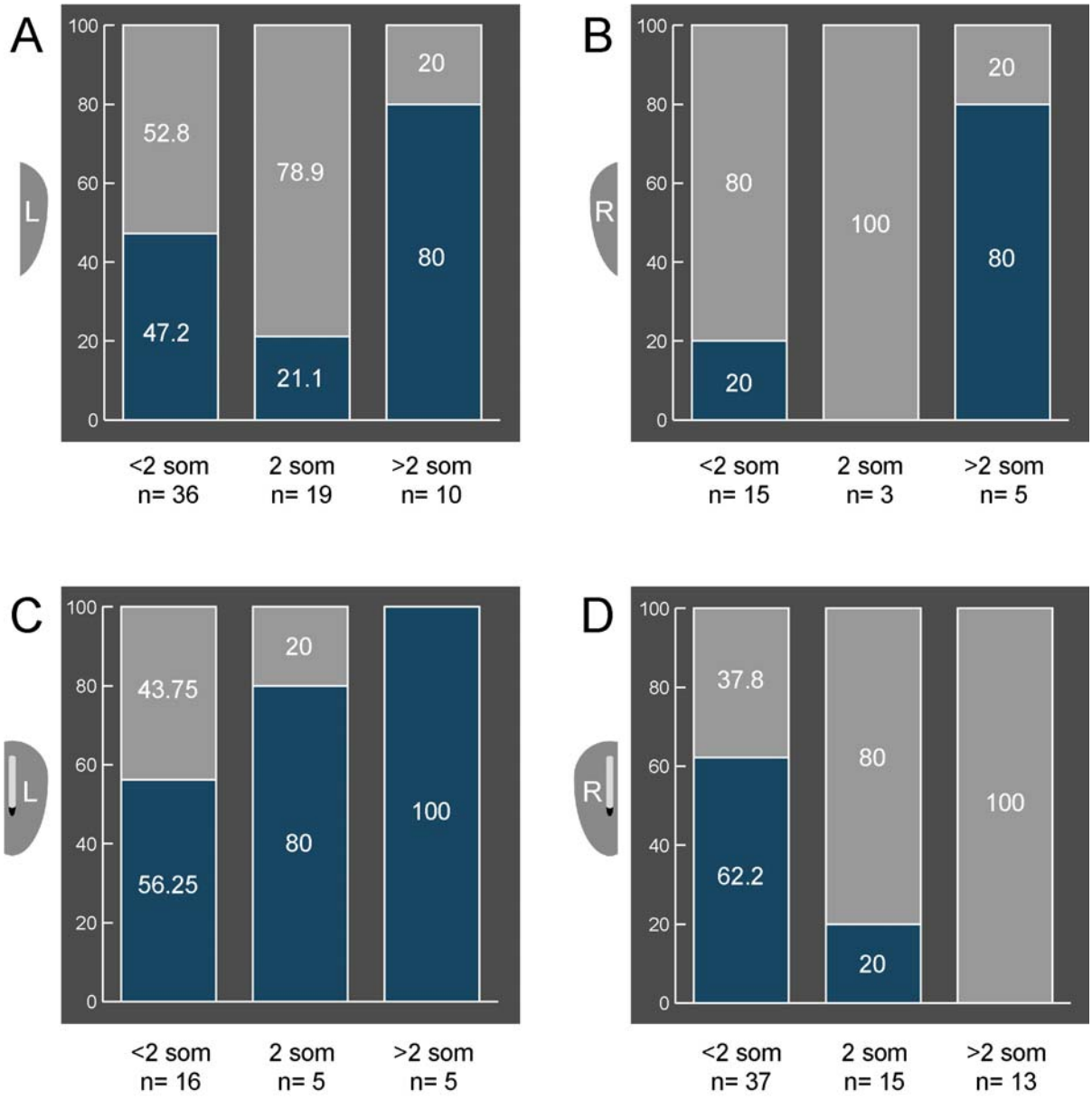

Fig. 17 The lateral plate receives left-right cues from the midline. Lateral plate tissue was dissected before, during and after the 2 somite stage, cultured with or without adhering midline structures and assessed for *Nodal* expression after culture to the 4-6 somite stage. (**A**) Left and (**B**) right lateral plate explants without midline structures. (**C**) Left and (**D**) right lateral plate tissue with adhering midline structures. Relative numbers of embryos expressing *Nodal* are shown in blue, grey bars represent embryos lacking *Nodal* expression. Note that presence of the midline in left lateral plate explants performed at the 2 somite stage (**C**) highly significantly elevated *Nodal* expression ($p<0.01$) as compared to left tissue without midline (**A**) explanted at the 2 somite stage. Presence of midline tissue highly significantly induced *Nodal* expression in right-sided explants performed before the 2 somite stage ($p<0.01$). Midline tissue also highly significantly stabilized lack of expression in right explants (**D**) performed after the 2 somite stage as compared to right lateral plate explants without midline (**B**; $p<0.001$).

The ratio of *Nodal* expression in explants cultured with adhering midline structures was comparable to whole embryo control cultures (no statistical differences between cultured explants with midline and cultured whole embryos, p-values >0.05). For example left LP tissue cultured with adhering midline showed *Nodal* expression in more than 50% of cases when taken into culture before the 2 somite stage and explants cultured from the 2 somite stage onwards stably expressed *Nodal* in the LPM (Fig. 17C). These results match the progression of expression observed in whole embryo control cultures, where expression in the left LPM was found in about two thirds of cases before the 2 somite stage and stable culture conditions were established from the 2 somite stage onwards (cf. Fig. 12A). Similarly about two thirds of the right LP explants with adhering midline expressed *Nodal* when explanted before the 2 somite stage and this expression decreased so that when dissected after the 2 somite stage, none of the explants revealed *Nodal* transcripts (Fig. 17D). This progression was comparable to the right LPM in control cultured embryos which showed expression in about 60% of cases and this expression was lost after the 2 somite stage (cf. Fig. 12A). The data obtained from the lateral plate explant culture show that on the right side, presence of the midline promotes *Nodal* expression in younger stages and is indispensable to repress transcription after the 2 somite stage. Furthermore, the results strongly suggest that during the 2 somite stage, the left LPM depends on signals from the midline to initiate the Nodal cascade.

Inhibition of GJC in isolated right LP tissue does not initiate *Nodal* expression

The previous experiments have shown that both left-sided initiation and right-sided suppression of the Nodal cascade depended on signals emanating from the midline. Furthermore, GJC was identified as a mechanism which synergizes with FGF8 during the 2 somite stage to repress *Nodal* in the right LPM. The GJ gene *Cx43* was expressed in the LPM as well as in mesodermal cells connecting midline and LPM (cf. Fig. 8). This expression pattern suggests that GJs might either be necessary in the LPM to directly inhibit *Nodal* transcription or required for the transfer of inhibitory

cues from the midline to the right LPM. To examine both possibilities, right-sided LP tissue of 2 somite stage embryos was dissected, cultured with or without adhering midline tissue and treated with heptanol.

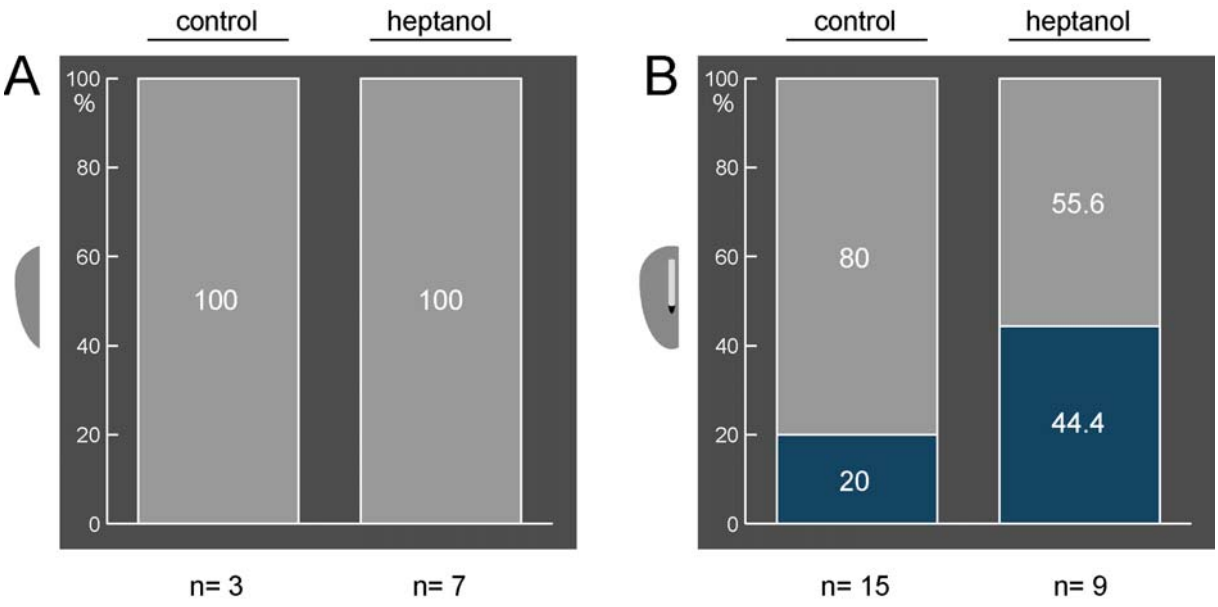

Fig. 18 Ectopic right-sided *Nodal* expression caused by inhibition of gap junctional communication at the 2 somite stage requires presence of the midline. Right lateral plate tissue was dissected at the 2 somite stage, incubated with or without adhering midline tissue in the presence of heptanol and assessed for *Nodal* expression by in-situ hybridization after culture to the 4-6 somite stage. (**A**, **B**) Right lateral plate without (**A**) and with (**B**) adhering midline structures. Relative numbers of control untreated (cf. Fig. 17) and heptanol treated embryos expressing *Nodal* are shown in blue, grey bars represent embryos lacking *Nodal* expression. Note that in the presence of midline tissue, treatment with heptanol significantly elevates ectopic expression of *Nodal* in the right lateral plate mesoderm ($p<0.05$).

When right-sided LP tissue was isolated from the midline and taken into culture at the 2 somite stage, the right LPM showed no expression of *Nodal* in untreated LP-explant cultures (Fig. 18A, cf. Fig. 17B). Likewise, inhibition of GJC by treatment with heptanol in the isolated right LP did not induce *Nodal* expression (n= 7, Fig. 18A). When dissected during the 2 somite stage and cultured untreated, the right LPM with adhering midline tissue developed mostly normal marker gene expression, as judged by a predominant lack of *Nodal* expression (Fig. 18B, cf. Fig. 17D). However, when such explants were treated with heptanol (n= 9), ectopic expression of *Nodal* was

induced in 44.4% of cases (n= 4, Fig. 18B), which was a significant increase in ectopic *Nodal* expression as compared to explants cultured without adhering midline tissue. These results show that presence of the midline is indispensable for ectopic induction of *Nodal* by heptanol and suggest that GJC is required for the transfer of inhibitory cues from the midline to the right LP during the 2 somite stage.

No FGF8-mediated repression of *Nodal* in isolated left LP tissue

Application of FGF8 onto the left side of the embryo next to the PNC inhibited *Nodal* expression in the left LPM of the rabbit (Fischer et al., 2002), mimicking the *in vivo* right-sided repressive function of this growth factor. However, FGF8 could only inhibit *Nodal* transcription before embryos had reached the 2 somite stage. This repressive effect of FGF8 on *Nodal* transcription might be achieved by inhibition in the LPM directly. Alternatively, FGF8 might prevent the transfer of inductive signals from the midline towards the left LPM. To test both possibilities, explants of left LP tissue were prepared before, during and after the 2 somite stage and a bead soaked in 0.5µg/µl FGF8 protein, which was sufficient to repress *Nodal* in whole-mount embryos, was incubated together with the piece of tissue. The tissues were cultured until the contra-lateral part with adhering midline and paraxial tissue had reached the 4-6 somite stage.

Left LP tissue of untreated control cultures dissected and taken into culture before the 2 somite stage expressed *Nodal* in 47.2% of cases (Fig. 19A, cf. Fig. 12A). When similar explants were incubated together with a FGF8-bead (n= 19), *Nodal* transcription was not significantly down-regulated ($p>0,05$) as transcripts were found in the LPM of 42.1% of explanted LPs (n= 8, Fig. 19B). When explants were performed during the 2 somite stage, FGF8 hardly affected the expression of *Nodal*. Transcripts were found in 21.1% of untreated control explants (Fig. 19A, cf. Fig. 12A), while none of the explants cultured in the presence of FGF8 expressed *Nodal* (n= 7, Fig. 19B). This moderate reduction however was not statistically significant ($p>0,05$). When left LP tissue was explanted after the 2 somite stage, FGF8 had no

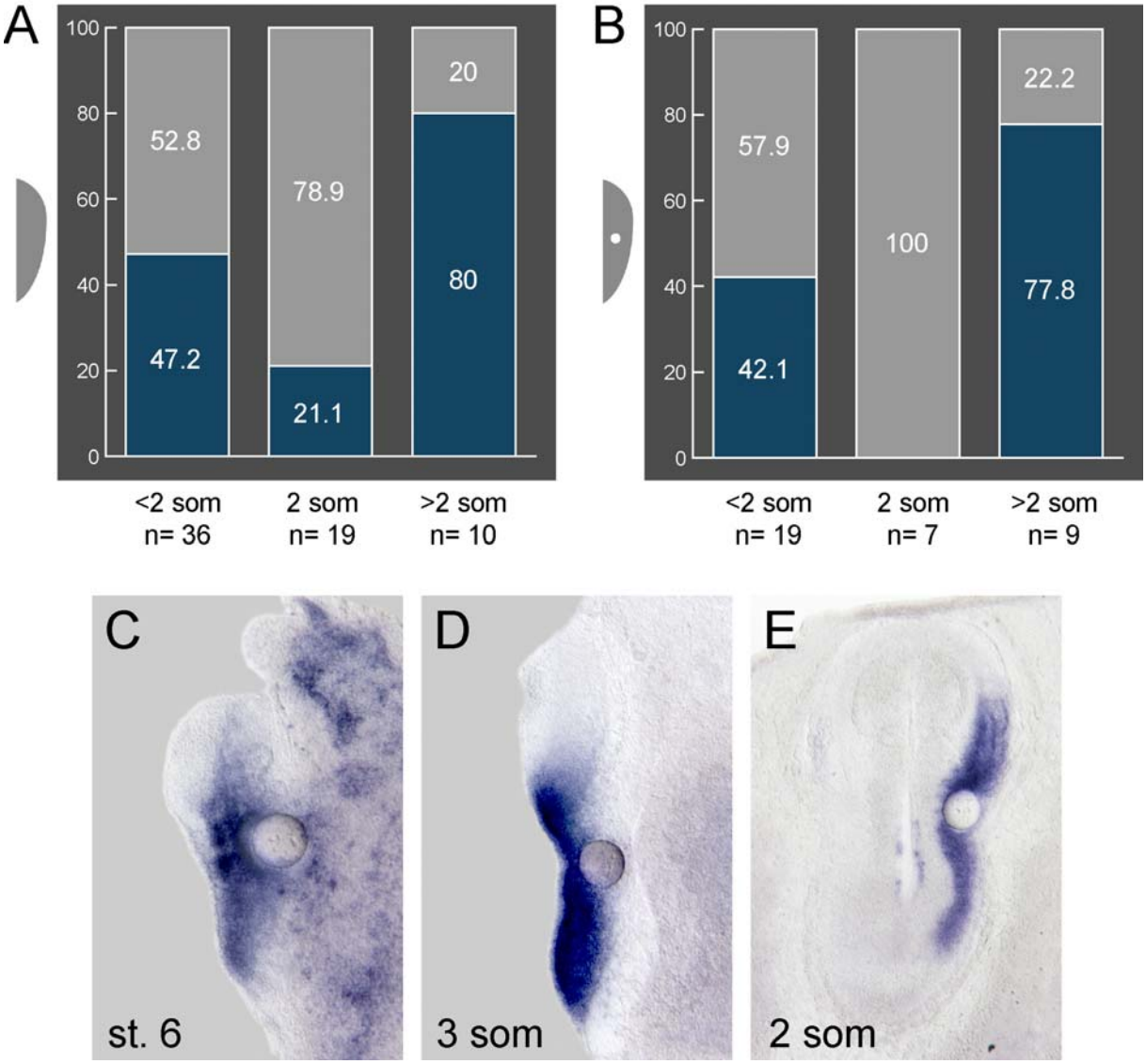

Fig. 19 *Nodal* expression is not altered by application of FGF8 to isolated left lateral plate tissue. Left lateral plate tissue was dissected before, during and after the 2 somite stage, treated with a FGF8 bead and assessed for *Nodal* expression after culture to the 4-6 somite stage. (**A**, **B**) Control untreated (**A**) and FGF8-treated (**B**) lateral plates. Relative numbers of lateral plates expressing *Nodal* are shown in blue, grey bars represent lateral plates lacking *Nodal* expression. (**C, D**) Lateral plate tissue taken into culture before (**C**) and after (**D**) the 2 somite stage showing *Nodal* expression unaltered by the FGF8 bead. (**E**) The *Nodal* domain was unaltered in whole embryos taken into culture from the 2 somite stage onwards when a bead with FGF8 was placed onto the lateral plate. Embryos are shown in ventral view with anterior to the top.

effect on the expression of *Nodal*, as 80% of untreated LPs (Fig. 19A, cf. Fig. 12A) as well as 77.8% (n= 7) of FGF8-treated LPs (n= 9, Fig. 19B) expressed *Nodal* after culture. Additionally, when FGF8-beads were placed onto dissected LPs of pre-

somite (Fig. 19C) or somite stages (Fig. 19D) or onto LPs of whole embryos taken into culture after the 2 somite stage (Fig. 19E), neither the rostro-caudal nor the lateral extension of the *Nodal* domain were altered. Thus FGF8 signaling did not directly influence *Nodal* transcription. Taken together these results demonstrate that FGF8 does not alter *Nodal* expression in LP tissue and thus indicate that FGF8 acts in the transfer of LR-signals from the midline to the LPM rather than in the LPM itself.

Discussion

Cilia on the notochordal plate of the rabbit

The posterior notochord (PNC) is an evolutionary conserved entity of the mammalian embryo, which is represented by the caudal widening of the notochordal plate in the rabbit blastodisc and the distal indentation of the mouse egg cylinder commonly addressed as ‘node’ (Blum et al., 2006). Homologous structures are found in amphibian (gastrocoel roof plate; GRP; Essner et al., 2002; Shook et al., 2004; Blum et al., 2006) and teleost fish embryos (Kupffer’s vesicle; KV; Essner et al., 2002; Essner et al., 2005; Kramer-Zucker et al., 2005; Okada et al., 2005; Hirokawa et al., 2006). This structure is characterized by a number of distinctive features that distinguishes it from any other ciliated tissue in the animal kingdom: (1) it is directly derived from the embryonic organizer, and (2) harbors motile monocilia of the 9+0 and/or 9+2 type. It is the only epithelial structure in which conical wave forms have been described to (3) result in an asymmetric vectorial fluid flow in the extracellular space (4). The present study adds further evidence to these known particularities and extends the list by a new feature: the presence of three different types of axonemes at the rabbit PNC including the novel 9+4 type. Because of the consistent rotational movement of all PNC cilia in the rabbit (Okada et al., 2005 and A. Rietema, personal communication) this finding implies that 9+2 and 9+4 cilia can display conical wave forms as well.

Cilia-driven fluid flow in the mouse was originally described as ‘nodal-flow’, implying that it occurred at the embryonic organizer, the equivalent of Hensen’s node (Nonaka et al., 1998). The previous morphological and histological analysis has demonstrated that the structure in question, the distal indentation of the E7.5 mouse egg cylinder, in

fact represents the posterior portion of the notochordal plate (PNC), and that the organizer itself, recognized by gene expression patterns and tissue organization, resides at the anterior end of the primitive streak but caudal to the PNC (Blum et al., 2006). The detailed SEM analysis presented here demonstrates that cilia started to protrude at the apical surface of PNC cells from stage 5 onwards (Fig. 2D, Fig. 3A, E), and that the polarization of cilia, which is a prerequisite for directed flow, was first observed at stage 6 (Fig. 2E, Fig. 3B, F, J). Cilia were never observed on Hensen's node, even after the hypoblast/endoderm cell layer had receded from the node at the 3-4 somite stage (Fig. 2G). Gene expression patterns of ciliary markers, however, were consistently found in the organizer itself (Fig. 1). Expression started at stage 4, when the node formed, and faded around the time when the first pairs of somites condensed (Fig. 1). Expression within the node was not uniform but restricted to the ventral cells (Fig. 1C', F', K'), from which the prechordal and notochordal cells emerge. Thus, although morphologically indistinguishable, node cells from the very beginning seem to be specified towards their future fates through the initiation of particular gene programs such as that governing ciliogenesis (Fig. 1). Subdivisions of the avian node were previously reported based on gene expression patterns and cell fate analysis (Charrier et al., 1999) but have not been reported for mammalian organizer tissue as yet. Expression in the notochordal plate was observed as well, however in a gradient which diminished towards the anterior end. This finding implies that the ciliogenic program only acts during a very short time period, and that cells as they migrate out of the node into the notochordal plate already begin to down-regulate their transcription rates. At the subcellular level it will be interesting to analyze whether ciliary protein assembly into larger complexes such as IFT rafts, dynein arm complexes and microtubule subsets already starts in Hensen's node before ciliogenesis begins upon exit of cells into the notochordal plate. The primary embryonic organizer, Spemann's organizer in the amphibian embryo, Hensen's node in rabbit and mouse, and the embryonic shield in the teleost fish embryo, from which the dorsal forerunner cells and hence Kupffer's vesicle (KV) is derived, thus sets the stage for the development of the PNC/GRP/KV or its equivalent in other vertebrates, which functionally may turn out to be primarily involved in LR axis development.

Experimental manipulation of the organizer thus affects all three body axes, while defects in PNC/GRP/KV cause laterality defects without affecting the main body axes (Herrmann and Kispert, 1994; Nonaka et al., 1998; Krebs et al., 2003; Przemeck et al., 2003; Abdelkhalek et al., 2004).

A likely common denominator of this LR axis determining entity seems to be the leftward cilia-driven fluid flow which is required for subsequent asymmetric induction of the Nodal signaling cascade in the left lateral plate mesoderm. A leftward flow was recently found at the GRP in *Xenopus laevis* which underscores the conserved nature of this module (Schweickert et al., 2007). Based on theoretical considerations it was postulated that cilia in order to produce a leftward flow should be polarized to the posterior pole of cells (Cartwright et al., 2004). This tilt should be accomplished by the posterior localization of the cilium on a mound-shaped notochordal cell, a prediction which has been verified in mouse (Cartwright et al., 2004; Nonaka et al., 2005; Okada et al., 2005). As the mouse *inv* mutant, in which the polarization process is disturbed, shows flow and laterality defects (Okada et al., 2005), polarization of cilia seems to be a general constituent of the LR program in vertebrates. The present study demonstrates that rabbit cilia display a posterior localization as well. The first cilia which are apparent on notochordal cells however are positioned medially on the cell surface. Progressive localization of the ciliary base to the posterior margin of the cell is observed concomitant with the lengthening of cilia from stage 5 to stage 6 (Fig. 3A, B, E, F, I, J). This polarization thus most likely represents a process which is initiated only after notochordal cells have surfaced from under the endoderm. In the ascidian notochord, nuclei are displaced posteriorly concomitant with a localization of planar cell polarity (PCP) pathway components during convergence and extension of the notochord (Jiang et al., 2005). Cilia are known to be tightly associated with the nucleus via the trans-golgi-network (Poole et al., 1997) and recent work has shown that the PCP-pathway is linked to ciliary function (Ross et al., 2005; Park et al., 2006). In the rabbit convergence and extension movements become visible in the narrowing of the notochordal plate during its elongation. It should be informative to examine whether the posterior

localization of notochordal cilia is reflected by a displacement of the nucleus and how these processes are connected to the PCP pathway in mammals. Cilia serve as the cell's antennae and could thus sense extracellular cues instructing the cells in the notochordal plate epithelium to undergo polarization movements. Whatever might be the initiating event for ciliary polarization, it is quite clear that a connection exists between the developmental progress of the notochord and the evolution of flow (Okada et al., 1999; Okada et al., 2005 and A. Rietema, personal communication). Laminar leftward fluid flow has only been observed in early somite stage embryos and never during presomite stages. Fluid movements manifest as local vortices around the beginning of somitogenesis and a slow turbulent flow is found from the 1-2 somite stage onwards in the rabbit (A. Rietema, personal communication). Flow only becomes laminar around the 2-3 somite stage which is accompanied by progressive ciliary lengthening and polarization (Fig. 4). This underlines that a certain length and the posterior tilt of a certain number of cilia is necessary to set up a leftward flow and suggests that with the increase of posteriorly tilted cilia leftward fluid flow becomes more laminar.

The most unexpected finding of the present study certainly was that after more than a century of cilia research a new axoneme was discovered at the PNC of the rabbit embryo. Other non-typical axonemes have occasionally been described, particularly in spermatids of arthropods. For example 12+0 and 14+0 axonemes were found in spermatozoans of protura (Baccetti et al., 1973), 9+3 axonemes in spider sperm (Baccetti et al., 1970), 3+0 cilia in parasitic protozoans (Prensier et al., 1980), and 9+1 axonemes in platyhelminthes (Henley et al., 1969). In no single case the functional significance of these cilia was assessed. In vertebrates no cilia besides 9+2 and 9+0 have been described so far. The 9+4 cilia of the rabbit PNC represent the first example of an axoneme with four inner singlets. These cilia have been found with significant frequency in every single embryo analyzed, amounting to about 15 percent of the totally analyzable 357 cilia in this study (Fig. 5). These 9+4 cilia, thus, mark a highly significant structural trait of rabbit PNC cells.

The investigation of the distribution of cilia types along the notochordal plate revealed two highly significant features. First, no domains were found in which one type of axoneme was exclusively present. In all cross sections analyzed cilia types were intermingled with no recognizable patterns. In mouse differences have been described with respect to motility of cilia at the PNC ("node"), such that a subset of immotile cilia was found at the left and right margin and motile cilia at the center (McGrath et al., 2003). If such differences existed in rabbit, they were not reflected by distinct axonemes. In addition, all cilia showed dynein arms irrespective of axoneme type (Fig. 4 and data not shown), suggesting that all cilia were motile. Second, distribution of cilia types along the length of the notochordal plate was unequal, with 9+4 axonemes being absent from the anterior-most region (Fig. 5B). A comparison of relative proportions of cilia with (9+2, 9+4) and without (9+0) central apparatus proves this inhomogeneity even more drastically. While in the posterior and medial part of the notochordal plate about half the cilia had a central apparatus, this proportion dropped to about 15% in the anterior region, where axonemes without central microtubules made up >80% of cilia (Fig. 5B). This pattern may indicate that the central microtubules arise in PNC cells, probably as these cells move out of the anterior node region. They might get lost progressively as cells are displaced anteriorly by the lengthening of the notochordal plate at its posterior end. Such a scenario would imply that 9+2 and 9+4 cilia were present only during a very transient phase of early PNC development.

The intermingled occurrence of three types of axonemes might at first glimpse look like a very enigmatic finding. However, different types of axonemes have been described at the teleost KV, namely 9+0 cilia in medaka (Okada et al., 2005) and 9+2 cilia in zebrafish (Kramer-Zucker et al., 2005). In mouse only 9+0 cilia were published at the PNC (Sulik et al., 1994; Nonaka et al., 1998), yet the knockout of *Foxj1*, a gene which selectively affects 9+2 cilia, revealed laterality defects nevertheless (Blatt et al., 1999; Brody et al., 2000). As probably in all of these studies a limited number of cilia was analyzed ultrastructurally in cross sections, and likely not the entire critical time period from the first appearance of cilia to the asymmetric induction of the Nodal

signaling cascade was investigated in mouse and fish, its seems possible that at least 9+0 and 9+2 cilia could in fact occur together in the PNC and KV of mammalian and teleost fish embryos, respectively. Unexpectedly, a re-evaluation of ciliary ultrastructure in mouse has recently revealed 9+2 and, most notably, 9+4 axonemes at the mouse PNC ("node") as well (Tamara Caspary and Kathryn Anderson, personal communication). Further ultrastructural studies in other species should help to resolve this issue.

The novel 9+4 axoneme most likely represents a duplication of the CP of a standard 9+2 cilium. The evaluation of a total of 56 axonemes of the 9+4 type revealed in quite a number of cases an apparent 2 x 2 arrangement of the CP similar to those depicted in Fig. 4F and I. As the CP microtubules are asymmetric with respect to accessory proteins a clear assignment of individual central microtubules to the C1 or C2 type should be possible by immuno electron microscopy. In the light of the recent finding of different axonemes in mouse (Tamara Caspary and Kathryn Anderson, personal communication), the three different cilia types might reflect a PNC-specific gene program, and probably be functionally required for LR axis formation. Short of a means of eliminating either kind of axoneme in any defined way in the rabbit or mouse, no testable predictions can be made at present. One attractive avenue to further characterize PNC cilia might be to analyze the specific localization of members of the growing list of axoneme associated marker proteins such as for example CaM Kinase II (Smith, 2002; Marshall and Nonaka, 2006).

Whatever the reason for three axoneme types at the PNC might be, one important conclusion can be drawn in any case, namely that all three cilia types are able to perform rotational movements. Hirokawa and colleagues published time-lapse movies of mouse and rabbit PNC cilia which show uniform clockwise rotations throughout (Nonaka et al., 1998; Nonaka et al., 2005; Okada et al., 2005). Ciliary beat patterns have been carefully analyzed at pre- and early somite stages in rabbit embryos as well, and also predominantly clockwise rotations were seen (A. Rietema, personal communication). What, if any, function might the 9+4 cilium exhibit? An attractive possibility would be to involve this axoneme in LR specific signaling

processes, be it the generation, perception or transduction of the initial asymmetric signal. With the recent burst of interest in cilia in contexts as diverse as signaling, morphogenesis, motility, sensation and disease it is to be expected that the enigmatic 9+4 axoneme might find its niche in the foreseeable future.

GJC and FGF8 are required for the relay of LR cues

In frog and chick, establishment of LR asymmetry during embryogenesis relies on intercellular coupling mediated by Cx43. It has been shown experimentally that in *Xenopus*, GJC was required during cleavage stages (Levin and Mercola, 1998), while LR asymmetric patterning in the chick depended on GJC during formation of the primitive streak (Levin and Mercola, 1999). Surprisingly, no laterality defects were recorded in a *Cx43* knockout mouse (Reaume et al., 1995). However, *Cx43* is important for situs determination in humans, as mutations in this gene have been identified in laterality patients (Britz-Cunningham et al., 1995). These divergences might be due to anatomical differences between rodent and other mammalian embryos, as comparative data from chick, mouse and rabbit suggested that, regardless of phylogenetic relation, embryonic architecture plays a crucial role for LR determination (Boettger et al., 1999; Meyers and Martin, 1999; Fischer et al., 2002). The rabbit develops via a flat blastodisc, an appearance which is typical for mammalian embryos including human. Rabbit embryos were thus ideally suited to examine the function of GJC during symmetry breakage in the mammalian embryo. This study provided the first demonstration that GJC is necessary for the determination of LR asymmetry in a mammalian blastodisc embryo, the rabbit. It shows that GJC is required for the relay of LR initiating cues from the midline to the LPM.

GJs relay LR information from the midline to the LPM

Left-sided initiation of the Nodal cascade is a prerequisite for subsequent asymmetric morphogenesis of the visceral organs. In the rabbit, this restriction of *Nodal* initiation to the left side requires intercellular communication specifically during the 2 somite stage. This could be shown by inhibition of GJC in embryos taken into culture at the 2 somite stage, a treatment which induced ectopic right-sided expression of *Nodal* (Fig. 11, Fig. 12). The overall inhibition of GJ permeability however did not alter endogenous left-sided expression of *Nodal*, as no loss of expression and no temporal delay or spatial restriction of the *Nodal* domain was observed upon treatment with the GJ blocker heptanol (Fig. 11, Fig. 12). Treatment of whole embryos with RA also induced ectopic right-sided expression when embryos were taken into culture at the 2 somite stage (Fig. 15). Likewise, the left-sided domain was unaltered upon RA treatment (Fig. 15). RA is a known modulator of GJC, acting by decreasing GJ permeability (Zhang and McMahon, 2001), and might therefore act similar to heptanol. Taken together, three conclusions can be drawn from the inhibition of GJC in whole embryos: (1) GJC is specifically important during the 2 somite stage. (2) On the right side of the embryo, intercellular communication via open GJs leads to inhibition of *Nodal* expression. (3) On the left side GJ permeability is down-regulated which initiates the Nodal cascade. This asymmetric regulation of GJC could be controlled by events occurring at the embryo's midline.

Differential regulation of GJC by a functional PNC

In the embryonic midline of vertebrates one entity specifically harbors the potential to determine LR asymmetry: the PNC (or KV in fish and GRP in frog; Shook et al., 2004; Essner et al., 2005; Kramer-Zucker et al., 2005; Blum et al., 2006; Schweickert et al., 2007). A functional PNC in mouse and rabbit is characterized by (1) bilateral expression of *Nodal* bordering a widening of the posterior notochordal plate where (2) leftward fluid flow driven by rotating monocilia occurs. These two important

features of the rabbit PNC develop in successive steps and the present work showed that a biphasic gain of functionality determines the sequence of LR asymmetry development.

In the early phase of PNC development from late stage 5 until the 1 somite stage, the LPM is initialized to express *Nodal* at later stages. This initiation requires *Nodal* expression in the PNC domain. Towards the end of stage 5, when the notochordal process surfaces from under the hypoblast (Fig. 3D), paranotochordal expression of *Nodal* can be detected for the first time. This expression of *Nodal* at the PNC is likely to be induced by the combined action of Shh and Foxa2. Both proteins are expressed in the PNC and interact in the formation of node, notochord and floorplate (Dufort et al., 1998; Sasaki et al., 1999). In the PNC-specific enhancer region of the *Nodal* gene binding sites for Foxa2 have been identified (Brennan et al., 2002) and Shh has been shown to induce *Nodal* expression in chick (Levin et al., 1995).

When LP tissue was explanted before the appearance of *Nodal* at the PNC (i.e. before late stage 5), *Nodal* expression was never observed in the isolated LPM. This matches the data from (Pagan-Westphal and Tabin, 1998) in chick, where LPM expression of *Nodal* was never induced when LP tissue was explanted at stage 5, which is before the appearance of paranotochordal *Nodal* expression in the chick. When rabbit LP tissue was removed after *Nodal* expression had been established at the PNC, isolated LPM had been rendered capable of expressing *Nodal* after culture. Likewise, in left LP tissue of the chick isolated after the onset of paranotochordal *Nodal* expression, *Nodal* transcripts were found after culture (Pagan-Westphal and Tabin, 1998). The same is true for *Xenopus*, where LP explants were performed at stage 15 (Lohr et al., 1997), which is after establishment of the *Xnr1* domain bordering the GRP but before left-sided expression in the LPM. LPM from both sides was capable of expressing *Xnr1* after culture (Lohr et al., 1997). Furthermore, it has been shown in mouse that induction of *Nodal* in the LPM requires signals emanating from the midline (Brennan et al., 2002; Saijoh et al., 2003). Saijoh and colleagues (2003) demonstrated that loss of *Nodal* induction in the LPM of mice homozygous for a hypomorphic *Nodal* allele was due to the lack of paranotochordal *Nodal* expression. This loss of LPM-*Nodal* could be rescued by reconstitution of the PNC-

Nodal domain, evidencing that *Nodal* is the signal determining the inductive function of the PNC. As Nodal can act as a long-range morphogen (Chen and Schier, 2001) and its expression in the LPM is *Nodal*-responsive (Norris et al., 2002; Yamamoto et al., 2003; Saijoh et al., 2005), it is likely that Nodal produced at the PNC initiates its own transcription in the LPM. Alternatively, Nodal signaling could induce a relay mechanism which in turn bridges the distance and activates the LPM domain.

Initiation of the competence to express *Nodal* is not restricted to the left LPM. Signals originating in the PNC region spread into every direction and render LPM on both sides competent to express *Nodal* at later stages. This is demonstrated by the fact that LP tissue from both sides expressed *Nodal* when isolated at late stage 5, at stage 6 or the 1 somite stage (Fig. 17). Additionally, presence of midline tissue increased the level of expression in explants from either side (Fig. 17).

In the late phase of PNC development the supply of LR cues by the midline is maintained (*Nodal* continues to be expressed at the PNC), but a regulation biasing *Nodal* initiation in the LPM sets in at the 2 somite stage. While the left LPM now crucially requires midline-derived signals, the right LPM does not experience significant regulation from the midline during the 2 somite stage (Fig. 17). In line with the above assumption on the differential regulation of GJC, signals from the midline towards the left side might decrease left-sided GJC to initiate *Nodal* expression. The right side does not receive these midline-derived signals so that right-sided GJC remains unaltered (i.e. permeable GJs) and *Nodal* initiation is repressed.

From the 3 somite stage onwards regulation from the midline is also required to maintain the right-sided fate, i.e. no activation of the Nodal cascade. A lack of these regulatory signals resulted in ectopic *Nodal* expression (Fig. 17), yet this loss of *Nodal* repression was not due to alterations in gap junctional conductance (Fig. 12B).

It has been shown in the mouse that *Nodal* expression in the left LPM induces *Lefty* in the midline (Yamamoto et al., 2003). Since Lefty proteins act as feedback inhibitors of Nodal signaling (Chen and Shen, 2004), Lefty could be the factor which takes over the repression of *Nodal* in the right LPM from the 3-4 somite stage onwards.

The late phase of PNC functionality, during which *Nodal* expression is differentially regulated, is characterized morphologically by the caudal widening of the notochordal plate (Fig. 3G) and by the formation of a leftward-directed cilia-driven fluid flow above the PNC (Okada et al., 2005). Stage-specific analyses in rabbit embryos have shown that leftward flow can be reliably detected from the 2 somite stage onwards (A. Rietema, personal communication), which coincides with the emergence of a mechanism regulating GJC identified in this work. The most important readout of the flow were transient elevations in intracellular calcium observed at the left border of the PNC in mouse (McGrath et al., 2003; Tanaka et al., 2005) and fish (Sarmah et al., 2005) embryos. Additionally, membrane-sheathed vesicles filled with RA and Shh have been detected as a cargo of leftward flow in the mouse (Tanaka et al., 2005). These so called NVPs (node vesicular parcels) were found to be fragmented on the left side of the mouse PNC, which could lead to a release of their contents onto adjacent cells. Both elevated levels of calcium and RA are known to reduce GJC (Zhang and McMahon, 2001) and RA has been identified in this study to induce *Nodal* expression. Together with a rise of intracellular calcium induced by leftward-directed fluid flow, RA could lead to an inhibition of GJC on the left side of the PNC, inducing *Nodal* expression. Leftward-directed fluid flow could thus be considered the midline signal providing the differential regulation of GJC on the left vs. the right side. How could a left-sided reduction in GJ permeability then lead to initiation of the Nodal cascade? This might be accomplished by an interplay between Cx43 and FGF8 signaling.

LR differences in GJC define the asymmetric function of FGF8

In the rabbit embryo, FGF8 acts as an *in vivo* inhibitor of *Nodal* expression exclusively on the right side (Fischer et al., 2002). Although it exerts an asymmetric function, *Fgf8* is expressed symmetrically in and around the node and PNC in rabbit and mouse embryos (Crossley and Martin, 1995; Fischer et al., 2002) and RTK activity, indicating activation of the FGF receptor, was found to be symmetrical in and

around the mouse PNC (Tanaka et al., 2005). Growth factor signaling is known to affect GJC in various ways - by regulating expression of connexins, by modulating channel assembly or through other posttranslational modifications like e.g. phosphorylation of mature channels (Makarenkova et al., 1997; Solan and Lampe, 2005). On the one hand, regulation by FGFs increased Cx43-mediated GJC. This was accomplished by e.g. up-regulation of Cx43 protein levels in chick limb bud explants (Makarenkova et al., 1997) or without increasing connexin protein level or channel assembly in primary cultures of embryonic chick lens cells (Le and Musil, 2001). On the other hand, activation of the MAPK/ERK pathway, which occurs downstream of FGFR1 activation, led to an inhibition of GJC by the phosphorylation of specific serine residues of Cx43 (Warn-Cramer et al., 1998).

In the above cases FGF8 regulates GJC, however, GJC can also regulate FGF8 signal transduction. It has been demonstrated that about 50% of the cell's activated ERK can arise from an amplification of ERK-signaling by Cx43-mediated GJC (Stains and Civitelli, 2005). Reducing the permeability of GJs decreases ERK activation which in turn results in the diminished activation of the transcription factor Sp1 and a marked down-regulation of target gene expression (Stains and Civitelli, 2005). Based on these observations a model was proposed in which the cell in a primary response to a growth factor stimulus activates ERK and produces a second messenger. Upon passage through GJs, the second messenger activates the ERK pathway in adjacent cells and thus the growth factor response spreads and amplifies itself (Stains and Civitelli, 2005). This model could be adapted to the LR-context if GJC would have a regulatory influence on ERK-mediated FGF8 signaling. FGF8, which is expressed in and caudo-lateral to the PNC, activates the ERK pathway at the embryo's midline. As the experiments presented in Fig.11 and Fig. 12 show, GJs are permeable on the right side of the midline. ERK activation would thus be multiplied on the right side leading to a right-sided intensification of FGF8 signaling. It has been shown that ERK-mediated FGF8 signaling can inactivate Smad2, the downstream effector of Nodal signaling, which results in inactivation of Nodal signaling (reviewed by Massague, 2003). Thus *Nodal* initiation on the right side could be inhibited by high levels of activated ERK which inactivate Smad2. On the left side however, due to the

presumably decreased permeability of GJs, only low levels of activated ERK would be produced. This would attenuate the repressive effect of FGF8 and additionally restrict its range. This restriction of FGF8 signaling would finally result in activation of the Nodal cascade.

Indeed the repressive effect of FGF8 signaling on *Nodal* expression required intact GJC in the rabbit embryo. When conductance of GJs was decreased in whole embryos, which according to Stains and Civitelli (2005) would lead to a dampening of FGF signaling, repression of *Nodal* by FGF8 was not observed. Only when the dose of FGF8 protein was increased, *Nodal* transcription could be repressed during the inhibition of GJC (Fig. 13). Additionally, ectopic expression of the Nodal cascade in the right LPM induced by inhibition of GJC was most likely due to an impairment of FGF8 function, as FGF8 applied to the right LP restored the wild type situation, i.e. no induction of the Nodal cascade. An asymmetric regulation of the FGF8 stimulated MAPK/ERK pathway would satisfyingly explain the right-sided repressive effect of FGF8 despite its symmetric expression (Fischer et al., 2002) and the uniform activation of its receptors (Tanaka et al., 2005). In addition to their asymmetric function, GJC and FGF8 proved to be required in the paraxial and intermediate mesoderm and not in the LPM directly (Fig. 18, Fig. 19). This suggests that the repressive mechanism provided by the interplay of GJs and FGF8 does not directly inhibit *Nodal* expression in the LPM, but might instead prevent further "*Nodal*-inducing" input from the midline.

A model for the relay of LR initiating cues from the midline to the LPM

The present work showed that LR determination in the rabbit is a multi-step process which requires a functional PNC and GJs for the relay of LR-instructive signals from the midline to the LPM. This process can be broken down into the four distinct phases depicted in Fig. 20. (A) Before the development of functionality, the PNC emits no LR-instructive signals. Due to permeable GJs FGF8 signaling from the streak is not impaired. If LP tissue is explanted at this point in development, no LPM

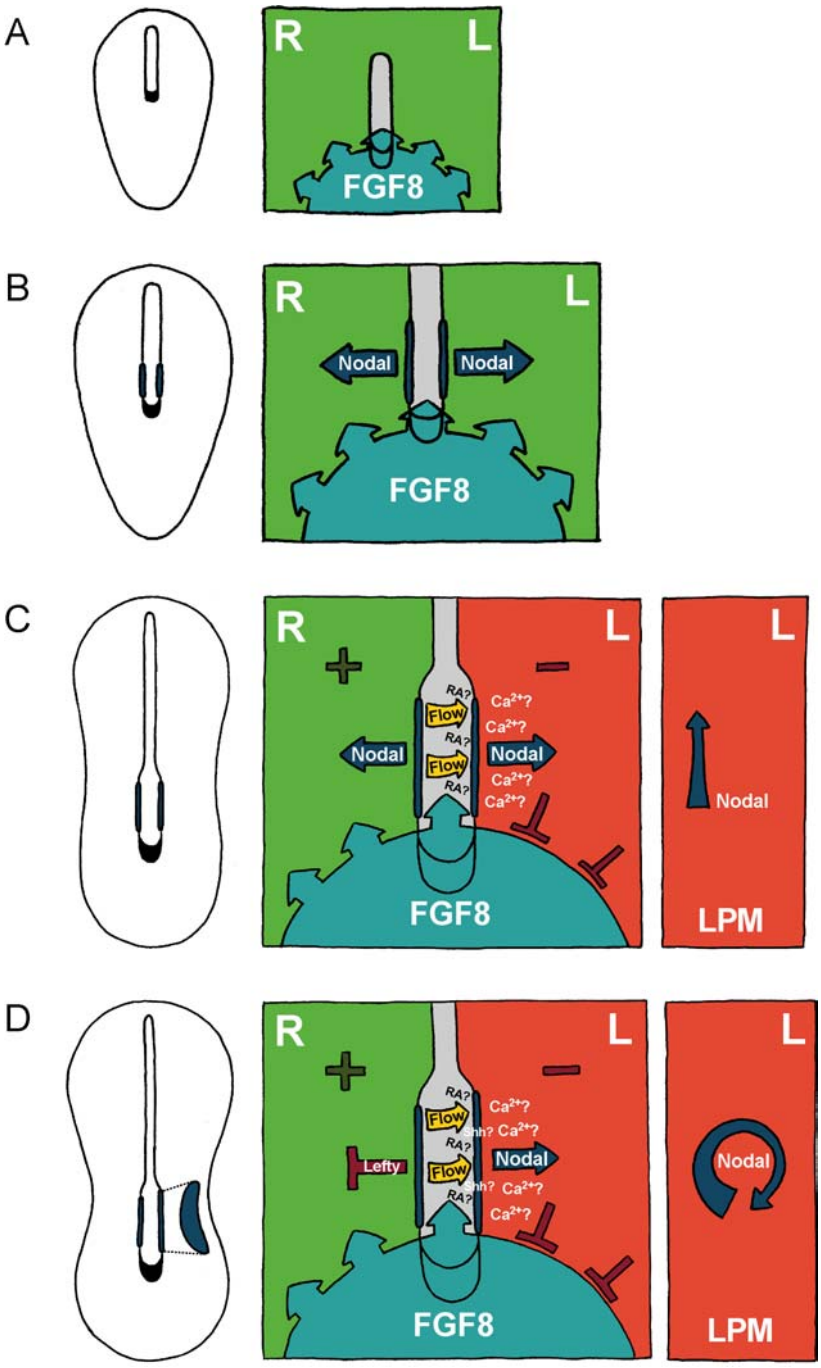

Fig. 20 GJC and FGF8 relay LR information from the PNC to the LPM. Schematic representation of embryos and signal transduction at the PNC at (**A**) early stage 5, (**B**) at stage 6, (**C**) at the 2 somite stage and (**D**) at the 3 somite stage. Permeable GJs are represented by green coloring, reduced permeability of GJs is indicated by red coloring. Expression and range of FGF8 signaling is indicated by light blue coloring. Note that from the 2 somite stage onwards (**C**, **D**) FGF8 signaling is attenuated on the right side as illustrated by the lack of light blue arrows. Stippled lines in schematic embryo shown in (**D**) indicate that expression of Nodal in the left lateral plate mesoderm (LPM) commences at the level of paranotochordal expression.

expression is observed after culture, as the cells have not received initiating signals. (B) From late stage 5 until the 1 somite stage, signals from the paranotochordal expression domain of *Nodal* spread towards the LPM on both sides. FGF8 function is not impaired as GJs are permeable on either side of the midline. Explants from both sides isolated at this stage are now capable of expressing *Nodal* after culture, as they have received inductive signals from the PNC domain. (C) Full functionality of the PNC is characterized by *Nodal* expression and leftward directed fluid flow at the 2 somite stage. The flow-mediated left-sided accumulation of RA together with a wave of Ca^{2+} initiated at the left margin of the PNC reduces the permeability of GJs on the left side of the embryo. This left-sided inhibition of GJC reduces the range of FGF8 signaling and will lead to a release of *Nodal* repression. Many left lateral plates isolated at that stage lack *Nodal* expression, as they are separated from the instructive midline signal (Nodal protein?) and have not fully experienced the release of repression by FGF8. Right lateral plates do not express *Nodal* as they are now under the full repressive influence of FGF8. (D) After its initiation at the 2-3 somite stage, *Nodal* expression is maintained by the positive feedback of Nodal signaling on *Nodal* transcription and stabilized by a continued input from the PNC. Additionally, a flow-mediated accumulation of Shh at the left margin of the PNC may stimulate the enlargement of left-sided PNC-*Nodal* expression and enhance the instructive signal originating from the PNC. Left lateral plate explants performed after the 2 somite stage confirm the requirement for a combination of positive feedback and continued input, as 80% of explants do express *Nodal* but the rest lacks *Nodal* expression. Towards the right side, repression of the Nodal cascade after the 2 somite stage is maintained by the competitive inhibitor Lefty (Yamamoto et al., 2003; Nakamura et al., 2006). A continued repressive effect of midline Lefty may be required as long as *Nodal* persists in the left LPM. Consistent with this assumption, right lateral plates explanted after the 2 somite stage and therefore lacking midline signals started to express *Nodal*.

Taken together the presented model rests on three main mechanisms: (1) a bilateral spread of Nodal protein to both LPs conferring competence for the left signaling

cascade, (2) a bilateral repression of this very cascade mediated through the FGF8/GJC module and (3) a flow-mediated compensation of this repression acting at the 2 somite stage specifically at the left side. This model is particularly attractive as it accounts not only for all experimental data presented within this thesis but is consistent with genetic and experimental data generated in other vertebrate model organisms such as zebrafish, *Xenopus* and mouse. Yet, if leftward flow at the PNC plays such a decisive role for LR-determination in these organisms, how can asymmetry be created in an embryo in which no flow is generated?

Ciliation and *Nodal* expression in the pig embryo suggest a second, flow-independent mode of LR-specification

The chick is the only model organism in which cilia have been described (Manner, 2001; Essner et al., 2002), but no fluid flow has been detected as yet. A relay of asymmetry information from the midline to the LPM must thus be accomplished by an independent mechanism. Experimental data in chick suggest that despite the absence of flow, the module consisting of GJC and FGF8 has been implemented in this process.

The earliest obvious asymmetry in the chick is the asymmetric morphology of Hensen's node (Dathe et al., 2002). Expression of *Shh* in the node mirrors this morphological asymmetry (Levin et al., 1995) and GJC has been shown to be required to establish this left-asymmetric *Shh* expression (Levin and Mercola, 1999). It was found that Shh induces ectopic right-sided expression of *Nodal* when a pellet of Shh-producing cells was placed on the right side of the embryo next to Hensen's node (Levin et al., 1995). Pagan-Westphal and Tabin (1998) however showed that Shh could not directly induce *Nodal* in the LPM but required the presence of at least paraxial tissue for *Nodal* induction. The authors thus proposed that the inductive capacity of Shh on *Nodal* might be relayed from the node to the LPM via a secondary signal residing in the paraxial mesoderm, yet the nature of the signal was still unknown at that time (Pagan-Westphal and Tabin, 1998). In the initial Shh

experiments performed by Levin and colleagues it can be seen that the application of Shh induced a large right-sided paranotochordal domain of *Nodal* next to the posterior notochord (cf. Levin et al., 1995, Fig. 5E). Deduced from these observations Shh, which is expressed on the left side of Hensen's node, induces the unilateral left-sided paranotochordal expression of *Nodal*. This signal can spread towards the left LPM and initiate the Nodal cascade. FGF8 however is required on the right side: it is expressed right-asymmetrically in Hensen's node and suppresses initiation of *Nodal* (Boettger et al., 1999), similar to its function in rabbit (Fischer et al., 2002). The asymmetric patterning of Hensen's node in chick could thus make a flow-based mechanism for the relay of LR signals from the midline to the LPM dispensable. The morphological asymmetry of the node in the chick embryo supposedly is established by a blastodisc-wide gradient of morphogenic molecules (Levin and Mercola, 1999, Levin et al., 2002). Such a gradient is presumably set up by differences in membrane potential between the left and right side of the primitive streak (Levin et al., 2002). However, no such gradients were found in the rabbit embryo (Fig. 9) suggesting that in the rabbit, patterning of Hensen's node may not be required which is supported by the fact that the rabbit node itself does not exhibit any morphological or molecular asymmetries.

The present study revealed that pig embryos show morphological and molecular characteristics strikingly similar to chick. Both pig and chick embryos (1) show unilateral expression of Nodal on the left side of the notochord, (2) have a morphologically asymmetric node and (3) a notochord forming a multi-layered rod instead of a single-layered plate. Furthermore, (4) the notochord is covered by a continuous layer of endoderm bearing (5) monocilia which are short and stubby, sparsely distributed and not confined to the PNC region. As no flow has been detected in the chick, it seems very unlikely that similar cilia in the pig could produce a leftward fluid flow.

The lack of a cilia-driven leftward fluid flow in chick suggested that birds might represent a side branch which has lost the "flow-module" during evolution. If flow is indeed missing in pig embryos as well, this view of a "peculiarity" of avian embryos will have to be put into perspective. The morphological and molecular homology of

the PNC in chick and pig suggests that vertebrates display two modes of paranotochordal *Nodal* expression: In species in which *Nodal* is expressed bilaterally, a flow-based mechanism biases signaling towards the left side. In agreement with this notion, all model organisms in which a bilateral paranotochordal domain has been described (zebrafish and medaka, *Xenopus*, mouse and rabbit) show a cilia-driven fluid flow in the region encompassed by *Nodal* expression (Nonaka et al., 1998; Fischer et al., 2002; Long et al., 2003; Essner et al., 2005; Okada et al., 2005; Schweickert et al., 2007). Ciliary motility and ensuing fluid flow requires the at least transient exposure of the PNC region to the archenteron cavity. In contrast, species in which notochord morphogenesis occurs without epithelialization and integration into the archenteron (chick and pig), *Nodal* expression at the PNC is unilateral (left-asymmetric). The molecular asymmetry at the midline of these species seems to be sufficient to induce left-sided activation of *Nodal*, making a flow-based mechanism dispensable. Although these observations rest on two species only, both display remarkably high similarity at the morphological as well as the molecular level. GJC has been shown to be involved in establishing molecular asymmetry at the chick node (Levin and Mercola, 1999). It should be interesting to see whether the GJ/FGF8 module is required to generate morphological asymmetry in the first place which in consequence results in unilateral *Nodal* expression. In the light of this reasoning it remains to be determined whether cilia-driven fluid flow truly provides the basic mechanism for symmetry breakage in all vertebrates species.

Material and methods

Embryological procedures

All embryos used in this work were derived from timed matings of either NZW rabbits or German Landrace pigs. All steps involving isolation and culture of embryos were conducted under sterile conditions using sterile buffers, media, labware and instruments. Fixation in a solution of 4% paraformaldehyde in PBS^- (4% PFA) was conducted for 1h at room temperature (RT) or overnight at 4°C unless stated otherwise.

Dissection and storage of embryos

After the abdominal cavity of the dead animal had been opened, the uterus was removed as a whole and transferred to PBS^+.

Dissection and fixation of pig embryos

To collect pig embryos, each uterine horn was flushed with about 2l of PBS^+. The embryos were harvested from the through-flow, washed in PBS^+ and separated from extraembryonic tissue using fine tweezers and iridectomy scissors under a stereomicroscope. They were either fixed in 4% PFA or processed for electron microscopy.

Dissection and fixation of rabbit embryos

If rabbit embryos were to be used for *in vitro* culture, the uterus was only rinsed in PBS^+ and then processed natively. If intended for *in situ* hybridization, rabbit uteri

were prefixed as a whole in 4% PFA for 10-15min at RT and washed in PBS^+ afterwards. Uteri from both procedures were transferred to fresh PBS^+ where excess fat and mesenteria were removed and the uterus was separated into pieces between the embryo implantation sites. Single parts of the uterus were further dissected under a stereomicroscope using fine tweezers and iridectomy scissors. The bulging uterine tissue opposite of the implantation site was carefully cut and removed until the embryo covering the mucosa became accessible. The embryo together with some of the surrounding extraembryonic tissue was cautiously detached from the mucosa, transferred to another culture dish with fresh PBS^+ and further trimmed in a circular fashion. Embryos were either left natively for direct use in an *in vitro* culture experiment, fixed in 4% PFA or processed further for electron microscopy.

Dehydration and storage

If desired, all embryos fixed in PFA could be stored until further utilization. After fixation had been completed, they were washed three times for 10min in PBS^+ and then dehydrated in an ascending methanol series (25, 50, 75% methanol in PBS^-, 2x 100% methanol). Embryos were stored in 100% methanol at -20°C.

In vitro culture of rabbit embryos

Rabbit embryos intended for *in vitro* culture were dissected as described above, then processed for in vitro culture and cultured in a small incubator under humidified air with 5% CO_2 at 38°C until they reached the desired stage.

Preparation of culture dishes

A substratum for the embryo during culture was prepared from 0,5% agarose in PBS^- which had been sterilized by autoclaving and then stored at room temperature. 100µl of remelt agarose were pipetted into small culture dishes (4cm in diameter) and spread to create a circular mound as flat as possible. Enough culture medium to

cover the agarose mound was added to the dishes which were then pre-incubated until further usage.

Preparation of substance soaked beads

To place proteins and chemical compounds onto the embryo during culture, small beads known from affinity chromatography columns were used. Heparin-coated acrylic beads (for FGF-8) or Affi-Gel Blue Gel beads (for SU5402) were washed three times in 50ml PBS^+ and stored on ice until further usage. The lyophilized proteins were reconstituted according to the manufacturer's suggestions and aliquots were stored at -80°C. SU5402 was dissolved in DMSO at a concentration of 1mg/ml and stored in aliquots of 10µl at -20°C. Because SU5402 is likely to deteriorate if exposed to light the substance was kept and handled in the dark whenever possible. Single tubes were thawed and a droplet of 5-10µl was pipetted into a Parafilm-coated culture dish. Beads were added to the substances by gently tapping a bead-filled pipette tip onto the droplet and allowing the beads to sink into the solution. This procedure prevented the droplet from being further diluted by PBS^+ in the pipette tip. The beads were incubated on ice (proteins) or at room temperature (SU5402) for at least 1h before use.

Preparation of modified medium

If it was desirable to have the whole embryo in contact with a drug, the substance was applied directly in the culture medium. An emulsion of 1µl heptanol in 1ml culture medium (1:1000) was freshly prepared before each experiment by heavy vortexing and ultrasonication until the liquid appeared milky. Further dilutions were prepared as required. A 1.6mM stock solution of retinoic acid in 70% EtOH was prepared in the dark, stored in aliquots at -20°C and directly diluted into the culture medium as desired.

Microsurgical dissection of embryos

To prepare explants of lateral plate tissue, a freshly dissected embryo was placed into a culture dish with fresh PBS^+. The lateral plate was removed with fine

iridectomy scissors by cutting in a straight line along the paraxial mesoderm. Care was taken to leave the presomitic and somitic mesoderm with the midline.

Placement of embryos onto agarose mounds

Single embryos prepared from native uteri were carefully transferred into a medium filled culture dish using a plastic pipette. With fine tungsten needles the embryo was gently pulled up the agarose mound and spread out, ectoderm down, on top of the mound. Surplus medium was now removed with a pulled out glass pipette and the fluid level was adjusted so that it just reached the extraembryonic tissue. In this way, the embryo was constantly wetted by a thin liquid film and also held in place by the surface tension of the medium. The procedure was performed in the same way for embryos that had been microsurgically dissected before culture.

When embryos should be cultured in modified medium, dishes were taken from the incubator, the pre-incubated medium was removed and replaced by fresh modified medium. The embryo was then transferred directly into the modified medium and placed onto the agarose mound as described above.

Implantation of substance soaked beads

Using a sharpened tungsten needle a small lesion was scraped into the embryo at the respective site of bead implantation. With a little hook bent into the tip of a tungsten needle, a bead was picked from the droplet in which it had been incubated. It was placed onto the embryo and carefully pushed into place with a second needle so that it came to lie between ecto- and endoderm. After positioning the bead, the embryo was put into the incubator and cultured to the desired stage.

Fixation of cultured embryos

After culture was completed, the embryo was gently rinsed with a few drops of culture medium to remove cell debris that had accumulated during the incubation period. The medium was then aspirated and replaced by 4% PFA which was filled in high enough to lift the embryo off the agarose mound and let the tissue float on the

surface of the fixative. Embryos were either fixed for 1h at room temperature or overnight at 4°C and then prepared for storage as described above.

Cloning of gene sequences and expression analysis

Partial sequences of genes originally described in other organisms were cloned and analyzed for their expression patterns in rabbit and pig embryos.

Isolation and handling of nucleic acids

Isolation of RNA from embryos and adult tissues

Tissue from E12 embryos and adult kidney was prepared freshly, cut into small pieces and frozen immediately in liquid nitrogen. Total RNA was extracted following the Promega “SV Total RNA Isolation System” using the spin column method. RNA was eluted in 100µl sterile DDW, measured photometrically and stored at -80°C.

Preparation of small amounts of plasmid DNA (mini-prep)

Plasmid DNA from *E. coli* cultures was isolated using a modified alkaline lysis protocol. All centrifugation steps were done at 4°C. 3ml of selective LB medium (100µg/ml Ampicillin) were inoculated with a single bacteria colony from a selective plate and grown overnight with vigorous shaking at 37°C. 2ml of the culture were poured into a microcentrifuge tube and bacteria were pelleted in a microcentrifuge at 6000g for 15min. The supernatant was discarded and the pellet resuspended by heavy vortexing in 100µl P1 buffer. When the bacteria suspension appeared uniform, 200µl of P2 buffer were added and the tube was inverted several times to thoroughly mix the reagents. Alkaline lysis was allowed to proceed for 5min and was then stopped by neutralizing with 150µl of P3, again inverting the tube several times. After

20min of incubation on ice, the lysate was cleared from the fluffy white precipitate containing genomic DNA, cell debris, proteins and potassium dodecyl sulphate by centrifugation in a microcentrifuge at full speed for 10min. 400µl of the clear supernatant were transferred to a fresh microcentrifuge tube and mixed well with 1ml of 100% Ethanol to precipitate the plasmid DNA. After precipitation for 30min at -20°C the plasmid DNA was pelleted by centrifuging at full speed for 10min. The pellet was washed in 70% ethanol, centrifuged briefly, dried and resuspended in 50µl sterile DDW.

Preparation of medium amounts of plasmid DNA (midi-prep)

100ml of selective LB medium (100µg/ml ampicillin) were inoculated with 1ml of a positively tested bacteria culture and grown overnight in a 1000ml conical flask with vigorous shaking at 37°C. Bacteria were harvested by centrifugation, lysed and DNA was purified following the Promega “PureYield Plasmid Midiprep System” using the vacuum method.

Measuring the concentration of nucleic acids

The concentration of nucleic acids in aqueous solutions was determined via spectrophotometry. The ratio of absorption (A) at 260nm and 280nm wavelength indicated the purity of the solution (pure nucleic acid solution: 1.8 for DNA, 2.0 for RNA). The content of either DNA or RNA was inferred from the A_{260} value with 1 unit corresponding to 50µg/µl DNA and 40µg/µl RNA.

Restriction enzyme digests of DNA

To check for insertion of the correct PCR product after a mini-prep, inserts were released from the plasmids by digestion with a restriction enzyme cutting on both sides of the multiple cloning site. EcoRI could be used for both pCRII-TOPO and pGEMTeasy vectors. Typically to 10µl of plasmid-DNA 1.5µl 10x buffer and 1µl enzyme were added, the mixture was filled up with 2.5µl sterile DDW to a final volume of 15µl and incubated at 37°C for 2hrs. After digestion the whole volume of the reaction was analyzed on a 1% agarose gel.

For linearization digests typically 20µg of plasmid-DNA was used in a 100µl reaction. Depending on the concentration, about 5µl of restriction enzyme were used and the digestion was incubated for at least 7hrs or preferably overnight. 1µl of the digestion was controlled on a 1% agarose gel.

Agarose gel analysis

The products of each reaction were checked on a standard 1% agarose gel supplemented with an end concentration 0,4µg/ml ethidium bromide solution.

Polymerase Chain Reaction (PCR)

First strand synthesis of cDNA

cDNA was synthesized from total RNA preparations by reverse transcription using M-MLV Reverse Transcriptase. A standard protocol started with 1µg of total RNA to which 1µl of random hexamers was added and filled up with sterile water to a total volume of 14µl. The solution was heated to 70°C for 5min to melt secondary structures within the template and immediate cooling on ice thereafter prevented these structures from reforming. The reagents were then supplemented with 5µl 5x M-MLV Reaction Buffer, 1.25µl 10mM dNTPs, 1µl (200units) of M-MLV RT and filled up to a volume of 25µl. After an initial incubation for 10min at room temperature, the reaction was put to 42°C for another 50min to complete first strand synthesis.

Oligonucleotides and PCR conditions

For the design of primers, already available sequences of interest preferably from mouse or human were run against a genomic database (NCBI Blastn) or were directly aligned to each other. Alignments derived from such searches were checked for regions of high sequence homology and oligonucleotides of about 25 bases length spanning these regions were designed as primers for the following PCR reactions. About three forward and reverse primers per gene were used to amplify products of different lengths. The primer combination giving the best PCR results

was used to obtain a fragment subjected to further amplification in bacteria. The following primer combinations and PCR conditions were used:

Foxj1 (rabbit, 825bp)

forward for2 5' CTG TCG GCC ATC TAC AAG TGG ATC A 3'

reverse rev4 5' CCA CAC TGG CCC AGT CCT GCA GGT C 3'

primer concentration: 10µM

annealing conditions: 66°C, 1'

Kif3a (rabbit, 660bp)

forward: for1 5' GAA AGC TGC GAT AAT GTG AAG GT 3'

reverse: rev1 5' TCT ATA GTA ATT GTA AAG ATG GC 3'

primer concentration: 25µM

annealing conditions: 52°C, 1'

Ird (rabbit, 995bp)

forward: for2 5' TGT GAA GCT GAC TTA CTC AAG GCT G 3'

reverse: rev6 5' CTT GAT CCA CTT AAT TCC CTG TTG C 3'

primer concentration: 5µM

annealing conditions: 52°C, 1'

Nodal (pig, 611bp)

forward for1 5' CAG AAC TGG ACI TTC ACI TTT GAC TT 3'

reverse rev2 5' TAI GCA TTG TAC TGC TTI GGG TA 3'

primer concentration: 25µM

annealing conditions: 55°C, 1'

polaris (rabbit, 773bp)

forward: for3 5' AGA AAT TAT TCC AAA GCC ATT AA 3'

reverse: rev6 5' GCC TTC TCA TAA TCA CCA TTT GCA A 3'

primer concentration: 25µM

annealing conditions: 58°C, 1'

Rfx3 (rabbit, 832bp)

forward for2 5' TCA CTC AGT GAC ACA CAC AAC TCG G 3'

reverse rev5 5' CTC ATG TTT GCA CAG AGT TAT CAG C 3'

primer concentration: 25µM

annealing conditions: 60°C, 1'

Standard PCR protocol

For a 25µl PCR reaction 100ng of previously prepared template cDNA (see 2.?.2.1) was mixed with 2mM dNTPs, 1U of Taq DNA polymerase, 5µl 5x Buffer, 1µl of each forward and reverse primer (concentration indicated below) and filled up to 25µl with sterile double distilled water (DDW). If necessary, DDW was substituted with varying amounts of DMSO (4-12%) to enhance specific hybridization of the oligonucleotides.

A standard PCR cycling program started with (1) 1' at 95°C, followed by (2) 30'' at 95°C, (3) 30'' or 1' at the annealing temperature indicated below and (4) 1' at 72°C. Steps (2) to (4) were repeated for 39 times before the reaction was (5) stopped and kept in the cycler at 8°C. Step (1) and (2) yield a denaturation of the double-stranded template DNA, step (3) allows hybridization of the primers to the single-stranded DNA and during step (4) the Taq polymerase elongates the sequences at the primer's 3' end.

If the PCR product was intended to be further amplified in bacteria, an extra 15min at 72°C were added after the 40 cycles to make use of the Taq Polymerase's Terminal Transferase activity, that adds an extra deoxyadenosine onto each 3' end of already existing double-stranded PCR product. This creates a single 3'-A overhang that can be utilized for ligation into a cloning vector.

Subcloning of PCR products and bacteria culture

Two different cloning systems were used for the subcloning of PCR products: the desired sequences were either amplified using the TOPO TA Cloning Kit with pCRII-TOPO vector and OneShot chemically competent cells or were ligated into the pGEMTeasy vector and transformed into chemically competent XL1-blue cells. Both vectors have their multiple cloning site within the coding region of β-galactosidase, so that clones can be selected by color screening.

Ligation of PCR products into cloning vectors

The linearized pCRII-TOPO vector has the enzyme topoisomerase covalently bound to 3'-T overhangs at the multiple cloning site. This enables the direct ligation of Taq-amplified PCR products with 3'-A overhangs into the vector. A cloning reaction was set up by combining 4µl of fresh PCR product with 1µl Salt Solution. To this 1µl of vector was added and the reaction was incubated for 10min at room temperature. The reaction tube was then placed on ice or stored at -20°C until needed for transformation.

PCR-products were ligated into the linearized pGEMTeasy vector with the help of T4 ligase. In a standard reaction, 5µl of ligation buffer, 1µl of vector and 1µl of T4 ligase were combined with 3µl of fresh PCR product. The reaction was incubated for 1h at RT or overnight at 4°C and then transformed into bacteria.

Transformation and clonal selection

The ligated vectors were transformed into chemically competent bacteria using the heat shock method. Different volumes (typically 50, 100, 150µl) of transformed bacteria were plated on LB-agar selective plates (100µg/ml ampicillin / 80µg/ml X-Gal for TOPO-cloning, 100µg/ml ampicillin / 0.5mM IPTG / 80µg/ml X-Gal for pGEMTeasy-cloning) and incubated overnight. Clones with white color, indicating insertion of a PCR product into the multiple cloning site, were selected for further amplification and analysis using a mini-prep procedure.

Sequencing and database analysis

Inserts of plasmids were sequenced at Seqlab, Göttingen. The obtained sequences were run against the NCBI database using the “blastn” algorithm (www.ncbi.nlm.nih.gov/BLAST).

Whole mount in situ hybridization

In vitro transcription of RNA probes

For in vitro transcription of RNA probes 200ng linearized plasmid with the insert of interest was used as a template. Depending on the orientation of the insert, 20units of either Sp6 or T7 polymerase were added to a mixture of template, 4µl Transcription Buffer, 0.5µl (= 20units) RNasin, 2µl DTT and 2µl 10x Dig-Mix. Sterile DDW was added to a final volume of 20µl and the mixture was incubated at 37°C for 2hrs. After transcription, 1µl of the transcription was mixed with 8µl sterile DDW and 1µl 10x Loading Buffer and checked on a 1% agarose gel for appropriate size and integrity of the product. 115µl 100% EtOH and 3.75µl 4M LiCl were added to the incubated transcription mixture and RNA was precipitated at -20°C for at least 30min. The tube was then centrifuged at full speed in a tabletop centrifuge at 4°C for 20min, the resulting pellet was rinsed in 70% EtOH and centrifuged again for 5min. The pellet was allowed to dry shortly before it was resuspended in 20-50µl of a 1:1 mixture of sterile DDW and formamide. The resuspended RNA was stored at -80°C until further use.

In situ hybridization

Whole mount in situ hybridization was used to detect the expression pattern of specific genes in whole rabbit or pig embryos. Expression of e.g. ciliary genes was tested in wild-type embryos whereas embryos after in vitro culture were assessed for LR marker gene expression.

Day 1: On the first day of the procedure, tissue was prepared for taking up the antisense RNA probe, which hybridizes to the endogenous target RNA. Embryos

were either used directly after fixation with 4% PFA or were rehydrated from storage in 100% methanol through a graded series of 75%, 50% and 25% methanol in PBS⁻. Embryos were washed three times for 5min in PBS⁻w and then the tissue was permeabilized for 5-10min in 10µg/µl Proteinase K in PBS⁻w at RT. Digestion was stopped in 2mg/ml glycine followed by three washing steps in PBS⁻w for 5min each. The tissue was then refixed for 15min at RT in 4% PFA supplemented with 0.2% glutaraldehyde. After washing three times in PBS⁻w for 5min the embryos were transferred into a 1:1 mixture of hybridization solution and PBS⁻w. After equilibration in 100% hybridization solution, a pre-hybridization period in 900µl hybridization solution at 65°C for 2-3hrs eliminated endogenous phosphatases. Depending on the concentration of the RNA, about 1µl of antisense probe (~20ng) was added to the vial and the embryo was incubated with the probe overnight at 70°C.

Day 2: On the second day excess antisense probe was removed in high strigency washing steps and the tissue was prepared for incubation with the anti-digoxygenin antibody. In a first step, the hybridization solution containing the antisense probe was replaced by 800µl hybridization solution without probe and embryos were washed in it for 5min at 70°C. In three steps each 400µl of 2xSSC (pH 4.5) were added and the embryo was washed twice in 2xSSC (pH 7) at 70°C afterwards. The washing steps in SSC were followed by four washing intervals in MAB, twice at RT for 10min and another two times at 70°C for 30min. Afterwards, embryos were washed three times in PBS⁻w at RT for 10min each and were then pre-incubated in antibody-blocking buffer at 4°C for 2hrs. In a second tube, the anti-digoxygenin antibody coupled to alkaline phosphatase was diluted 1/10.000 and pre-blocked for the same time. After the 2hrs of pre-incubation, the blocking buffer was replaced with the antibody-solution and the embryos were incubated with the antibody overnight at 4°C.

Day 3: On the third day, unbound antibody was removed in extensive washing steps and the staining reaction was started. Embryos were rinsed and then washed five times for 45min each in PBS⁻w containing 0.1% BSA. The washing in BSA was followed by two washing steps with PBS⁻w for 30min each and embryos were then transferred into AP1 buffer, which adjusts the pH of the tissue for the optimal reaction

of the alkaline phosphatase. AP1 buffer was changed twice and then replaced by a 1:1 mixture of AP1 buffer and BMPurple, the substrate for the alkaline phosphatase. The staining process was controlled and stopped by washing in PBS^{-}w, when the expected signal had reached a dark blue to violet color. A gradual methanol series intensified the signal and the embryos were afterwards stored in glycerol at 4°C.

Histological analysis of embryos after in situ hybridization

While embryos were equilibrated in a small volume of embedding medium (~1ml) the embedding mold was prepared. 2ml of embedding medium were mixed shortly but vigorously with 140µl of glutaraldehyde and poured into the two metal brackets arranged to form a square mold. The mixture was allowed to harden and the equilibrated embryo was transferred and spread evenly upon the surface of the block, excess embedding medium was carefully removed. Another 2ml of embedding medium mixed with glutaraldehyde were poured into the mold so that the embryo was now sandwiched between two layers of embedding mix. The hardened block was trimmed with a razor blade and glued onto a plate. The plate was mounted into the holder of the vibratome and 30µm thick sections were prepared. The sections were arranged onto glass slides, embedded with mowiol and protected with glass cover slips.

Structural analysis of notochordal plate cilia

Notochordal plate morphogenesis and ciliogenesis as well as ultrastructure of notochordal cilia were analyzed by scanning and transmission electron microscopy.

Scanning electron microscopy

Embryos were freshly dissected in PBS^+ and immersion fixed in either 2,5% glutaraldehyde (GA) or a mixture of 2-4% paraformaldehyde (PFA) and 2,5% GA for 1h at room temperature or overnight at 4°C. The specimens were washed three times for 10 minutes in 0,1M phosphate buffer (PB) and were then postfixed for 1hr in 1% OsO_4 in 1M PB at 4°C. After extensive washing embryos were gradually dehydrated in an ethanol series and stored in 100% EtOH at 4°C until submitted to the drying procedure. Critical point drying was performed using CO_2 as drying agent. Embryos were sputter with gold and viewed under a LEO DSM 940A.

Transmission electron microscopy

Embryos were dissected and fixed in a solution of 4% paraformaldehyde / 2.5% glutaraldehyde in Soerensen's phosphate buffer for 1hr at room temperature (RT) or at 4°C overnight. Postfixing was performed in 1% osmium tetroxide in Soerensen's buffer for 1hr at 4°C. In order to contrast microtubules, specimens were treated with tannic acid (1%) in Soerensen's buffer for 30min at RT. Following dehydration embryos were embedded in araldite CY212 (Plano, Germany), and polymerized for up to 48hrs at 60°C. Ultrathin sections (70nm) of NP tissue were cut using a Leica Ultracut S, mounted on copper grids, post stained with lead citrate, and viewed under a LEO 912 AB TEM at 80 kV.

Analysis of intracellular pH

BCECF-AM is a vital dye used to determine intracellular pH in living cells and tissues. The inactive AM ester is cell permeant and is cleaved by intracellular esterases into the active form. Loading of embryos was performed in PBS^+ to which pluronic had been added. Pluronic acts as a mild detergent and increases the loading efficiency of the AM ester. BCECF-AM was dissolved in anhydrous DMSO at 1mg/ml and further diluted 1:1000 in PBS^+ yielding a ~1.6µM solution. Embryos were incubated in BCECF-AM for 10-20min, washed briefly in PBS^+ and viewed under a Zeiss LSM for optical sections of the tissue or under a Zeiss Axioskop for widefield fluorescence images.

Buffers, Solutions and Media

For in situ hybridization:

Phosphate Buffered Saline 10x (PBS, 1l)

80g NaCl
2g KCl
14.4g Na_2HPO4
2.4g KH_2PO4
800ml DDW
adjust pH to 7.4, add DDW to 1L, autoclave.

Alkaline Phosphatase Buffer (AP1, 1l)

100ml 1M TRIS pH 9.5
20ml 5M NaCl
50ml 1M MgCl
add DDW to 1l.

Maleic Acid Buffer 5x (MAB, 1l)

58.05g (100mM) Maleic Acid

43.83g (150mM) NaCl
800ml DDW
adjust pH to 7.5 with 10N NaOH, add DDW to 1l, autoclave.

Sodium Sodium Citrate Buffer 20x (SSC, 1l)

175.3g NaCl
88.2g Sodium citrate
800ml DDW
adjust pH to 7.0, add DDW to 1l, autoclave.

Hybridization solution (1l)

10g Boehringer Block
500ml Formamide
250ml SSC 20x
Heat to 65°C for 1 hour
120ml DDW
100ml Torula RNA (10mg/ml in DDW; filtered)
2ml Heparin (50mg/ml in 1x SSC pH 7)
5ml 20% Tween-20
10ml 10% CHAPS
10ml 0.5M EDTA

Antibody Blocking Buffer

10% Heat Inactivated Goat Serum
1% Boehringer Block
0.1% Tween-20
dissolve in PBS at 70°C, vortexing frequently, then filter (0.45µm).

For bacteria culture:

Super Optimal Catabolite repression medium (S.O.C.)

0.5% Yeast extract
2.0% Tryptone
10mM NaCl
2.5mM KCl
10mM $MgCl_2$
10mM $MgSO_4$
20mM Glucose
autoclave

Lysogeny Broth (LB) medium

1% Tryptone
1% NaCl
0.5% Yeast extract
adjust pH to 7.0, autoclave.

LB agar

1% Tryptone
1% NaCl
0.5% Yeast extract
adjust pH to 7.0, add 15g/l agar before autoclaving.

For electron microscopy:

Sörensen phosphate buffer

Stock solution A: 0.2M NaH_2PO_4
Stock solution B: 0.2M Na_2HPO_4
for 0.1M pH 7.4: 19ml A, 81ml B, 100ml H_2O
for 0.1M pH 7.0: 39ml A, 61ml B, 100ml H_2O

Araldite resin mixture

23g Araldite CY 212
22g DDSA
mix well, then add
1.2g BDMA

Lead citrate (after Reynolds)

Lead Nitrate 1.33g
Sodium Citrate 1.76g
add
30ml DDW (carbonate free)
shake vigorously for 1min, then shake intermittently for 30min.
add
8ml 1N NaOH (carbonate free)
invert slowly, fill up to 50ml with DDW (carbonate free).

For DNA preparation:

P1
50mM TRIS HCl
10mM EDTA pH 8
add RNaseA (DNase free) to a final concentration of 100µg/ml

P2
0,2M NaOH
1% SDS

P3
3M Potassium acetate, pH 5.5

For other applications:

Medium for rabbit embryo *in vitro* culture

F-10 Nutrient Mixture with L-Glutamine
20% Fetal Bovine Serum
2% Penicillin/Streptomycin

Embedding medium for vibratome sections

2.2g Gelatine
135g Bovine Serum Albumin
90g Saccharose
dissolve in 450ml PBS.

Mowiol (Mounting medium)

96g Mowiol 488
24g Glycerol
24ml DDW
stir for 2h, then add
48ml TRIS 0.2M pH 8.5
stir for 20min at 50°C
centrifuge for 15min at 5000rpm, keep supernatant
and store at -20°C.

Tris Acetate EDTA Buffer (TAE)

40mM Tris-acetate
2mM EDTA
adjust pH to 8.0.

Sources of supply

Chemicals and labware:

Affi-Gel Blue Gel	BIO RAD, Munich
Agarose	Roth, Karlsruhe
Ampicillin	Applichem, Darmstadt
BCECF-AM	Molecular Probes (Invitrogen) Karlsruhe
Boehringer Block	Roche, Mannheim
Bovine serum albumin	Applichem, Darmstadt
BM Purple	Roche, Mannheim
CAS-Block	Zymed (Invitrogen) Karlsruhe
CHAPS	Sigma, Schnelldorf
Dig-Mix	Roche, Mannheim
Disodium hydrogen phosphate	Applichem, Darmstadt
Glass slides	Roth, Karlsruhe
Glass coverslips	Roth, Karlsruhe
DigMix	Roche, Mannheim
DTT	Promega, Mannheim
DMSO	Roth, Karlsruhe
EDTA	Roth, Karlsruhe
Ethanol	Roth, Karlsruhe
Ethidiumbromide	Roth, Karlsruhe
F10 medium	Gibco (Invitrogen) Karlsruhe
Fetal bovine serum	Sigma, Schnelldorf
Formamide	Roth, Karlsruhe
Gelatine	Roth, Karlsruhe
Glutaraldehyde	Applichem, Darmstadt
Glycerol	Roth, Karlsruhe
Goat serum	Sigma, Schnelldorf
Grids	Plano, Wetzlar
Heparin	Sigma, Schnelldorf

Heparin-Acrylic beads	Sigma, Schnelldorf
Heptanol	Roth, Karlsruhe
Iridectomy scissors	Fine Science Tools, Heidelberg
Lead nitrate	Serva, Heidelberg
Lithium chloride	Serva, Heidelberg
Loading Buffer	Applichem, Darmstadt
Lucifer Yellow	Molecular Probes (Invitrogen) Karlsruhe
Maleic acid	Roth, Karlsruhe
Magnesium chloride	Roth, Karlsruhe
Methanol	Roth, Karlsruhe
Oligonucleotides	Operon, Cologne
Osmium tetroxide	Plano, Wetzlar
Parafilm	Roth, Karlsruhe
Paraformaldehyde	Applichem, Darmstadt
PBS^{+} (10x)	Gibco (Invitrogen) Karlsruhe
Penicillin/Streptomycin	Gibco (Invitrogen) Karlsruhe
Plastic pipettes	Sarstedt, Nümbrecht
Pluronic F-127	Molecular Probes (Invitrogen) Karlsruhe
2-Propanol	Roth, Karlsruhe
Propylenoxide	Serva, Heidelberg
Proteinase K	Roth, Karlsruhe
Rhodamine dextran	Molecular Probes (Invitrogen) Karlsruhe
RNAse A	Roth, Karlsruhe
RNAsin	Promega, Mannheim
Saccharose	Applichem, Darmstadt
Sodium acetate	Roth, Karlsruhe
Sodium chloride	Roth, Karlsruhe
Sodium citrate	Roth, Karlsruhe
Sodium dihydrogen phosphate	Applichem, Darmstadt
Sodium hydroxide	Applichem, Darmstadt
SU5402	Calbiochem, Bad Soden

T61	Hoechst, Frankfurt
Tannic acid	Roth, Karlsruhe
Tissue culture dishes	Greiner, Frickenhausen
Torula RNA	Sigma, Schnelldorf
TRIS base	Applichem, Darmstadt
TRIS HCl	Applichem, Darmstadt
Triton-X100	Serva, Heidelberg
Tryptone	Applichem, Darmstadt
Tungsten wire	Plano, Wetzlar
Tween-20	Applichem, Darmstadt
Tweezers (#3, #5)	Fine Science Tools, Heidelberg

Kits:

Araldite CY212 Kit	Plano, Wetzlar
SV Total RNA Isolation System	Promega, Mannheim
TOPO TA Cloning Kit	Invitrogen, Karlsruhe
pGEM-T Easy Vector System	Promega, Mannheim
PureYield Plasmid Midiprep System	Promega, Mannheim

Proteins and Antibodies:

Recombinant mouse FGF8b	R&D Systems, Wiesbaden
Restriction enzymes and buffers	Promega, Mannheim
Modifying enzymes and buffers	Promega, Mannheim
Mouse anti-acetylated tubulin	Sigma, Schnelldorf
Anti-mouse IgG Alexa 488	Molecular Probes, Invitrogen, Karlsruhe
Anti-digoxigenin AP	Roche, Mannheim

Animals:

Rabbits (New Zealand White)	Haussler, Schwäbisch Hall

Pigs (German Landrace)	Unterer Lindenhof, Eningen

Special Hardware:

Vibratome	Leica, Bensheim
Ultracut S	Leica, Bensheim
Stereo microscope	Zeiss, Oberkochen
LEO EFTEM 912AB	Zeiss, Oberkochen
LEO DSM 940A	Zeiss, Oberkochen
LSM 5 Pascal	Zeiss, Oberkochen
Axioplan 2	Zeiss, Oberkochen
Critical point dryer CPD 030	Balzers, Austria
Sputter coater SCD 050	Balzers, Austria
Incubator Gasboy C42	Labotect, Göttingen
Heat Sterilizer	Fine Science Tools, Heidelberg

Supplement

A

Foxj1

```
1   ctg tcg gcc atc tac aag tgg atc acc gac aac tcc tgc tac ttc cgc cac gca gac ccc  60
1    L   S   A   I   Y   K   W   I   T   D   N   S   C   Y   F   R   H   A   D   P   20

61  acc tgg cag aac tcg atc cgc cac aac ctg tct ctg aac aag tgc ttt atc aaa gtc ccc 120
21   T   W   Q   N   S   I   R   H   N   L   S   L   N   K   C   F   I   K   V   P   40

121 cgg gag aaa gac gag ccg ggc aag ggg ggc ttc tgg cgc atc gac ccc cag tac gcc gag 180
41   R   E   K   D   E   P   G   K   G   G   F   W   R   I   D   P   Q   Y   A   E   60

181 cgg ctg ctg agc ggc gcc ttc aag aag cgg cgg ctg ccc ccg gtc cac atc cac ccg gcc 240
61   R   L   L   S   G   A   F   K   K   R   R   L   P   P   V   H   I   H   P   A   80

241 ttc gcc cgc cag gcc tcg cag gag ccc ggc gcc gcc ccc tgg gcc gcg ccg ctg gcc gtg 300
81   F   A   R   Q   A   S   Q   E   P   G   A   A   P   W   A   A   P   L   A   V  100

301 aac acg gag gcc cag cag ctg ctc cgg gag ttc gag gag gcc acg ggg gag gcg ggc tgg 360
101  N   T   E   A   Q   Q   L   L   R   E   F   E   E   A   T   G   E   A   G   W  120

361 ggc gcg ggc gag ggc agg ctc ggg cac aag cgc aag cag ccg ctg ccc aag cgg gtg gcc 420
121  G   A   G   E   G   R   L   G   H   K   R   K   Q   P   L   P   K   R   V   A  140

421 aag gtc ccg cgg gcc ccc agc acc ctg ctg ctg acc cag gag gag cag ggc gag ctg gaa 480
141  K   V   P   R   A   P   S   T   L   L   L   T   Q   E   E   Q   G   E   L   E  160

481 ccc ctt aag ggc agc ttc gac tgg gaa gcc atc ttc gag gcg ggc act ctg ggc ggg gag 540
161  P   L   K   G   S   F   D   W   E   A   I   F   E   A   G   T   L   G   G   E  180

541 ctg ggc aca ctg gag gcc ctg gag ctg agc ccg cca ctc agc ccc gcc tcg cac ggg gac 600
181  L   G   T   L   E   A   L   E   L   S   P   P   L   S   P   A   S   H   G   D  200

601 gtg gac ctc acc gtc cac ggc cgc cac atc gac tgc ccc acc ccc tgg ggg ccc ccg gca 660
201  V   D   L   T   V   H   G   R   H   I   D   C   P   T   P   W   G   P   P   A  220

661 gag cag gct gcc aac agc ctg gac ttc gac gag acc ttc ctg gcc acg tcc ttc ctg cag 720
221  E   Q   A   A   N   S   L   D   F   D   E   T   F   L   A   T   S   F   L   Q  240

721 cac ccg tgg gac gag agc ggc agc ggc tgc ctg ccc cca gag ccc ctc ttc gag gct ggg 780
241  H   P   W   D   E   S   G   S   G   C   L   P   P   E   P   L   F   E   A   G  260

781 gac gcc acg ctg gcc gcc gac ctg cag gac tgg gcc agt gtg g                      823
261  D   A   T   L   A   A   D   L   Q   D   W   A   S   V                      274
```

B

Rfx3

```
1 t cac tca gtg aca cac aca act cgg gcc tcc cca gcg aca att gaa atg gcg att gag acg  61
1    H   S   V   T   H   T   T   R   A   S   P   A   T   I   E   M   A   I   E   T   20

62  ctg caa aag tct gac ggt ctg tct act cac aga agt tct ctt ctc aac agc cat ctc cag 121
21   L   Q   K   S   D   G   L   S   T   H   R   S   S   L   L   N   S   H   L   Q   40

122 tgg ctg ctg gac aat tat gag aca gca gaa gga gta agc ctt ccc aga agc act ctg tac 181
41   W   L   L   D   N   Y   E   T   A   E   G   V   S   L   P   R   S   T   L   Y   60

182 aac cac tac ctt cga cac tgt cag gaa cac aaa ctg gac cca gtc aat gct gcc tct ttt 241
61   N   H   Y   L   R   H   C   Q   E   H   K   L   D   P   V   N   A   A   S   F   80

242 gga aaa ctt ata agg tca att ttt atg ggg cta cga acc aga aga ttg ggc act aga gga 301
81   G   K   L   I   R   S   I   F   M   G   L   R   T   R   R   L   G   T   R   G  100

302 aac tcc aag tac cat tac tat ggg att tgt gtc aag cca gat tcc cct ctt aat cgt ctg 361
101  N   S   K   Y   H   Y   Y   G   I   C   V   K   P   D   S   P   L   N   R   L  120

362 caa gaa gat atg cag tat atg gct atg aga caa caa ccc atg caa cag aaa caa agg tac 421
121  Q   E   D   M   Q   Y   M   A   M   R   Q   Q   P   M   Q   Q   K   Q   R   Y  140

422 aag cct atg cag aaa gtg gat ggg gtt gca gat ggt ttc aca gga agt ggt caa cag aca 481
141  K   P   M   Q   K   V   D   G   V   A   D   G   F   T   G   S   G   Q   Q   T  160

482 ggc aca tct gtt gag caa act gta att gcc caa agt caa cat cat cag cag ttt tta gat 541
161  G   T   S   V   E   Q   T   V   I   A   Q   S   Q   H   H   Q   Q   F   L   D  180

542 gca tct cga gcc ctt cca gag ttt gga gaa gtt gaa atc tct tcc ctg cca gat ggt act 601
181  A   S   R   A   L   P   E   F   G   E   V   E   I   S   S   L   P   D   G   T  200

602 acc ttt gag gat atc aag tca ctg cag agt ctt tat cga gag cac tgt gag gca ata ttg 661
201  T   F   E   D   I   K   S   L   Q   S   L   Y   R   E   H   C   E   A   I   L  220

662 gac gtt gtt gtg aat ctc cag ttt agc ctg ata gaa aaa ttg tgg caa aca ttc tgg cgc 721
221  D   V   V   V   N   L   Q   F   S   L   I   E   K   L   W   Q   T   F   W   R  240

722 tat tct ccc acg act cca gct gac ggc act acc att act gaa cca agc aat ctg agt gaa 781
241  Y   S   P   T   T   P   A   D   G   T   T   I   T   E   P   S   N   L   S   E  260

782 ata gaa agt cga ctt ccg aaa gca aag ctg ata act ctg tgc aaa cat gag            832
261  I   E   S   R   L   P   K   A   K   L   I   T   L   C   K   H   E            277
```

C

```
Lrd

1   tgt gaa gct gac tta ctc aag gct gag cct gcg ctg gtg gct gcc aca gcc gcg ctc aac  60
1    C   E   A   D   L   L   K   A   E   P   A   L   V   A   A   T   A   A   L   N   20

61  aca ctc aac agg atc aac ctt act gag ctg aaa gtc ttt ccc aat ccc cca aat gcc gtc 120
21   T   L   N   R   I   N   L   T   E   L   K   V   F   P   N   P   P   N   A   V   40

121 acc aac gtc act gcg gcc gtg atg gtc ctt ctg gca ccc cgg ggc cga gtg cca aag gac 180
41   T   N   V   T   A   A   V   M   V   L   L   A   P   R   G   R   V   P   K   D   60

181 cga agc tgg aaa gca gcg aaa gtc ttc atg gga aag gtt gat gat ttc ttg caa gcg tta 240
61   R   S   W   K   A   A   K   V   F   M   G   K   V   D   D   F   L   Q   A   L   80

241 att aac tac gac aaa gag cac att cca gac aac tgt ctc caa gtg gtc aag gaa cag tat 300
81   I   N   Y   D   K   E   H   I   P   D   N   C   L   Q   V   V   K   E   Q   Y  100

301 ttg aaa gac ccc gag ttc aat cca aac ttc att cgg acc aaa tcc ttt gca gca gct ggt 360
101  L   K   D   P   E   F   N   P   N   F   I   R   T   K   S   F   A   A   A   G  120

361 ctg tgc gcc tgg gtc atc aac att gtg aaa ttc tac gag gtc tac tgt gat gtg gaa ccc 420
121  L   C   A   W   V   I   N   I   V   K   F   Y   E   V   Y   C   D   V   E   P  140

421 aaa cgc caa gcc tta gcc cag acg aac ttg gag ttg gcc gca gcc acc gag aaa cta gag 480
141  K   R   Q   A   L   A   Q   T   N   L   E   L   A   A   A   T   E   K   L   E  160

481 act atc agg aaa aag ctg gtg gat ctg gat cgc cat ctg agc aga ctc acc gct tcc ttt 540
161  T   I   R   K   K   L   V   D   L   D   R   H   L   S   R   L   T   A   S   F  180

541 gaa aag gcc ata gct gag aag atc cgc agt cag gag gag gcg aac cga acc aac acg acc 600
181  E   K   A   I   A   E   K   I   R   S   Q   E   E   A   N   R   T   N   T   T  200

601 atc gcc ctg gcg aac agg ctc gtc acg gag ctg gag aca gag aag act cgc tgg ggt cag 660
201  I   A   L   A   N   R   L   V   T   E   L   E   T   E   K   T   R   W   G   Q  220

661 tcc atc cgc tcg ttt gaa gct cag gag aag acg ctg tgt gga gac gtc ctg ctt gcg gct 720
221  S   I   R   S   F   E   A   Q   E   K   T   L   C   G   D   V   L   L   A   A  240

721 gcc ttt gtg tct tac ggg ggn cct ttc acc aga ctg tac cgc cgg gac ctg gtg gcc tgc 780
241  A   F   V   S   Y   G   G   P   F   T   R   L   Y   R   R   D   L   V   A   C  260

781 gag tgg gtc ccc ttt ctc cac aag act tcc atc cca ata acc aaa ggc ctg gac gtg att 840
261  E   W   V   P   F   L   H   K   T   S   I   P   I   T   K   G   L   D   V   I  280

841 gcc atg ttg acg gat gac gcc aca gtt gcc gcc tgg aat aac gaa ggg ctg ccc agt gac 900
281  A   M   L   T   D   D   A   T   V   A   A   W   N   N   E   G   L   P   S   D  300

901 aga atg tcc acg gaa aat gcc acc atc ctc acc cag tgg gag cgc tgg ccc ctg atg ata 960
301  R   M   S   T   E   N   A   T   I   L   T   Q   W   E   R   W   P   L   M   I  320

961 ggc ccc cag caa cag gga att aag tgg atc aag                                    993
321  G   P   Q   Q   Q   G   I   K   W   I   K                                    331
```

D

```
Polaris

1   aga aat tat tcc aaa gcc att aaa ttc tac cga atg gca tta gat caa att cca agt gtc  60
1    R   N   Y   S   K   A   I   K   F   Y   R   M   A   L   D   Q   I   P   S   V   20

61  cat aaa gaa atg agg att aaa ata atg cag aac att gga gtt aca ttt att aag act ggt 120
21   H   K   E   M   R   I   K   I   M   Q   N   I   G   V   T   F   I   K   T   G   40

121 caa tat tca gat gcc att aat tca ttt gag cat ata atg agt atg gcg cca aat ctg aag 180
41   Q   Y   S   D   A   I   N   S   F   E   H   I   M   S   M   A   P   N   L   K   60

181 gct ggc ttc aac cta att ctt agt tat ttt gct att gga gat caa gaa aaa atg aag aaa 240
61   A   G   F   N   L   I   L   S   Y   F   A   I   G   D   Q   E   K   M   K   K   80

241 tca ttc caa aaa ttg att gct gtt cca ttg gaa att gat gaa gat gat aaa tat att tca 300
81   S   F   Q   K   L   I   A   V   P   L   E   I   D   E   D   D   K   Y   I   S  100

301 cca agt gat gat cct cat act aat tta gtg att gaa gct ata aaa aat gat cat ctc agg 360
101  P   S   D   D   P   H   T   N   L   V   I   E   A   I   K   N   D   H   L   R  120

361 caa atg gaa cgt gaa agg aaa gcc atg gca gaa aaa tac atc atg aca gct gcg aaa ctc 420
121  Q   M   E   R   E   R   K   A   M   A   E   K   Y   I   M   T   A   A   K   L  140

421 att gct cct gta att gaa aca tct ttt gct gta ggt tat gat tgg tgt gtg gaa gtg gtg 480
141  I   A   P   V   I   E   T   S   F   A   V   G   Y   D   W   C   V   E   V   V  160

481 aaa gcg tct caa tat gta gag cta gcc aat gac ctg gaa ata aac aaa gca att aca tat 540
161  K   A   S   Q   Y   V   E   L   A   N   D   L   E   I   N   K   A   I   T   Y  180

541 ttg aga caa aag gac ttt acc caa gct gta gat acc tta aaa atg ttt gaa aag aag gac 600
181  L   R   Q   K   D   F   T   Q   A   V   D   T   L   K   M   F   E   K   K   D  200

601 agt aga gtg aaa agt gca gct gca acc aac ctc tcc ttc cta tat tat ctg gaa aac gaa 660
201  S   R   V   K   S   A   A   A   T   N   L   S   F   L   Y   Y   L   E   N   E  220

661 ttt gca caa gcc agc agc tat gca gat tta gct gtg aac tct gat aga tac aat cca tca 720
221  F   A   Q   A   S   S   Y   A   D   L   A   V   N   S   D   R   Y   N   P   S  240

721 gct ctt act aat aaa ggg aat act gtt ttt gca aat ggt gat tat gag aag gc          773
241  A   L   T   N   K   G   N   T   V   F   A   N   G   D   Y   E   K             257
```

E

Kif3a

```
1   gaa agc tgc gat aat gtg aag gtc gtt gtt agg tgc cgg ccc ctc aat gag aga gag aaa  60
1    E   S   C   D   N   V   K   V   V   V   R   C   R   P   L   N   E   R   E   K   20

61  tcc atg ttc tac aag cag gct gtc agt gtg gat gag atg agg ggg act atc act gtg cat 120
21   S   M   F   Y   K   Q   A   V   S   V   D   E   M   R   G   T   I   T   V   H   40

121 aag act gat tct tcc aat gaa cct ccg aag acc ttt act ttt gat act gtt ttt gga cca 180
41   K   T   D   S   S   N   E   P   P   K   T   F   T   F   D   T   V   F   G   P   60

181 gag agt aaa caa ctt gac gtt tat aac tta act gcg aga cct att att gat tct gtt ctt 240
61   E   S   K   Q   L   D   V   Y   N   L   T   A   R   P   I   I   D   S   V   L   80

241 gaa ggc tac aat gga act att ttt gca tat ggt caa act gga aca ggc aaa act ttc acc 300
81   E   G   Y   N   G   T   I   F   A   Y   G   Q   T   G   T   G   K   T   F   T  100

301 atg gaa ggt gtt cga gct gtt cct gaa ctt aga gga atc att ccc aat tca ttt gct cat 360
101  M   E   G   V   R   A   V   P   E   L   R   G   I   I   P   N   S   F   A   H  120

361 ata ttt ggt cat att gca aag gca gag ggt gac aca agg ttt ttg gtt cga gtt tct tat 420
121  I   F   G   H   I   A   K   A   E   G   D   T   R   F   L   V   R   V   S   Y  140

421 ttg gaa ata tat aat gaa gaa gtt cgt gac ctt ttg ggc aag gat cag aca cag agg tta 480
141  L   E   I   Y   N   E   E   V   R   D   L   L   G   K   D   Q   T   Q   R   L  160

481 gag gtt aaa gaa aga cct gat gtg gga gtt tat atc aaa gat tta tca gct tat gtt gta 540
161  E   V   K   E   R   P   D   V   G   V   Y   I   K   D   L   S   A   Y   V   V  180

541 aac aat gct gat gat atg gat agg att atg act cta ggc cac aaa aat cgt tct gtt ggt 600
181  N   N   A   D   D   M   D   R   I   M   T   L   G   H   K   N   R   S   V   G  200

601 gca act aat atg aat gaa cat agt tcc cgt tcc cat gcc atc ttt aca att act ata ga  659
201  A   T   N   M   N   E   H   S   S   R   S   H   A   I   F   T   I   T   I      219
```

Supplementary Fig. 1 Nucleotide- and deduced amino acid-sequence of rabbit ciliary gene-fragments cloned by RT-PCR. (**A**) 823bp fragment of *Foxj1*. (**B**) 832bp fragment of *Rfx3*. (**C**) 993bp fragment of *lrd* (*Dnahc11*). (**D**) 773bp fragment of *polaris*. (**E**) 659bp fragment of *Kif3a*.

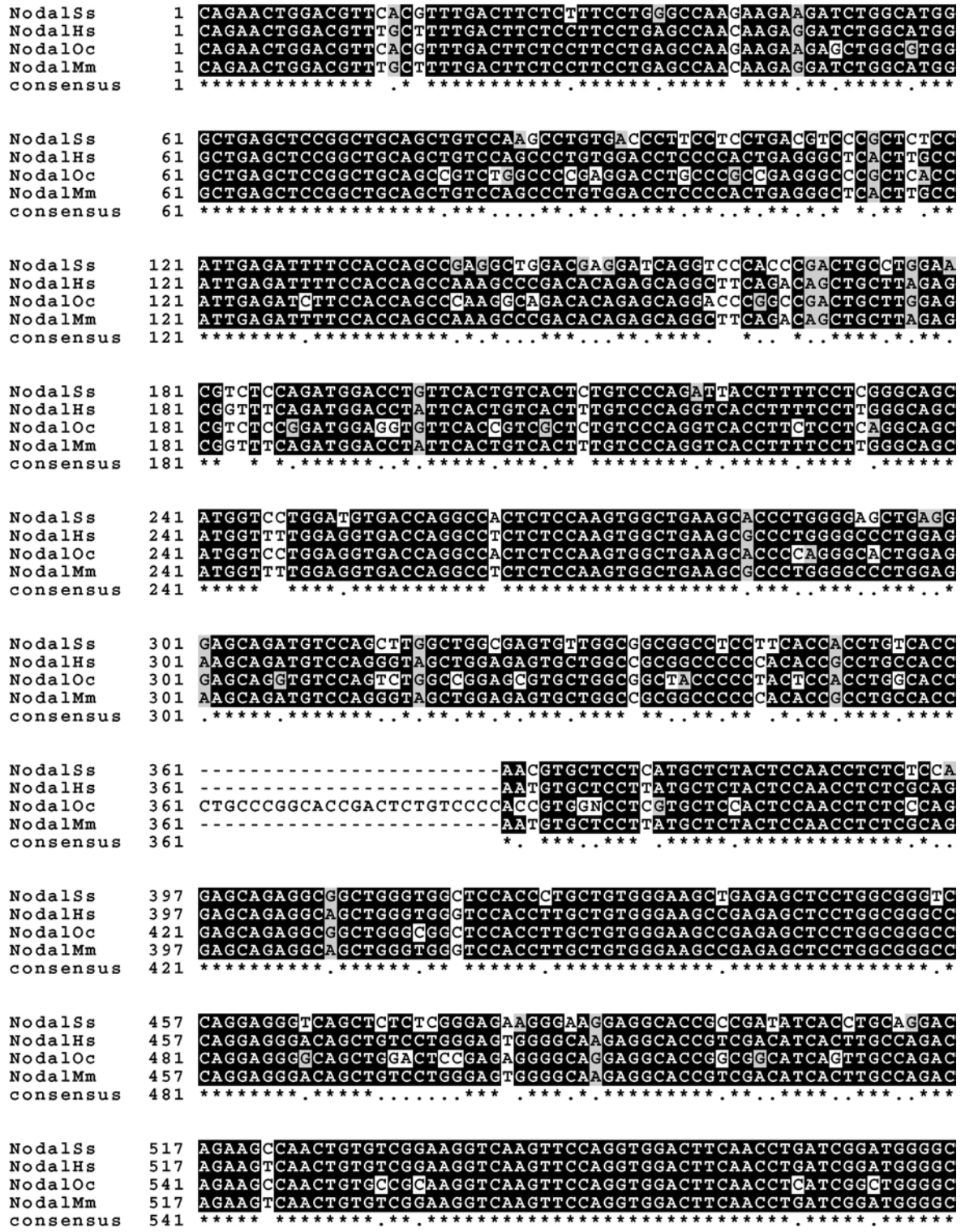

Supplementary Fig. 2 Nucleotide sequence alignment of a 611bp *Nodal* fragment cloned from pig (Sus scrofa, Ss) with nucleotide sequences from human (Homo sapiens, Hs), rabbit (Oryctolagus cuniculus, Oc) and mouse (Mus Musculus, Mm). Matching basepairs are shaded in black and indicated by an asterisk in the consensus line.

References

Abdelkhalek HB, Beckers A, Schuster-Gossler K, Pavlova MN, Burkhardt H, Lickert H, Rossant J, Reinhardt R, Schalkwyk LC, Muller I, Herrmann BG, Ceolin M, Rivera-Pomar R, Gossler A. 2004. The mouse homeobox gene Not is required for caudal notochord development and affected by the truncate mutation. Genes Dev 18:1725-1736.

Adachi H, Saijoh Y, Mochida K, Ohishi S, Hashiguchi H, Hirao A, Hamada H. 1999. Determination of left/right asymmetric expression of nodal by a left side-specific enhancer with sequence similarity to a lefty-2 enhancer. Genes Dev 13:1589-1600.

Baccetti B, Dallai R, Fratello B. 1973. The spermatozoon of arthropoda. XXII. The 12+0', 14+0' or aflagellate sperm of protura. J Cell Sci 13:321-335.

Baccetti B, Dallai R, Rosati F. 1970. The spermatozoon of arthropoda. 8. The 9 + 3 flagellum of spider sperm cells. J Cell Biol 44:681-682.

Blake JR, Sleigh MA. 1974. Mechanics of ciliary locomotion. Biol Rev Camb Philos Soc 49:85-125.

Blatt EN, Yan XH, Wuerffel MK, Hamilos DL, Brody SL. 1999. Forkhead transcription factor HFH-4 expression is temporally related to ciliogenesis. Am J Respir Cell Mol Biol 21:168-176.

Blum M, Andre P, Muders K, Schweickert A, Fischer A, Bitzer E, Bogusch S, Beyer T, van Straaten HWM, Viebahn C. 2006. Ciliation and gene expression distinguish between node and posterior notochord in the mammalian embryo. Differentiation:in press.

Boettger T, Wittler L, Kessel M. 1999. FGF8 functions in the specification of the right body side of the chick. Curr Biol 9:277-280.

Bonnafe E, Touka M, AitLounis A, Baas D, Barras E, Ucla C, Moreau A, Flamant F, Dubruille R, Couble P, Collignon J, Durand B, Reith W. 2004. The transcription factor RFX3 directs nodal cilium development and left-right asymmetry specification. Mol Cell Biol 24:4417-4427.

Brennan J, Norris DP, Robertson EJ. 2002. Nodal activity in the node governs left-right asymmetry. Genes Dev 16:2339-2344.

Britz-Cunningham SH, Shah MM, Zuppan CW, Fletcher WH. 1995. Mutations of the Connexin43 gap-junction gene in patients with heart malformations and defects of laterality. N Engl J Med 332:1323-1329.

Brody SL, Yan XH, Wuerffel MK, Song SK, Shapiro SD. 2000. Ciliogenesis and left-right axis defects in forkhead factor HFH-4-null mice. Am J Respir Cell Mol Biol 23:45-51.

Brown NA, Wolpert L. 1990. The development of handedness in left/right asymmetry. Development 109:1-9.

Cartwright JH, Piro O, Tuval I. 2004. Fluid-dynamical basis of the embryonic development of left-right asymmetry in vertebrates. Proc Natl Acad Sci U S A 101:7234-7239.

Chanson M, Bruzzone R, Bosco D, Meda P. 1989. Effects of n-alcohols on junctional coupling and amylase secretion of pancreatic acinar cells. J Cell Physiol 139:147-156.

Charrier JB, Teillet MA, Lapointe F, Le Douarin NM. 1999. Defining subregions of Hensen's node essential for caudalward movement, midline development and cell survival. Development 126:4771-4783.

Chazaud C, Chambon P, Dolle P. 1999. Retinoic acid is required in the mouse embryo for left-right asymmetry determination and heart morphogenesis. Development 126:2589-2596.

Chen C, Shen MM. 2004. Two modes by which Lefty proteins inhibit nodal signaling. Curr Biol 14:618-624.

Chen Y, Schier AF. 2001. The zebrafish Nodal signal Squint functions as a morphogen. Nature 411:607-610.

Crossley PH, Martin GR. 1995. The mouse Fgf8 gene encodes a family of polypeptides and is expressed in regions that direct outgrowth and patterning in the developing embryo. Development 121:439-451.

Dathe V, Gamel A, Manner J, Brand-Saberi B, Christ B. 2002. Morphological left-right asymmetry of Hensen's node precedes the asymmetric expression of Shh and Fgf8 in the chick embryo. Anat Embryol (Berl) 205:343-354.

Diez del Corral R, Olivera-Martinez I, Goriely A, Gale E, Maden M, Storey K. 2003. Opposing FGF and retinoid pathways control ventral neural pattern, neuronal differentiation, and segmentation during body axis extension. Neuron 40:65-79.

Dubruille R, Laurencon A, Vandaele C, Shishido E, Coulon-Bublex M, Swoboda P, Couble P, Kernan M, Durand B. 2002. Drosophila regulatory factor X is

necessary for ciliated sensory neuron differentiation. Development 129:5487-5498.

Dufort D, Schwartz L, Harpal K, Rossant J. 1998. The transcription factor HNF3beta is required in visceral endoderm for normal primitive streak morphogenesis. Development 125:3015-3025.

Essner JJ, Amack JD, Nyholm MK, Harris EB, Yost HJ. 2005. Kupffer's vesicle is a ciliated organ of asymmetry in the zebrafish embryo that initiates left-right development of the brain, heart and gut. Development 132:1247-1260.

Essner JJ, Vogan KJ, Wagner MK, Tabin CJ, Yost HJ, Brueckner M. 2002. Conserved function for embryonic nodal cilia. Nature 418:37-38.

Ewart JL, Cohen MF, Meyer RA, Huang GY, Wessels A, Gourdie RG, Chin AJ, Park SM, Lazatin BO, Villabon S, Lo CW. 1997. Heart and neural tube defects in transgenic mice overexpressing the Cx43 gap junction gene. Development 124:1281-1292.

Fischer A, Viebahn C, Blum M. 2002. FGF8 acts as a right determinant during establishment of the left-right axis in the rabbit. Curr Biol 12:1807-1816.

Gaio U, Schweickert A, Fischer A, Garratt AN, Muller T, Ozcelik C, Lankes W, Strehle M, Britsch S, Blum M, Birchmeier C. 1999. A role of the cryptic gene in the correct establishment of the left-right axis. Curr Biol 9:1339-1342.

Gibbons IR. 1981. Cilia and flagella of eukaryotes. J Cell Biol 91:107s-124s.

Henley C, Costello DP, Thomas MB, Newton WD. 1969. The "9+1" pattern of microtubules in spermatozoa of Mesostoma (Platyhelminthes, Turbellaria). Proc Natl Acad Sci U S A 64:849-856.

Herrmann BG, Kispert A. 1994. The T genes in embryogenesis. Trends Genet 10:280-286.

Hirokawa N, Tanaka Y, Okada Y, Takeda S. 2006. Nodal flow and the generation of left-right asymmetry. Cell 125:33-45.

Jiang D, Munro EM, Smith WC. 2005. Ascidian prickle regulates both mediolateral and anterior-posterior cell polarity of notochord cells. Curr Biol 15:79-85.

Jones CM, Kuehn MR, Hogan BL, Smith JC, Wright CV. 1995. Nodal-related signals induce axial mesoderm and dorsalize mesoderm during gastrulation. Development 121:3651-3662.

Kramer-Zucker AG, Olale F, Haycraft CJ, Yoder BK, Schier AF, Drummond IA. 2005. Cilia-driven fluid flow in the zebrafish pronephros, brain and Kupffer's vesicle is required for normal organogenesis. Development 132:1907-1921.

Krebs LT, Iwai N, Nonaka S, Welsh IC, Lan Y, Jiang R, Saijoh Y, O'Brien TP, Hamada H, Gridley T. 2003. Notch signaling regulates left-right asymmetry determination by inducing Nodal expression. Genes Dev 17:1207-1212.

Le AC, Musil LS. 2001. A novel role for FGF and extracellular signal-regulated kinase in gap junction-mediated intercellular communication in the lens. J Cell Biol 154:197-216.

Levin M, Johnson RL, Stern CD, Kuehn M, Tabin C. 1995. A molecular pathway determining left-right asymmetry in chick embryogenesis. Cell 82:803-814.

Levin M, Mercola M. 1998. Gap junctions are involved in the early generation of left-right asymmetry. Dev Biol 203:90-105.

Levin M, Mercola M. 1999. Gap junction-mediated transfer of left-right patterning signals in the early chick blastoderm is upstream of Shh asymmetry in the node. Development 126:4703-4714.

Levin M, Thorlin T, Robinson KR, Nogi T, Mercola M. 2002. Asymmetries in H+/K+-ATPase and cell membrane potentials comprise a very early step in left-right patterning. Cell 111:77-89.

Logan M, Pagan-Westphal SM, Smith DM, Paganessi L, Tabin CJ. 1998. The transcription factor Pitx2 mediates situs-specific morphogenesis in response to left-right asymmetric signals. Cell 94:307-317.

Lohr JL, Danos MC, Yost HJ. 1997. Left-right asymmetry of a nodal-related gene is regulated by dorsoanterior midline structures during Xenopus development. Development 124:1465-1472.

Long S, Ahmad N, Rebagliati M. 2003. The zebrafish nodal-related gene southpaw is required for visceral and diencephalic left-right asymmetry. Development 130:2303-2316.

Lowe LA, Supp DM, Sampath K, Yokoyama T, Wright CV, Potter SS, Overbeek P, Kuehn MR. 1996. Conserved left-right asymmetry of nodal expression and alterations in murine situs inversus. Nature 381:158-161.

Makarenkova H, Becker DL, Tickle C, Warner AE. 1997. Fibroblast growth factor 4 directs gap junction expression in the mesenchyme of the vertebrate limb Bud. J Cell Biol 138:1125-1137.

Makarenkova H, Patel K. 1999. Gap junction signalling mediated through connexin-43 is required for chick limb development. Dev Biol 207:380-392.

Manner J. 2001. Does an equivalent of the "ventral node" exist in chick embryos? A scanning electron microscopic study. Anat Embryol (Berl) 203:481-490.

Marshall WF, Nonaka S. 2006. Cilia: Tuning in to the Cell's Antenna. Curr Biol 16:R604-614.

Massague J. 2003. Integration of Smad and MAPK pathways: a link and a linker revisited. Genes Dev 17:2993-2997.

McGrath J, Somlo S, Makova S, Tian X, Brueckner M. 2003. Two populations of node monocilia initiate left-right asymmetry in the mouse. Cell 114:61-73.

Meyers EN, Martin GR. 1999. Differences in left-right axis pathways in mouse and chick: functions of FGF8 and SHH. Science 285:403-406.

Mohammadi M, McMahon G, Sun L, Tang C, Hirth P, Yeh BK, Hubbard SR, Schlessinger J. 1997. Structures of the tyrosine kinase domain of fibroblast growth factor receptor in complex with inhibitors. Science 276:955-960.

Nakamura T, Mine N, Nakaguchi E, Mochizuki A, Yamamoto M, Yashiro K, Meno C, Hamada H. 2006. Generation of robust left-right asymmetry in the mouse embryo requires a self-enhancement and lateral-inhibition system. Dev Cell 11:495-504.

Nonaka S, Shiratori H, Saijoh Y, Hamada H. 2002. Determination of left-right patterning of the mouse embryo by artificial nodal flow. Nature 418:96-99.

Nonaka S, Tanaka Y, Okada Y, Takeda S, Harada A, Kanai Y, Kido M, Hirokawa N. 1998. Randomization of left-right asymmetry due to loss of nodal cilia generating leftward flow of extraembryonic fluid in mice lacking KIF3B motor protein. Cell 95:829-837.

Nonaka S, Yoshiba S, Watanabe D, Ikeuchi S, Goto T, Marshall WF, Hamada H. 2005. De novo formation of left-right asymmetry by posterior tilt of nodal cilia. PLoS Biol 3:e268.

Norris DP, Brennan J, Bikoff EK, Robertson EJ. 2002. The Foxh1-dependent autoregulatory enhancer controls the level of Nodal signals in the mouse embryo. Development 129:3455-3468.

Norris DP, Robertson EJ. 1999. Asymmetric and node-specific nodal expression patterns are controlled by two distinct cis-acting regulatory elements. Genes Dev 13:1575-1588.

Ohi Y, Wright CV. 2006. Anteriorward shifting of asymmetric Xnr1 expression and contralateral communication in left-right specification in Xenopus. Dev Biol.

Okada Y, Nonaka S, Tanaka Y, Saijoh Y, Hamada H, Hirokawa N. 1999. Abnormal nodal flow precedes situs inversus in iv and inv mice. Mol Cell 4:459-468.

Okada Y, Takeda S, Tanaka Y, Belmonte JC, Hirokawa N. 2005. Mechanism of nodal flow: a conserved symmetry breaking event in left-right axis determination. Cell 121:633-644.

Omoto CK, Gibbons IR, Kamiya R, Shingyoji C, Takahashi K, Witman GB. 1999. Rotation of the central pair microtubules in eukaryotic flagella. Mol Biol Cell 10:1-4.

Onuma Y, Yeo CY, Whitman M. 2006. XCR2, one of three Xenopus EGF-CFC genes, has a distinct role in the regulation of left-right patterning. Development 133:237-250.

Pagan-Westphal SM, Tabin CJ. 1998. The transfer of left-right positional information during chick embryogenesis. Cell 93:25-35.

Park TJ, Haigo SL, Wallingford JB. 2006. Ciliogenesis defects in embryos lacking inturned or fuzzy function are associated with failure of planar cell polarity and Hedgehog signaling. Nat Genet 38:303-311.

Poole CA, Jensen CG, Snyder JA, Gray CG, Hermanutz VL, Wheatley DN. 1997. Confocal analysis of primary cilia structure and colocalization with the Golgi apparatus in chondrocytes and aortic smooth muscle cells. Cell Biol Int 21:483-494.

Prensier G, Vivier E, Goldstein S, Schrevel J. 1980. Motile flagellum with a "3 + 0" ultrastructure. Science 207:1493-1494.

Przemeck GK, Heinzmann U, Beckers J, Hrabe de Angelis M. 2003. Node and midline defects are associated with left-right development in Delta1 mutant embryos. Development 130:3-13.

Reaume AG, de Sousa PA, Kulkarni S, Langille BL, Zhu D, Davies TC, Juneja SC, Kidder GM, Rossant J. 1995. Cardiac malformation in neonatal mice lacking connexin43. Science 267:1831-1834.

Rebagliati MR, Toyama R, Fricke C, Haffter P, Dawid IB. 1998. Zebrafish nodal-related genes are implicated in axial patterning and establishing left-right asymmetry. Dev Biol 199:261-272.

Rosenbaum JL, Witman GB. 2002. Intraflagellar transport. Nat Rev Mol Cell Biol 3:813-825.

Ross AJ, May-Simera H, Eichers ER, Kai M, Hill J, Jagger DJ, Leitch CC, Chapple JP, Munro PM, Fisher S, Tan PL, Phillips HM, Leroux MR, Henderson DJ, Murdoch JN, Copp AJ, Eliot MM, Lupski JR, Kemp DT, Dollfus H, Tada M, Katsanis N, Forge A, Beales PL. 2005. Disruption of Bardet-Biedl syndrome ciliary proteins perturbs planar cell polarity in vertebrates. Nat Genet 37:1135-1140.

Saijoh Y, Oki S, Ohishi S, Hamada H. 2003. Left-right patterning of the mouse lateral plate requires nodal produced in the node. Dev Biol 256:160-172.

Saijoh Y, Oki S, Tanaka C, Nakamura T, Adachi H, Yan YT, Shen MM, Hamada H. 2005. Two nodal-responsive enhancers control left-right asymmetric expression of Nodal. Dev Dyn 232:1031-1036.

Sarmah B, Latimer AJ, Appel B, Wente SR. 2005. Inositol polyphosphates regulate zebrafish left-right asymmetry. Dev Cell 9:133-145.

Sasaki H, Nishizaki Y, Hui C, Nakafuku M, Kondoh H. 1999. Regulation of Gli2 and Gli3 activities by an amino-terminal repression domain: implication of Gli2 and Gli3 as primary mediators of Shh signaling. Development 126:3915-3924.

Schier AF, Shen MM. 2000. Nodal signalling in vertebrate development. Nature 403:385-389.

Schweickert A, Weber T, Beyer T, Vick P, Bogusch S, Feistel K, Blum M. 2007. A cilia-driven leftward flow specifies laterality upstream of asymmetric Nodal signaling in the frog Xenopus laevis. Curr Biol:in press.

Shook DR, Majer C, Keller R. 2004. Pattern and morphogenesis of presumptive superficial mesoderm in two closely related species, Xenopus laevis and Xenopus tropicalis. Dev Biol 270:163-185.

Sirbu IO, Duester G. 2006. Retinoic-acid signalling in node ectoderm and posterior neural plate directs left-right patterning of somitic mesoderm. Nat Cell Biol.

Smith EF. 2002. Regulation of flagellar dynein by calcium and a role for an axonemal calmodulin and calmodulin-dependent kinase. Mol Biol Cell 13:3303-3313.

Smith EF, Lefebvre PA. 1997. The role of central apparatus components in flagellar motility and microtubule assembly. Cell Motil Cytoskeleton 38:1-8.

Solan JL, Lampe PD. 2005. Connexin phosphorylation as a regulatory event linked to gap junction channel assembly. Biochim Biophys Acta 1711:154-163.

Stains JP, Civitelli R. 2005. Gap junctions regulate extracellular signal-regulated kinase signaling to affect gene transcription. Mol Biol Cell 16:64-72.

Sulik K, Dehart DB, Iangaki T, Carson JL, Vrablic T, Gesteland K, Schoenwolf GC. 1994. Morphogenesis of the murine node and notochordal plate. Dev Dyn 201:260-278.

Supp DM, Witte DP, Potter SS, Brueckner M. 1997. Mutation of an axonemal dynein affects left-right asymmetry in inversus viscerum mice. Nature 389:963-966.

Swoboda P, Adler HT, Thomas JH. 2000. The RFX-type transcription factor DAF-19 regulates sensory neuron cilium formation in C. elegans. Mol Cell 5:411-421.

Tabin CJ, Vogan KJ. 2003. A two-cilia model for vertebrate left-right axis specification. Genes Dev 17:1-6.

Tanaka Y, Okada Y, Hirokawa N. 2005. FGF-induced vesicular release of Sonic hedgehog and retinoic acid in leftward nodal flow is critical for left-right determination. Nature 435:172-177.

Wargo MJ, Smith EF. 2003. Asymmetry of the central apparatus defines the location of active microtubule sliding in Chlamydomonas flagella. Proc Natl Acad Sci U S A 100:137-142.

Warn-Cramer BJ, Cottrell GT, Burt JM, Lau AF. 1998. Regulation of connexin-43 gap junctional intercellular communication by mitogen-activated protein kinase. J Biol Chem 273:9188-9196.

Wasiak S, Lohnes D. 1999. Retinoic acid affects left-right patterning. Dev Biol 215:332-342.

Wemmer KA, Marshall WF. 2004. Flagellar motility: all pull together. Curr Biol 14:R992-993.

Whitman M, Mercola M. 2001. TGF-beta superfamily signaling and left-right asymmetry. Sci STKE 2001:RE1.

Ya J, Erdtsieck-Ernste EB, de Boer PA, van Kempen MJ, Jongsma H, Gros D, Moorman AF, Lamers WH. 1998. Heart defects in connexin43-deficient mice. Circ Res 82:360-366.

Yamamoto M, Mine N, Mochida K, Sakai Y, Saijoh Y, Meno C, Hamada H. 2003. Nodal signaling induces the midline barrier by activating Nodal expression in the lateral plate. Development 130:1795-1804.

Zhang DQ, McMahon DG. 2001. Gating of retinal horizontal cell hemi gap junction channels by voltage, Ca2+, and retinoic acid. Mol Vis 7:247-252.

Zhou X, Sasaki H, Lowe L, Hogan BL, Kuehn MR. 1993. Nodal is a novel TGF-beta-like gene expressed in the mouse node during gastrulation. Nature 361:543-547.